Population Genetic Investigation of the White-Nose Syndrome Pathogen,*Pseudogymonascus destructans*, in North America

Population Genetic Investigation of the White-Nose Syndrome pathogen, *Pseudogymnonascus destructans*, in North America

By Adrian Forsythe,

A Thesis Submitted to the School of Graduate Studies in the Partial Fulfillment of the Requirements for the Degree Doctor of Philosophy

McMaster University

Doctor of Philosophy (2020)

Hamilton, Ontario (Department of Biology)

TITLE: Population Genetic Investigation of the White-Nose Syndrome pathogen, *Pseudogymonascus destructans*, in North America

AUTHOR: Adrian Forsythe (McMaster University)

SUPERVISOR: Dr. Jianping Xu

NUMBER OF PAGES: xxi, 170

Abstract

Fungal infections of animals have become an increasingly important global issue. White-Nose Syndrome is an ongoing fungal epizootic of North American hibernating bats, caused by epidermal infections of the fungus, *Pseudogymnoascus destructans*. Infections emerged early in 2006 in New York State and have since spread to 35 US States and seven Canadian Provinces, with rates of mortality exceeding 90% in some bat colonies. As an emerging outbreak in North America, the transmission of *P. destructans* is assumed to occur in a radial fashion outwards from the point of origin. In addition, the factors that may influence *P. destructans* transmission have been postulated, but not tested before. Lastly, as reproduction is assumed to be strictly clonal in North America, invasive populations should have low genetic diversity, and may even accumulate deleterious mutations over time. The aim of my PhD research is to test these assumptions regarding the spread, evolution, and adaptation of *P. destructans* using combination of genotyping methods. My results showed how *P. destructans* isolates have shifted in terms of phenotypes and physiological capabilities since being introduced. In addition, I describe patterns of connectivity across the landscape, which are more consist with the level of anthropogenic activity than variation in climate. The mutations common to all invasive strains of *P. destructans* are associated with adaptations that have occurred since being introduced from Europe, some with relevant metabolic functions that fit their pathogenic lifestyle. Together, my results revealed significant phenotypic and genotypic changes during the spread of *P. destructans* in North America. The factors identified here that influence the phenotypic and genotypic changes should help developing better management strategies against the White-Nose Syndrome pathogen.

Acknowledgements

First I want to thank my supervisor, Dr. Jianping Xu, for his support, insight, and encouragement whenever I needed it. Over the years spent under JP's supervision, I came to understand how remarkable his life and academic path has been. I feel very grateful to have shared just a small part of it.

To my committee members, Dr. Ben Evans and Dr. Jonathon Stone, for providing constructive feedback during committee meetings, which have been a great help in completing this thesis.

I would also like the members of the Xu Lab, both past and present. You have all made my time at McMaster both more enjoyable, and less painful when times were rough.

All the friends from the Biology Department and across McMaster – it's the conversations we shared together that helped me to find purpose in my work. Conversations that withheld judgment or expectation were of immense benefit to me over the years.

Finally, my parents, extended family, and Ramsha who have always been a major source of support. All my past teachers, instructors, and supervisors who have all contributed to my journey in academia thus far.

Contents

List of Figures

List of Tables

Acronyms

AIC Akaike information criterion

CNV copy number variation

CTAB cetyl-trimethylammonium bromide

FDR False Discovery Rate

FGT Four Gamete Test

GO Gene Ontology

IBD Isolation by Distance

IBE Isolation by Environment

IBR Isolation by Resistance

Indel Insertion/Deletions

LD linkage disequilibrium

LD linkage equilibrium

MLG multilocus genotype

MLPE Maximum Likihood Population Effects mixed-effects models

MSAT microsatellite

MYA million years ago

N. America North America

P. destructans *Pseudogymnoascus destructans*

PIC Polymorphic index content

SDA Sabouraud Dextrose Agar

SNP Single Nucleotide Polymorphism

UV Ultraviolet radiation

WNS White-Nose Syndrome

Declaration of Authorship

I, Adrian FORSYTHE, declare that this thesis titled, "Population Genetic Investigation of the White-Nose Syndrome pathogen, *Pseudogymonascus destructans*, in North America" and the work presented in it are my own. I confirm that:

- Chapters 1 and 5

  These chapters are literature reviews written by myself with help from Jianping Xu.

- Chapter 2

  I conducted genome sequencing, bioinformatic analyses, statistical analyses, the majority of arthroconidial germination experiment, and drafting of manuscript. Victoria Giglio conducted part of the arthroconidial germination experiment. Jonathan Asa completed all of the phenotypic measurements. JP contributed to drafting of the manuscript and conceived of experiments.

- Chapter 3

  I conducted genotyping, bioinformatic analyses, statistical analyses, and manuscript drafting. Karen Vanderwolf supplied many of the *P. destructans* strains from the Canadian Maritimes and also contributed to manuscript drafting. JP helped with manuscript drafting and conceived of experiments.

- Chapter 4

  I conducted bioinformatic analyses, statistical analyses, and manuscript drafting. JP helped with manuscript drafting.

For my nieces Breah and Lydia, both younger than the work contained in this thesis.

Chapter 1

General Introduction

1.1 Fungal Pathogens in the Environment

Fungi are ubiquitous in almost all ecological niches. From single celled yeasts, to multicellular filamentous moulds, members of the fungal kingdom have evolved a wide range of different lifestyles in order to meet ecological demands. Many fungal species are well known for their saphrotrophic capabilities, digesting dead organic matter, such as cellulose and lignin, and recycling nutrients back into the food web (Robinson 1990). However, some fungal species form interactions with plants (Behie and Bidochka 2014), animals (Nguyen et al. 2007), and other microbes (Lutzoni et al. 2001). These interactions can be mutually beneficial, such as the relationship between arbuscular mycorrhizal fungi and land plants (Brundrett 2002). However, fungi do not always reciprocate the benefits provided by the other symbiont, this results in parasitism and disease.

The occurrence of infections by fungi have to be considered in the greater context of the microbial ecosystem as a whole. Fungal pathogens that are ubiquitous in the environment are often commensals to their hosts. Under certain circumstances, some level of exposure to these pathogens can be tolerated by the host. For example, the pathogenic yeast *Candida albicans*, colonizes the gastrointestinal mucosa and genitals in various

mammalian species (Ghannoum et al. 2010; Iliev et al. 2012), becoming pathogenic only with the suppression of host immune system function (Enoch et al. 2006). These infections only occur when the host is compromised as opportunistic fungal pathogens are generally well suited to stressful host conditions as a byproduct of tolerance to environmental stress normally experienced by these pathogens outside of their hosts.

Few fungal pathogens are well adapted to the conditions of the host during infection, and result in hosts that are not contagious. For instance, infections of another opportunistic pathogen *Aspergillus*, are acquired from environmental sources, and transmission between hosts does not occur (Seyedmousavi et al. 2015). The few pathogens that can spread between hosts have a drastically different host/pathogen relationship, as mutations acquired during infection can be passed on to next generation. Transmission between hosts in zoophilic pathogens, such as *Batrachochytrium dendrobatidis*, benefits from long-distance dispersal mediated by the host. Contagious individuals thereby enable direct transmission of the disease and often leads to exponentially expanding epizootics.

In most fungal infections, the main reservoir is from the environment, as most infections in hosts are acquired from propagules that originate from outside of the host. Such environmental pathogens have two life styles, combining opportunistic and zoophilic pathogen characteristics. As part of their life cycle can be completed in both environmental and host reservoirs, spread of these pathogens are not limited to the availability of host species. With such added flexibility, the expansion of infections between hosts sourced from the environment make them difficult to eradicate.

Currently, the fungal epizootics with the largest impact on host populations are initiated through the introduction of a non-native pathogen. A mycosis can be introduced via anthropogenic trade or other mechanisms, and further establishment in the novel environment can occur through spillover events leading the widespread infections of host

population(s). Adaptation to the novel environment can occur, refining pathogenesis, survival, or transmission of the pathogen (reviewed in Gladieux et al. 2015). The motivation for the research detailed in this thesis is to better understand the factors involved in the spread and adaptation of one such fungal pathogen, *Pseudogymnoascus destructans* (*P. destructans*), the causative agent of White-Nose Syndrome (WNS) in bats. These efforts are motivated by unprecedented loss in biodiversity that current fungal epizootics are responsible for, and the need to control current fungal epidemics and the prevention of epidemics in the future.

1.2 *Pseudogymnoascus destructans*, the Causative Agent of White Nose Syndrome

WNS is an epidermal infection of North America (N. America)n bat species, caused by the fungal pathogen, *P. destructans* (formerly *Geomyces destructans*; (Gargas et al. 2009). *P. destructans* is invasive from Europe, and is thought to have first been introduced into N. America in New York State in 2006, as a consequence of human movements between continents. Bats with WNS infections have characteristic white mycelial growth on their muzzle or wing tissue eventually leading to the formation of ulcers and the erosion of epithelial tissues (Meteyer et al. 2009). Torpid bats with WNS experience electrolyte imbalance, and evaporative water loss (Willis et al. 2011). Many exhibit an increased frequency of arousal from hibernation and have shortened bouts of torpor in general (Lorch et al. 2011). These additional arousal events are very energetically taxing (Thomas et al. 1990) and cause further depletion of fat reserves (Reeder et al. 2012). Surviving hibernation becomes more challenging for bats infected with *P. destructans*, as early and frequent arousals can lead to starvation and ultimately result in mortality (Cryan et al. 2010). Bats that do survive hibernation have been recorded with aberrant behaviours such as excessive grooming, day-flying, or aggregating near cave entrances.

The asexual isolates of *P. destructans* have expanded from a single point of introduction in N. America (Ren et al. 2012; Rajkumar et al. 2011), with relatively little genetic differentiation accumulated among clones since 2006 (Khankhet et al. 2014; Trivedi et al. 2017; Drees et al. 2017a). The point of introduction for *P. destructans* in N. America is thought to have been initially due to anthropogenic activity. Clothing or caving gear contaminated with arthroconidia are likely to have enabled the transfer of *P. destructans* between continents (Turner et al. 2011). Considering the bio-security risk, and that fungal spores are easily transferred across long distances, strict decontamination protocols for researchers studying WNS are implemented at caves within N. American (US Fish and Wildlife Service 2016).

P. destructans has caused well over 7 million deaths (Froschauer and Coleman 2012; Blehert et al. 2009) in 15 different species of hibernating bats within 35 US states and 7 Canadian provinces. Some regions of the northeastern United States impacted by these infections have recorded population collapse in certain bat species (Frick et al. 2010). Transmission of WNS is likely spread through bat movements. In general, bats live as fission-fusion societies, where larger groups periodically split into multiple smaller groups that later rejoin, or individuals move freely among a network of multiple social groups. The composition of each group is different depending on the species. Roost switching is widely documented. Populations of hibernating bats undergo swarming behaviour in autumn, where bats congregate in large groups. At this time, bats are likely to sweep up *P. destructans* spores and carry them to the next cave (Turner et al. 2011; Lorch et al. 2011), which can then spread into the environment, contaminating caves that were at once free of *P. destructans* and remain infected for multiple years after the inhabiting bat populations have been eradicated (Lorch et al. 2013).

The rapid spread and high mortality rate associated with WNS can be readily explained within the framework of the Novel Pathogen Hypothesis (Rachowicz et al. 2005).

Consistent with the expectations of this hypothesis, host-pathogen interactions in the ancestral range do not result in mortality. However, both N. American and European *P. destructans* cause mortaility in N. American bats (Puechmaille et al. 2011b; Warnecke et al. 2012). A long-standing evolutionary relationship has likely existed between *P. destructans* and Eurasian bats (Wibbelt et al. 2010; Leopardi et al. 2015). Within the genus *Pseudogymnoascus*, most species are not pathogenic and are commonly isolated within soil/permafrost in Europe. The last known common ancestor of *P. destructans* (*Pseudogymnoascus* sp. WSF3629) diverged approximately 23.5 million years ago (MYA) (Palmer et al. 2018). Based on fossil evidence, the oldest known ancestor of all chiropteran species, *Palaeochiropteryx*, was estimated to have lived 50–40 MYA (Novacek 1985; Springer et al. 2001). More recently, *Myotis* bat species have undergone adaptive speciation 9–6 MYA in Eurasia and more recently in N. America at 6–3.2 MYA (Ruedi and Mayer 2001). Since *P. destructans* divergence predates Eurasian *Myotis* species, it is indicative of the longstanding host/pathogen relationship.

1.3 Fungal Pathogenesis in Mammalian Hosts

Pathogenic species have to be able to survive host conditions in order to be successful. Host-pathogen interactions hang in the balance between mediation of host defences and mechanisms that provide resistance or avoidance of host defenses. For example, the main deterrence of fungal infections in homeothermic animals is ambient body temperature of $\sim 37\,^{\circ}\mathrm{C}$. Although fungi are pathogenic to many species throughout the tree of life, infections of vertebrate species remain extremely rare. Of the estimated 5.1 million species of fungi (Blackwell 2011), only 625 are known to cause disease in vertebrates (de Hoog et al. 2018) and only a fraction of these fungal pathogens are capable of infecting mammalian hosts. In contrast, fungal infections of poikilothermic animals present a major threat to biodiversity. For example, chytrid and snake fungal disease are among the most pervasive infections of reptile/amphibian, currently responsible for certain species

declines (Fisher et al. 2016). This has prompted conservation strategies that exploit such limits of fungal pathogens through artificial manipulation of the ambient temperatures of the host species (Boyles and Willis 2010).

Mammals present a particular challenging environment for most pathogenic fungi, as their ambient body temperatures is a hostile environment that few species can withstand (Casadevall 2005). Mammalian endothermy and homeothermy serve as defenses against many pathogens, but present a particularly strong evolutionary advantage against fungal diseases (Casadevall 2005). Every 1 °C increase from 30 °C to 40 °C excludes 6% of fungal species that are capable of infections in vertebrates (Robert and Casadevall 2009). This is usually a strong barrier to infection, where prolonged exposure to these conditions can be lethal, preventing infections by many species of fungi. Yet a handful of pathogenic fungi thrive under these conditions (Casadevall 2005; Casadevall 2008). Ambient body temperatures in the range of 30 °C to 40 °C already prevents infection by the majority of fungal species (Robert and Casadevall 2009) and further resistance can be bolstered through mammalian immune responses (i.e. fever Elliot et al. 2002).

1.3.1 Mechanisms for Thermotolerance

Environmentally acquired microbes are not usually expected to be thermotolerant to the conditions typical in mammalian hosts. Mechanisms allowing for thermotolerance in fungal pathogens are biochemically expensive to maintain, and are therefore not rapidly acquired. Recent emerging outbreaks in mammals have been attributed to fungal pathogens with environmental thermotolerance, a key virulence factor that is "dual-use" (Casadevall et al. 2003). Theromtolerance is a trait that is interspersed across Ascomycota and Basidiomycota (Robert and Casadevall 2009), suggesting separate origins/losses for this trait. The origins of thermotolerance have been suggested to be a relic of the ancient global climate, which prior to Eocene-Oligocene transition 34 MYA, was much

warmer than in recent geological time (Liu et al. 2009). Many species have lost thermotolerance since then, which can be easily lost through a single mutation (Robert and Casadevall 2009).

Responses to temperature stress involve various cellular pathways for membrane and protein stabilization. Heat shock proteins are primarily involved in these responses, but other responses incorporate the production of cryoprotective molecules. Trehalose is involved in stress response to abiotic stressors (e.g.: high salinity, drought, heat/cold tolerance) in plants and fungi. In yeast, trehalose accumulates in various levels after 12 hours of incubation at 10, 4, or 0 °C. Some of the key energy reserves in fungal arthrocondia, such as trehalose, mannitol, and lipids, are also cryoprotectant materials, useful in cold-temperature tolerance (Steele 1972). In particular trehalose is used as an energy and carbon source during germination (Inoue and Shimoda 1981; Hecker and Sussman 1973). Based on differential expression profiles in the black yeast *Exophiala dermatitidis*, growth in low temperatures is associated with lipid membrane fluidity, trehalose production and cytoskeleton rearrangement gene expression (Blasi et al. 2015).

The pathology of WNS is exclusive to hibernating bats, as the host environment during torpor are permissive infection of *P. destructans*, a psychrotolerant fungus. During hibernation, body temperatures of bats mirror that of the hibernacula. Normal mammalian body temperatures prevent the growth and progression of *P. destructans*. Yet during hibernation, all bodily functions, including immune responses, in hibernating N. American bats are reduced (Bouma et al. 2010; Thomas 1995). This decrease in the body temperature of these mammals to the near-ambient temperatures within the hibernacula are the ideal substrate for a slow growing and psychrophilic fungal pathogen such as *P. destructans*. Interestingly, growth of *P. destructans* at temperatures above 12 °C alters the morphology of hyphae, conidial structures and arthrospores, shifting to

primarily producing arthroconidia (Verant et al. 2012). As a clear barrier to *P. destructans* growth, thermal stress from the host or the surrounding environment needs to be overcome in order for this pathogen to persist with N. American bats (Forsythe et al. 2018). Adaptation to the ambient temperatures of bats not in torpor could enable to the spread of *P. destructans* within host communities during the summer months (Hoyt et al. 2018).

1.3.2 Fungal Dermatophytes

In mammals, the epithelial tissues of the epidermis are the first line of defense, preventing the invasion of the underlying tissues by microbial pathogens. Characterized by their ability to use keratin as their sole energy source, dermatophytes are among the most common fungal pathogens in mammals. Outbreaks of *Microsporum canis* in cats, *Trichophyton verrucosum* in cattle, and *T. benhamiae* in guinea pigs are a few of the most recent emerging zoontic infections in mammals (Hubka et al. 2018). In response to invasive infections, mammalian immune systems mount a targeted response to fungal dermatophytes. This usually involves the secretion of antimicrobial peptides and secretory antibodies, triggered by the recognition of fungal cell wall (Romani 2004; Steele and Wormley 2012). Usually, a local inflammatory is sufficient to deter infection from most of the commensal fungal species. However, in hibernating bats there is no local inflammatory response regardless of the severity of lesions caused by infection (Bouma et al. 2010). During infections of bat epithelium, hyphae invade hair follicles and sebaceous/apocrine glands. *P. destructans* is unlike other dermatophytes in that the mycelia invade connective tissues underlying the epidermis (Meteyer et al. 2009). Eventually, the erosions of these tissues can contain dense pockets of fungal hyphae and leave to sever ulcerations that can span the thickness of the wing membrane.

Genme sequencing of dermatophytes have revealed a high number of secondary metabolite gene clusters, which are upregulated during infection infection (Burmester et al.

2011). In particular proteases are produced to degrade host proteins including collagen, elastin, fibrinogen, immunoglobulin, leading to host tissue damage. The metabolic capabilities have been demonstrated with *in vitro* assays on various substrates (Raudabaugh and Miller 2013), which demonstrated in *P. destructans* is capable of proteinase secretion (Chaturvedi et al. 2010). Most notable of these proteases is Destructin-1, a serine protease capable of degrading collagen protein (O'Donoghue et al. 2015).

Interestingly, substantial differences between *P. destructans* and the closest sister species may reflect the changes that have occurred since the transition from saprophyte to zoonotic pathogen. Specifically, *P. destructans* has a reduced diversity of carbon metabolism enzymes, as the flexibility in carbon metabolism is likely not required during infection of host tissues (Palmer et al. 2018). Such changes are common in emerging fungal pathogens, as flexibility in metabolic capabilities are useful in a novel environment. The amount of divergence between the existing species in host and pathogen populations can be used to infer the extent of the host/pathogen relationship.

1.4 Characteristics of Successful Fungal Invasions

The majority of biological invasions are caused by microorganisms, and those caused by fungal pathogens tend to outnumber invasive plants and animal species (Gladieux et al. 2015). Yet, research on the disruptions caused by invasive fungal species have only recently come into focus (Desprez-Loustau et al. 2007). The success of an invasive species is dependent on its ability to overcome a series of obstacles during introduction, establishment, and spread into the novel environment (Kolar and Lodge 2001). Fungal pathogens that cause outbreaks generally have common traits that enable them to overcome these obstacles and explain why they are commonly so devastating to the species they infect.

Infections caused by some groups of fungal pathogens occur in the form of outbreaks,

referred to as epizootics in animals. The potential for fungal infections to spread through a population is determined by the basic reproductive rate, where an outbreak will only occur if the basic reproductive number, R_0, is greater than 1. R_0 will fall below 1 when the population build up immunity to infection, or the rate of transmission slows due to host availability or environmental pressures. In the case of an outbreak of transmissible fungal infections, R_0 is needed to determine the amount of intervention needed from control strategies in order to control the onwards spread of infection. However, in the scenario of a recently introduced pathogen in a naïve host population, host resistance factors may not be sufficient or may be missing entirely.

Typically, a trade-off exists between virulence and transmission of a pathogen. Within free-living fungal pathogens, this constraint is much more achievable since many species are not dependent on the host for replication. Alongside the benefits of the sapronotic lifestyle, pathogens with long-lived environmental stages, and those that infect generalist hosts, can result in highly lethal outbreaks where local extirpations or even complete extinction of the host population can occur (Fisher et al. 2012). Such processes have resulted in fungal pathogens having a reputation of being among the few organisms that are capable of causing extinctions (Olsen et al. 2011). The most recent example of this is the widespread extinction of at least 200 species of amphibians by *Batrachochytrium dendrobatidis* (Martel et al. 2018).

1.4.1 Population Biology of Fungal Pathogens

Within a population, adaptation occurs through an increased frequency of locally advantageous alleles and prevention of the immigration of locally deleterious ancestral alleles, in relation to the local conditions resulting in increased fitness in that environment (Giraud et al. 2010). A diversity of abiotic and biotic factors can drive adaptation in a fungal species. Climatic conditions have the most obvious impact on species survival or

proliferation, which often impact the distribution of a pathogen species in the environment (Vacher et al. 2008). Such examples of rapid adaptation in fungal pathogens occur during the spread of an epidemic into a novel environment with drastically different or unstable climate. Certain crop pathogens can adapt to different climates and seasons (Frenkel et al. 2010; Mboup et al. 2012; Enjalbert et al. 2005). In some cases the resulting adaptations are in the form of a tradeoff, gaining resistance to one abiotic factor while becoming susceptible to another. In response to non-optimal growing conditions, fungal pathogens may adapt through improving overwintering abilities by sporulating later in the growing season (Feau et al. 2012; Giraud et al. 1997). For many obligate or highly specialized fungal pathogens, adaptations occur in relation to the host environment. Pathogenic capabilities of such species are developed through adaptation of the host species to environmental conditions. The anther smut fungus, *Microbotryum violaceum*, has evolved through frequent host shifts, resulting in a number of strains that represent multiple independent evolutionary lineages, becoming highly specialized on a single or a few host species (Le Gac et al. 2007; Refrégier et al. 2008). However, sudden switching of host species is not uncharacteristic for some fungal pathogens, and can be a major factor in speciation (de Vienne et al. 2013).

Unlike many other larger organisms, fungi can have large distributions, and almost all are capable of producing a large number of spores, which have a crucial role in the life cycles of numerous species. The dispersion and resilience of spores enables species to reach novel environments and survive hostile conditions, as well as allowing for resilience to the host environment. For many fungal species, spores can be easily transmitted across long ranges to initiate growth in new environments. While promoting long-range dispersal, spores also increase the resilience of many species, allowing tolerance of stressful conditions, such as: desiccation, high temperatures, oxidative stress or UV radiation (Botts et al. 2009). When conditions change, spores enable an escape from environmental stressors (Brown and Hovmøller 2002). For example, only sexual spores are produced

in *Saccharomyces cerevisiae*, and their growth is stimulated by nitrogen-limitation and poor carbon sources (Freese et al. 1982). Dispersal through fungal spores provides an escape from geographical constraints that can limit the colonization success of an invasive fungal pathogen (Philibert et al. 2011).

It is of general concern whether a pathogen introduced to a novel environment has adapted the conditions of the invasive host/range or whether the successful invaders were already well suited for establishment prior to introduction (Facon et al. 2006). The point of origin for an invasive population coincides with the genetic diversity in the population due to the effects of a founder effect or population bottleneck (Gladieux et al. 2008; Munkacsi et al. 2008). For invasive pathogens that arise from the introduction of a single genetic lineage, we can observe these effects by comparing between the introduced and native populations of these pathogens (Raboin et al. 2007; Hovmøller et al. 2008). The process of introduction into the novel environment can be considered as having a bottleneck effect, especially if conditions differ from home and introduced ranges. After introduction, some pathogenic species have shown the opposite, with higher rates of diversity outside the center of origin for their current host. The occurrence of local adaptation despite low genetic diversity in the establishing population is known as the "genetic paradox of invasions". This is commonly though to be responsible for the recent occurrence of range expansion or host shifts in a pathogen population (Zaffarano et al. 2009; Ali et al. 2014). The expansion of a pathogen into novel host population(s) provides a means for rapid increase of the colonizing lineage and an escape from pressures/competition in the ancestral population. The range expansion of a pathogen into a novel host population can result in specialization (Gladieux et al. 2008; Gladieux et al. 2010) or increased aggressiveness and the acquisition of new virulence traits (Le Van et al. 2012). The colonization of a new host species can occur with evolutionary changes that permit infection of the naïve host populations. (Giraud et al. 2010; de Vienne et al. 2013).

Mating in fungi can involve multiple mating types, but "sex" is not determined by sex chromosomes, as in animals. Instead, mating types are determined by a single genetic locus. The mating-type locus consists of idiomorphs (Heitman et al. 2013) and mating events most commonly occur with the proper pairing of cells of opposite mating types. Invasive fungal species with the capacity for multiple modes of reproduction have a higher probability of successful establishment in a novel environment compared to strictly sexual or asexual population (Bazin et al. 2013). Fungi relying solely on asexual reproduction may benefit from rapidly increasing their population size, yet they lack the genetic stability provided by sexual reproduction. As described by the genetic paradox of invasions describes, pathogens with low diversity in their founder populations must adapt despite their initial low genetic diversity. In theory, a mixed mating system has the highest probability of fostering a successful invasion (Bazin et al. 2013). For example, cinnamon tree blight, caused by *Phytophthora cinnamomi*, has been able to establish in novel environments with limited occurrence of sexual reproduction and a limited genetic diversity of the migrants (Hardham 2005). In some cases, a lower capacity for sexual reproduction has evolved in the invasive population (Ali et al. 2010), and a complete loss of sexual reproduction events can be the result of the absence of compatible mating types (Dobrowolski et al. 2003), hybridization events (Lin et al. 2007), or of the result of a complex life cycle dependent on the host (Mboup et al. 2009). There are some examples where considerable variation can occur within a single clonal lineage without sex (Dilmaghani et al. 2012), where variation may arise through the occurrence of mitotic recombination events (Gusa and Jinks-Robertson 2019).

In *P. destructans* the asexual state is represented by arthroconidia, a thallic conidium that is produced via budding from the conidiophore and released into the environment. *P. destructans* produces other asexual spores called aleurioconidia, which bud directly off of the hyphae, although their function or contribution to the spread of infections

is currently not known. With each *P. destructans* individual only carrying one ideomorph, heterothalic mating occurs. Although the sexual has not yet been described in *P. destructans*, the sexual structure are likely similar to other closely related *Pseudogynoascus* species, like *P. roseus*. In *P. roseus*, the sexual state consists of the formation of an asci containing 8 ascospores, with the haploid spores produced following karyogamy and meiosis.

1.5 Patterns of Adaptation and Genome Evolution in Fungi

1.5.1 Genomic factors contributing to adaptation

More than 6 000 fungal species have some been sequenced to some degree, representing species with diverse lifestyles and distinct evolutionary history that play important roles in both ecosystems and human activity. Genomic studies of fungi have significantly influenced not only our understanding of their evolutionary history but have also revealed novel mechanisms for survival, reproduction, and adaptation in their diverse ecological niches (Gladieux et al. 2014). With current methods in genomic sequencing (i.e. high throughput sequencing technologies), it is possible to identify areas of the genome that are associated with changes in life history traits or ecological strategies of pathogens. The ecological impact of genomic diversification is most commonly investigated through comparative studies measuring mutations causing amino acid substitutions, the occurrence of genomic rearrangements, and alteration of gene copy number.

Amino acid substitutions are quite prevalent in underlying fungal adaptation, and can often be found in the same gene, or even at the same site within separate species (Aguileta et al. 2010; Aguileta et al. 2012). Through studies of closely related *Saccharomyces* species, only a small subset of the total genes are subject to recurrent selection (Li et al. 2009). In the context of adaptation to a novel environment, regions of the genome that are hot-spots for mutation may be the result of a selective sweep, in which

beneficial mutations increase in frequency and become fixed, generally after the population has gone through a bottleneck event. During adaptation, genes with host-specific functions are a constraint to diversification in the novel environment. As such, in the fungal pathogen *Microbotryum*, genes related to transporter activity and cell-cell or cell-environment communication pathways are frequently found to be under positive selection during adaptation.

Gene families are often the target of expansion, duplication, or loss in fungal pathogens during adaptation. The reduction or complete loss of gene families of secreted proteins, nutrient transporters, and enzymes have often been found to reflect ecological shifts (Casadevall 2008; Xu et al. 2007; Joneson et al. 2011; Martinez et al. 2004; Duplessis et al. 2011; Ohm et al. 2012). The expansion or contraction of certain gene families can also be facilitated by the activity of mobile genetic elements. Transposable elements acquire cellular genes or gene fragments between their terminal inverted repeats and replicate them throughout the genome. Within the genome of a fungal pathogen, transposable elements can act to increase the copy number and diversity of genes coding for effector proteins/molecules, which can increase or decrease enzyme activity, gene expression, or cell signaling. In the pathogen *Pyrenophora trici-repentis*, diversification of such genes is manifested through copy number variation (CNV)s, mediated by transposable elements (Manning et al. 2013). Whole-genome duplication events can contribute to adaptation as duplicate genes diversify and become specialized. In most cases of diverging paralogs, neofunctionalization commonly occurs when one copy evolves slowly, retaining ancestral function, whereas the other copy evolves much more rapidly, acquiring novel functionality. For example, the manipulation of *Saccharomyces cerevisiae* metabolism to survive anoxic conditions was facilitated by a large duplication event in which genes became specialized (Kellis et al. 2004).

The specific regulation of genes may also play an important role in the adaptation

of fungal pathogens (Wohlbach et al. 2009; Spanu and Kämper 2010). Genes encoding proteins involved in growth and general metabolism have conserved expression patterns. However, genes involved in responses to external and internal signals, or that code for nonessential functions, tend to display divergent patterns of expression between species (Tirosh et al. 2006; Thompson and Regev 2009). Amplification of gene copies can be involved with tolerance to host conditions, as in the adaptation of *Cryptococcus* to high concentrations of arsenite during pathogenesis (Chow et al. 2012). As an abundant environmental toxin (Zhu et al. 2014), arsenite accumulates to high abundance in vertebrate hosts (Sattar et al. 2016). Likely these concentrations are higher than environmental levels experienced by microbial pathogens. Furthermore, pathogens that switch from an obligate biotrophic to symbiotic lifestyle commonly lose genes involved with functions that are made redundant by the available resources from the host (Spanu et al. 2010; Duplessis et al. 2011; McDowell 2011). For instance, powdery mildew fungus, a common pathogen of many plants, has lost genes involved in primary and secondary metabolic functions reflected by the redundancy of these genes in the host environment (Spanu 2012).

1.6 Thesis Outline

There have been qualitative descriptions of significant phenotypic diversification among isolates of *P. destructans* during the clonal expansion in eastern N. America. Within these cultures we wanted to test if changes in phenotype have been accumulated along a geographic gradient and if these phenotypic variations could be indicative of local adaptation to environmental conditions. To test this hypothesis, in Chapter 2 I analyse geographic patterns of phenotypic variation and temperature tolerance during the invasion of *P. destructans* into eastern N. America. The research in this chapter tests one of the main assumptions made regarding the transmission of WNS: conditions during the summer in N. America deactivate *P. destructans* cells from causing recurrent infections

when bats return to hibernacula in the fall.

The population structure of a host population is often reflected in that of the pathogen population, provided the absence of additional transmission events. The bat species in N. American experience a high variation in climate across the landscape, which has likely influenced the rates of spread/transmission for WNS. The purpose of the analyses in Chapter 3 is to understand how landscape features influence the rate of gene flow between *P. destructans* populations, and thereby influence the spread of WNS. The landscape features analyzed in Chapter 3 include geographical, environmental, or anthropogenic factors. The relationships of environmental variables with genotype distributions of *P. destructans* strains across the landscape can also help infer the presence/absence of barriers to *P. destructans* spread and inform conservation strategies for N. America bats.

Tracking the spread of an invasive population is made more difficult with predominately asexual reproduction in the introduced population due to the slow rate at which mutations can be accumulated. In Chapter 4, I characterize the abundance, location, and functional association of rapidly evolving genomic motifs (CNVs) and measure signatures of selection within a collection of *P. destructans* genomes from N. America, Europe, and Asia. The dynamics of CNVs in a clonal population can be complex, but useful in monitoring the spread and diversification of clonal lineages in nature. Furthermore, beneficial mutations that provide adaptive advantage in the invasive population would indicate the occurrence of specialization to local host or environmental conditions. Such patterns of genomic adaptation in *P. destructans* could contribute to the continued rapid spread of WNS and extirpation of N. American bats.

Chapter 2

Phenotypic Divergence along Geographic Gradients Reveals Potential for Rapid Adaptation of the White-Nose Syndrome Pathogen, *Pseudogymnoascus destructans*, in North America

2.1 Preface

This works builds directly off of previous work in our lab. Initially, there were only small scale investigations into the patterns genetic diversification of *Pseudogymnoascus destructans* (*P. destructans*) in North America (N. America). Work published by a previous Masters student, Jordan Khankhet (Khankhet et al. 2014), expanded on what was known about phenotypic and genotypic diversity within this clonal pathogen in N.

America. Here, I expand on Khankhet et al. 2014 by demonstrating the geographical patterns in phenotypic traits. In addition, at specific geographical points of the White-Nose Syndrome (WNS) distribution, there are different responses to temperature stress which may be of adaptive significance in WNS. In order to demonstrate this concretely, this work needs to be followed up with *in vitro* experiments comparing the fitness of invasive and native *P. destructans* conidia. This chapter has been published as Forsythe et al. 2018, and has been cited multiple times since. Some of the main conclusions of this publication have been independantly tested in Campbell et al. 2020.

2.2 Abstract

WNS is an ongoing epizootic affecting multiple species of N. America bats, caused by epidermal infections of the psychrophilic filamentous fungus *P. destructans*. Since its introduction from Europe, WNS has spread rapidly across eastern N. America and resulted in high mortality rates in bats. At present, the mechanisms behind its spread and the extent of its adaptation to different geographic and ecological niches remain unknown. The objective of this study was to examine the geographic patterns of phenotypic variation and the potential evidence for adaptation among strains representing broad geographic locations in eastern N. America. The morphological features of these strains were evaluated on artificial medium, and the viability of asexual arthroconidia of representative strains was investigated after storage at high (23 °C), moderate (14 °C), and low (4 °C) temperatures for different lengths of time. Our analyses identified evidence for a geographic pattern of colony morphology changes among the clonal descendants of the fungus, with trait values correlated with increased distance from the epicenter of WNS. Our genomic comparisons of three representative isolates revealed novel genetic polymorphisms and suggested potential candidate mutations that might be related to some of the phenotypic changes. These results show that even though this pathogen arrived in N. America only recently and reproduces asexually, there has been substantial

evolution and phenotypic diversification during its rapid clonal expansion.

2.3 Importance

The causal agent of WNS in bats is *P. destructans*, a filamentous fungus recently introduced from its native range in Europe. Infections caused by *P. destructans* have progressed across the eastern parts of Canada and the United States over the last 10 years. It is not clear how the disease is spread, as the pathogen is unable to grow above 23 °C and ambient temperature can act as a barrier when hosts disperse. Here, we explore the patterns of phenotypic diversity and the germination of the fungal asexual spores, arthroconidia, from strains across a sizeable area of the epizootic range. Our analyses revealed evidence of adaptation along geographic gradients during its expansion. The results have implications for understanding the diversification of *P. destructans* and the limits of WNS spread in N. America. Given the rapidly expanding distribution of WNS, a detailed understanding of the genetic bases for phenotypic variations in growth, reproduction, and dispersal of *P. destructans* is urgently needed to help control this disease.

2.4 Introduction

White-Nose Syndrome (WNS) is an epidermal infection of North America (N. America) bat species, caused by the psychrophilic fungal pathogen, *Pseudogymnoascus destructans* (*P. destructans*) (formerly *Geomyces destructans*, Gargas et al. 2009). WNS infection is characterized by the presence of white mycelial growth on the muzzle or wing tissues of bats, and eventually leads to the formation of ulcers and the erosion of epithelial tissues (Meteyer et al. 2009). Torpid bats with WNS experience electrolyte imbalance, evaporative water loss (Willis et al. 2011), and tend to rouse more frequently from hibernation than non-infected bats (Lorch et al. 2011). These additional arousal events

are very energetically taxing (Thomas et al. 1990) and cause further depletion of fat reserves, starvation, and death (Reeder et al. 2012; Cryan et al. 2010). Indeed, since its discovery in 2006 (Blehert et al. 2009), *P. destructans* has caused an estimated 5.7 – 6.7 million cases of mortality (Froschauer and Coleman 2012) in 31 US States and 5 Canadian Provinces and resulted in population collapses within some regions of the northeastern United States and Canada (Frick et al. 2010). In contrast, the ancestral *P. destructans* populations from Europe do not cause obvious diseases in European bats (Flory et al. 2012; Davis 1970). The rapid spread and high mortality rate of N. America bats associated with WNS is consistent with the Novel Pathogen Hypothesis (Reynolds et al. 2015). However, despite significant efforts in monitoring and controlling the spread of the WNS epizootic, the timing, route, and mode of WNS expansion remain largely unknown.

Several factors have been proposed to influence WNS transmission, including the sociality of the host species, population density, and the local climate (Davis 1970; Flory et al. 2012; Langwig et al. 2012). Research has shown that WNS can be transmitted by direct bat-to-bat contacts right before hibernation (Reynolds et al. 2015). Within N. America, the current distribution of *P. destructans* and WNS covers a large latitudinal and longitudinal range and a great variation in climate and other conditions. One of the factors is temperature. N. America bat species hibernate in sites with temperatures that generally range between 3 °C to 15 °C (McNab 1974; Swezey and Garrity 2011). Within the hibernacula, the conditions conducive to *P. destructans* growth, 12.5 °C to 15.8 °C and greater than 70% relative humidity (Reynolds et al. 2015), may mirror those outside of the hibernacula, but perhaps with greater stability than those outside. However, this is only true of caves with limited air circulation (Swezey and Garrity 2011). Generally, the variance of cave temperatures decreases with increasing latitude (Moore and Sullivan 1978). Within individual hibernacula, a temperature gradient may also exist (Swezey and Garrity 2011; Figure. 2.3A). Overall, with decreasing seasonal

temperatures at increasing latitudes (Figure. 2.3B), northern caves and hibernacula are more likely to maintain cooler temperatures for longer periods of time than southern caves and hibernacula. Since *P. destructans* growth is known to be extremely limited at temperatures greater than 20 °C (Langwig et al. 2015), such differences in temperature could impact the direction of adaptation, and influence the transmission and spread of WNS differently between the southern and northern regions. The rapid expansion is especially intriguing because the N. America *P. destructans* population is known to be descended from a single clone through asexual reproduction (Rajkumar et al. 2011). However, whether the different ecological conditions among regions in N. America have impacted the adaptation and phenotypic characteristics of *P. destructans* remains unknown. Analyzing the geographic patterns of phenotypic changes in this pathogen and how phenotypic changes may be influenced by environmental factors will help understand the evolution of this pathogen and protect the bat populations (Flory et al. 2012).

In many filamentous ascomycetes such as *P. destructans*, arthroconidia are the propagules that prolong the survival of the population during environmental stress and facilitate the dispersal of the fungi to other ecological niches. Previous research has shown that *P. destructans* produces abundant asexual spores, arthroconidia (Gargas et al. 2009), which likely play a significant role in the spread of this pathogen among geographic regions. While methods by which WNS transmission could be facilitated have been suggested (Lučan et al. 2016), the mechanisms behind the rapid geographic expansion of WNS in N. America has not been adequately explained. For example, if 90-100% of infections cause mortality, and the increased temperatures that these bats experience after the hibernation period ends could eliminate *P. destructans* (Langwig et al. 2015), then how does this epizootic continue to spread? Also, given the large differences in ecological niche conditions across the latitudinal gradients in eastern N. America, how might a clonal genotype respond to a diversity of ecological niches? In order for *P. destructans* to spread, arthroconidia must be able to withstand temperatures outside the

optimal range for vegetative growth.

Here we hypothesize that during the clonal expansion of *P. destructans* in eastern N. America, there has been significant phenotypic diversification along geographic gradients and that some of the phenotypic variations are associated with or are indicative of local adaptations. To test this hypothesis, we explored the geographic patterns of phenotypic changes among representative isolates from the WNS epizootic in eastern N. America. Our analyses identified evidence for geographic patterns of phenotypic variation and suggest that adaptation to low temperatures has likely occurred during its northern spread to eastern Canada. In addition, mutations potentially associated with such an adaptation were investigated using whole genome sequencing of representative isolates.

2.5 Methods

2.5.1 *P. destructans* Isolates

Our experiments involved a total of 62 isolates from various areas of the WNS epizootic (Figure. 2.1; Supplemental 1). All isolates were obtained by the Natural Resources Department (Canada) or the Fish and Wildlife Services (US), and were sub-cultured from single cell dissections. These purified cultures were preserved in Sabouraud-glycerol tubes at −80 °C. We revived each isolate by spotting cell suspensions onto Sabouraud Dextrose Agar (SDA) and incubating at 14 °C for 28 days. Cell suspensions were created in triplicate for each isolate; each suspension was then inoculated onto the center of each separate plate of SDA for colony morphology observations.

2.5.2 Phenotypic Characterizations

After incubating at 14 °C for 28 days, each strain was assessed for several phenotypic traits, including colony size, pigmentation on the surface of the colony, and pigment diffusion underneath the colony through the agar medium. To assess colony size of each

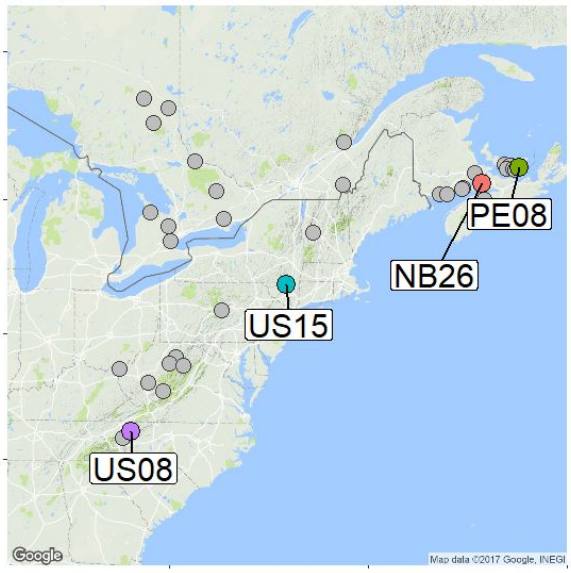

FIGURE 2.1: Geographic locations of the isolates analyzed in this study. While all isolates were examined for their colony phenotype, only the four highlighted ones (US8, US15, NB26, and PE8) were examined for their arthroconidia survival and genetic differences.

P. destructans isolate, we recorded digital images of all 62 isolates and these images were subsequently analysed using the spot densitometry function in FluroChem 8900 (Alpha Innotech – San Leandro, CA). Colony size was recorded as an estimate of the total amount of visible culture on the agar plate, from which the total area was calculated based on the shape of each colony. Similarly, pigmentation on both the colony surface and its diffusion in agar was approximated using the spot densitometry function using the tools available with FluroChem 8900, following the protocols described by Vogan et al. 2016.

2.5.3 Arthroconidia Survival

Here we examined the arthroconidia spore survival of four (US15, PE8, NB26, and US8) of the 62 isolates at 4 °C, 14 °C, and 23 °C environments. These four isolates came from different geographic areas and represented different colony phenotypes. Briefly, we first grew these isolates on SDA medium at 14 °C for two months, allowing enough time for

cultures to sporulate to produce arthroconidia. These cells were then collected from the surface of the colonies and adjusted to a density of 5×10^4 arthroconidia per mL. Three separate samples of 20 µl each for each isolate were transferred onto an 8mm diameter disc of sterile Whatman filter paper No.5 (2.5 µm pore size). These paper discs were allowed to dry at 14 °C temperature under sterile conditions, and were subsequently exposed to sub-optimal temperature of either 4 °C or 23 °C. The paper disks containing the arthroconidia were held at these two temperatures for various lengths of time: 0 days, one days, seven days, 14 days, 21 days, and 28 days. After each respective time period, the filter paper disks were re-hydrated with 200 µl of sterile water, with the arthroconidia released into the water and calibrated to a spore density of 2×10^4 arthroconidia per mL. Samples of 100 µl were taken from the suspension created from each paper disk in triplicate; each sample was then spread onto fresh SDA media. These plates containing the final cultures were incubated at 14, the optimal temperature for spore germination and growth, for a minimum of seven days before they were scored for arthroconidia germination. Each plate was imaged and the number of colony forming units was counted using the multipoint function on `ImageJ` (Schneider et al. 2012). In total, the experimental design consisted of 432 data points [4 isolates X 2 temperature levels X 6 exposure times X 3 tubes (per treatment) X 3 plates (per tube)].

2.5.4 Genotyping

To identify the potential genetic changes associated with phenotypic differences (including arthroconidia viability), three of the four isolates (NB26, US15, and PE8) were chosen initialy for whole-genome sequencing. Cells were harvested from SDA plates of one-month old cultures growing at 14 °C incubator. DNA was extracted using a standard cetyl-trimethylammonium bromide (CTAB) and phenol-chloroform protocol for filamentous fungal cultures (Katz and Cheetham 2009). Sequencing was conducted with a paired-end library on an Illumina MiSeq platform. A de novo assembly of the isolate

US15 (NHWC 20631-21) was constructed using an open source pipeline, specifically designed for use with MiSeq data and microbial genomes (Coil et al. 2015). Raw reads from all isolates were aligned to our de novo build (Supplemental 1), which had a total size of 30.9Mb, consisting of 8145 scaffolds with an N50 of 7747bp, at approximately 50X coverage. Variant calling was conducted on concatenated BAM files using `Freebayes` V1.1.0 (Garrison and Marth 2012). Variants that lacked coverage and quality scores were excluded, and were filtered based on quality and depth (QUAL & DP $>$ 20) using `bcftools` V1.3 (Li and Durbin 2010). With this final set, we performed a sequence homology search of fungal protein database, mapping of Gene Ontology (GO) terms, and functional annotation using the tools available on the `Blast2GO` platform (Conesa and Götz 2008). We then conducted an enrichment analysis using Fisher's Exact test to identify statistically significant enrichment within genes that contain variants. We investigated 30 loci that contained putative mutations based on genome sequence comparisons. Through locus-specific PCR and sequencing, we identified seven of the thirty loci were false positives (a rate of 30%) while 23 mutations were confirmed among the three isolates. In addition, the same sites were also investigated in the isolate US8, as its genome was not sequenced in the original Illumina MiSeq run. In addition to our three whole genome sequences, the genomic data from 60 *P. destructans* isolates were obtained from NCBI and were examined for the variants that we found in our MiSeq data described above. Genomic reads obtained from NCBI were aligned to whole scaffolds containing variant sequences from the US15 reference genome, using the same alignment and variant calling protocol described above. Variant site was considered robust if the quality and depth scores exceeded 20.

2.5.5 Statistical Analyses

All statistical tests on phenotypic data were carried out in `R` (V3.3.2, (R Core Team 2015). In order to evaluate the patterns of phenotypic variation across geographical

regions in the WNS epizootic, we used linear models for each trait. Relative geographical distances (in km) to the closest isolate from the epicenter of WNS outbreak (in William's Hotel Mine, NY, near Albany) were converted from geographical coordinates using the Haversine method (available in the `R` package `geosphere`, (Hijmans et al. 2012). When measuring trait variability, results from each trait were binned separately for every 50 km of relative distance in each cardinal direction. Relative to the early isolate, US15, geographic distance to the north and east are considered to be positive change along the x-axis, whereas distance to the south and west are considered to be negative relative change. Variation among strains within each geographic distance class was calculated using these bins, and a separate linear model was conducted for each trait and geographic direction.

To compare phenotypic patterns among multiple traits, we used a mixed-effects linear model to approach to perform multivariate analysis of variance. Results from all three phenotypic measures (colony area, pigment, and pigment diffusion) were first scaled prior to construction of the model (Supplemental 1). Using the `lme4 R` package (Bates et al. 2015), a mixed-effects linear model was used to measure the variance/co-variance of multiple traits among individuals, using the identity of the isolates set as a random effect.

The proportions of arthroconidia that germinated after storing at various temperatures for different lengths of times were analyzed using linear models for each temperature group. We log-transformed the raw data points to normalize our dataset, applied an offset value to adjust for data points that were zeros, and excluded outliers that exceeded three standard deviations of the mean for each isolate/temperature/day grouping. We then computed an analysis of variance table for each linear model fit and extracted significant groups for each factor via multiple-comparison Tukey tests using default settings (`R` package `agricolae`, (De Mendiburu 2014).

Enrichment analysis determines the probability that the GO Terms within a given subset of genes, compared to a background set of genes, were assigned by chance. Using the built-in functions in Blast2GO, we compared the set of genes containing variants (Table 2.2) to all other genes that were assigned GO Terms. The results from Fisher's Exact Test were corrected for False Discovery Rate (FDR), with a significance cut-off of < 0.05.

2.6 Results

We surveyed the colony morphology of 62 *P. destructans* isolates, including 47 Canadian isolates from four Provinces and 15 isolates from six US States (Figure. 2.1). The total area represented by these isolates covers 2×10^6 km^2 (approximately 1/5 of the area of the US). This collection of clonal strains has been preserved in $-80\,^{\circ}$C since isolation from their natural environment and the isolations spanned five years, from 2008 to 2013. Based on multilocus sequence typing and PCR-fingerprinting (Khankhet et al. 2014), all these isolates were assumed to have descended clonally from a single genotype in N. America, as represented by the early isolate, US15.

2.6.1 Geographical pattern of phenotypic differences

The strains showed variation in all three colony morphology traits: colony size, colony surface pigmentation, and the extent of pigment diffusion through agar. To analyze the geographic patterns of phenotypic variations, we first considered the variation of each trait as a function of the relative distance from the location of the earliest *P. destructans* sample, William's Hotel Mine in New York State (Figure. 2.2; Figure. 2.4). We then compared variance/co-variance of the collection of phenotypic traits using a multivariate linear mixed model (Figure. 2.5). Overall, colony phenotype divergences (colony size, pigment production, and pigment diffusion) were correlated with increased geographic distance from the epicenter. However, we also observed heterogeneity among isolates

from the same geographical regions, especially within eastern Canadian Provinces. Below we describe results for each of the traits.

P. destructans colony size

Mycelial growth can provide insights into the efficiency of substrate utilization and reproduction under specific environmental conditions . Overall, we found a positive correlation between the variability in measurements of colony size on petri plates and geographic distance to epicenter (Figure. 2.4A). Furthermore, the positive correlation was statistically significant along both the South/North axis (F = 2.8, r = 0.2, p = 0.008; Figure. 2.2A) and the West/East axis (F = 3, r = 0.19, p = 0.01; Figure. 2.2B). Isolates from eastern Canada, particularly cultures from New Brunswick generally recorded larger colony sizes at 14 °C than those from the US (Figure. 2.2A). Though the change in colony size showed a significant correlation with geographic distance from the epicenter of the outbreak, the amount of variation among all strains at each distance bin (of every 50km) were overall very similar (Figure. 2.4A). However, as isolates spread further in the western direction, there was an increased variation among the strains in their mycelial growth (F = 0.4776, r = -0.6, p = 0.02; Figure. 2.4B).

Surface pigmentation

Pigmentation is considered a virulence factor in many pathogenic fungi and contributes to resistance towards multiple environmental stressors (Jacobson 2000). In this study, the majority of the 62 isolates displayed dense pigmentation on the tested medium and incubation condition. However, significant variations in pigmentation were observed among strains. A small proportion of the isolates in this survey lacked surface pigmentation. Over a geographical gradient, the amount of colony surface pigmentation showed moderate but statistically significant correlations with increasing northern/southern (F = 2.5, r = 0.2, p=0.007; Figure. 2.2C) and eastern/western distances (F = 3.5, r = 0.25,

p = 0.001; Figure. 2.2D) from the epicenter. Furthermore, we found a positive correlation between the variance in surface pigmentation and the distance from the epicenter as the pathogen spread northward (F = 6.7, r = 0.6, p = 0.02; Figure. 2.4C) and eastward (F = 0.05835, r = 0.78, p = 0.04; Figure. 2.4D). However, there was no increase in the variance of surface pigmentation in the pathogen's spread either westwards (F = 7.8, r = 0.1, p = 0.7; Figure. 2.4D), or southwards (F = 0.06, r = 0, p = 0.8; Figure. 2.4C).

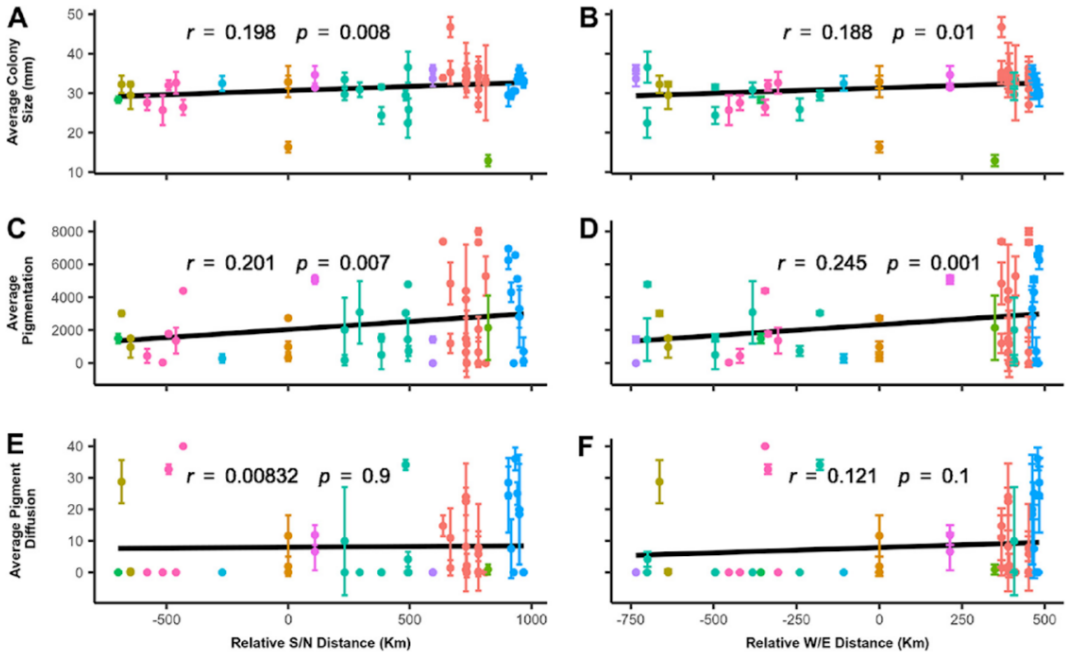

FIGURE 2.2: Measurements of *P. destructans* colony phenotypic traits at 14 °C after 28 days of growth. A: Fungal colony area on agar plates over West/East (S/N) relative distance. B: Fungal colony area on agar plates over west/east (W/E) relative distance. C: Fungal colony surface pigmentation along the S/N relative distance. D: Fungal colony surface pigmentation over W/E relative distance. E: Fungal colony pigment diffusion over S/N relative distance. F: Fungal colony pigment diffusion over E/W relative distance.

Pigment diffusion through agar

Whereas the secretion of pigments within hyphae of *P. destructans* likely confers some form of resistance to exogenous stresses, the deposition of pigments into surrounding medium may contribute to their competitiveness within the substrate. Though variation

was observed among strains in deposition of pigments into surrounding solid medium, in contrast to that observed for colony surface pigmentation, there was no correlation between the amount of pigment diffusion through the agar medium and the relative geographic distances from the epicenter of the outbreak, either in total geographic distance or in longitudinal/latitudinal distances ($F = 0.25$, $r < 0.1$, $p > 0.05$; Figure. 2.2E & 2F). Interestingly, though statistically not significant, as WNS spread, there were increasing variances among strains in pigment diffusion in all directions, with the eastward showing the strongest correlation ($F = 2.5$, $r = 0.422$, $p = 0.3$; Figure. 2.4F). This result is consistent with continued divergence among strains.

Relationships among the three colony phenotypes

A summary of the results from the multivariate linear mixed model is presented in a correlogram, shown in Figure. 2.5. Our analyses showed that colony surface pigmentation was positively correlated with pigment diffusion in agar ($r = 0.5$, $p < 0.001$). Similarly, colony size and pigment diffusion were positively correlated. However, their correlation was weak ($r = 0.09$, $p = 0.04$). Interestingly, though the correlation coefficient was larger than that between colony size and pigment diffusion, that between colony size and surface pigmentation was statistically insignificant ($r = 0.15$, $p = 0.23$).

2.6.2 Arthroconidia Survival

From the 62 isolates we selected four representatives, based on their geographical origin and divergent colony phenotypes, to further examine the effect of storage at various temperatures on arthroconidia viability. For each isolate, we created arthroconidia suspensions in sterile water, air-dried them, and exposed them to 4 °C, 14 °Cand 23 °Cfor various lengths of time before they were rehydrated and germinated on SDA plates. A reference arthroconidia germination rate was obtained for each isolate using rehydrated asexual spores immediately after they were dehydrated instead of being stored at their

respective temperature. The reference germination rates varied from 21.1% to 38.2% among the four isolates. In general, storage of arthroconidia at all three temperatures led to steadily decreased germination rates (Table 2.1). Among the three temperatures, arthroconidia stored at 4 °C had the highest germination rate for the greatest length of time. In general, the two isolates (NB26 and PE8) from further north fared better than the two from the south (US15 and US8) after long-term exposure under 4 °Cand 14 °Ctemperatures. Lastly, exposure to 23 °Cresulted in no germination after 28 days of storage. Interestingly, arthroconidia from the early isolate in the WNS epizootic, US15, had the highest germination rate after stored at 23 °C for 21 days. The detailed germination rates for all four isolates at the five specific time points after storage at each of the three temperatures are presented in Table 2.1. Also shown in Table 2.1 are the F-statistic test values of the comparisons between pairs of strains in their arthroconidia germination rates at each of the 18 treatments (3 temperatures x 6 time points of storage).

Table 2.1: Viability of arthroconidia of four strains of *P. destructans* stored at three different temperatures for various lengths of time. Arthroconidia were first extracted from colonies then stored on an inert substrate (filter paper), before being rehydrated and plated on fresh media after the pre-determined storage times. A linear model for each temperature group was run on colony forming units, adjusted for zero-inflation. Statistical differences between groups were determined from an analysis of variance on the fit of each linear model and post-hoc Tukey Honest Significant Difference tests.

Day	0			1			7			14			21			28		
							4°C											
NB26	42.8 ± 37.5		a	59.3 ± 25.1		a	35.9 ± 18.2		ab	14.4 ± 2.6		ab	31.8 ±17.2		a	9.4 ± 2.5		b
PE8	33.2 ± 8.5	F=1.1	a	37.6 ± 14.3	F=3.7	a	49.8 ± 26.1	F=2.54	a	15.3 ± 2.7	F=3.92	a	46.7 ± 7.4	F=5.53	a	13.8 ± 1.9	F=30.39	a
US15	36.9 ± 3.7	p=0.36	a	52.3 ± 13.2	p=0.02	a	27.9 ± 9.2	p=0.074	b	10.3 ± 2.2	p=0.017	b	15.1 ± 10.9	p=0.004	b	2.7 ± 1.5	p<0.001	c
US8	20.4 ± 6.2		a	34.6 ± 10.4		a	34 ± 8.1		ab	11.9 ± 5.6		ab	34.6 ± 12		a	9 ± 3.9		b
							14°C											
NB26	13.7 ± 3.2		b	9.7± 3.5		a	10.3 ± 3.1		a	4.8 ± 4.1		bc	6.9 ± 1.8		a	2.4 ± 1.2		b
PE8	7 ± 2	F=6.7	c	18.2 ± 10.6	F=2.84	a	4.5 ± 2.6	F=27.6	b	8 ± 1.9	F=11.9	a	2.1 ± 0.4	F=8.1	b	12.2 ± 7.5	F=14.8	a
US15	6.5 ± 1.7	p=0.001	c	9.5 ± 4.2	p=0.054	a	2 ± 0.4	p<0.001	c	2.3 ± 0.8	p<0.001	c	1.7 ± 0.2	p<0.001	b	0.3 ± 0.1	p<0.001	b
US8	22.3 ± 5		a	12.3 ± 3.1		a	2 ± 0.4		c	7.5 ± 1.8		ab	4.2 ± 4.4		ab	9.3 ± 7.2		a
							23°C											
NB26	11.2 ± 7.7		c	13.8 ± 7.9		b	1.1 ± 0.2		b	0.3 ± 0.2		b	0.3 ± 0.2		b	0 ± 0		a
PE8	81.4 ± 13.1	F=23	a	26.9 ± 6.4	F=6.85	b	3.8 ±1.3	F=20	b	0.5 ± 0.3	F=49.7	b	0.2 ± 0	F=5.9	b	0 ± 0	F=10.7	a
US15	25.2 ± 5.7	p<0.001	b	21.7 ± 6.1	p=0.001	ab	10.4 ± 6.8	p<0.001	a	2.7 ± 0.6	p<0.001	a	1 ± 0.8	p=0.003	a	0 ± 0	p<0.001	a
US8	31.6 ± 13.4		b	13.8 ± 8.7		b	1 ± 0.5		b	0.5 ± 0.1		b	0.5 ± 0.4		ab	0 ± 0		a

2.7 Genotyping

Of the four isolates analyzed for both their colony morphology traits and arthroconidia germination, the potential mutations were investigated using whole genome sequencing for three isolates. For the fourth isolate, high-quality whole genome sequence was not obtained. Instead, we used Sanger sequencing to assay the mutations identified in the other three isolates. In total, we identified 23 mutations that differ between strain US15 and the other two sequenced strains NB26 and PE8, including 16 Single Nucleotide Polymorphism (SNP)s and 7 Insertion/Deletions (Indel). Fifteen of the 23 mutations were shared between isolates NB26 and PE8, while 8 mutations were unique to PE8 including those found in genes encoding a putative function COP9 signalosome, retrotransposon, and reverse transcriptase (Table 2.2). A single missense variant was found in all three derived isolates (NB26, PE8, and US8) in a gene putatively identified as a velvet factor, pertaining to a family of fungus-specific transcription factors linked to the regulation of morphological development and production of secondary metabolites in other filamentous fungi (Calvo et al. 2016). Of the 16 SNPs, nine were G:C $\rightarrow$ A:T transitions and six were A:T $\rightarrow$ C:G transversions. Among the seven Indels, six mutations affected protein translation, and one caused a nonsense mutation resulting in the truncation of its protein product.

A subsequent search of GO Terms provided functional annotation information for each of the genes impacted by the identified mutations. Our analysis revealed that several mutations were in genes involved in catalytic enzyme activity, cellular respiration, cell wall components, and other constituents of cell metabolism – among others (Table 2.3). The majority of regions containing variants were significantly enriched with GO Terms.

Aside from comparing the mutations among representative strains in our own collections, we also surveyed the sequenced genomes of other *P. destructans* strains at the specific variant sites by querying the Short Read Archive on NCBI submitted by other

TABLE 2.2: Collection of SNPs from whole-genome sequencing conducted on three isolates (NB26, US15, and PE8). These SNPs were all confirmed using custom primers and Sanger sequencing among the isolates.

Variant	Mutation Type	Putative Annotation	AA Change	REF	ALT	Scaffold	Position
NB26/PEI8/US8	missense	Velvet Factor	p.Asp309Glu	T	G	4871	927
NB26/PEI8	stop gained	nucleic acid binding; zinc ion binding; DNA integration	p.Arg749*	C	T	720	2245
	missense	hydroxyacid-oxoacid transhydrogenase	p.Arg261Leu	G	T	6034	782
		N/A	p.Asp4453Asn	G	A	355	13357
		growth factor receptor cytosine rich domain	p.Ala142Ala	A	G	322	426
		transposase (AF333034.1)	p.Gly957Gly	T	C	1928	2871
	synonymous	related to PDE2-High affinity 3‘,5‘-cyclic-nucleotide phosphodiesterase	p.Thr188Thr	C	T	3235	564
		hypothetical protein (GMDG_02575)	p.Leu1526Leu	T	A	1536	4578
		ribonuclease H	p.Phe1700Phe	T	C	1498	5100
PEI8	missense	DNA binding	p.Thr1813Lys	C	A	104	5438
		retrotransposon nucleocapsid: nucleic acid binding; DNA integration	p.Ala114Ser	G	T	5792	340
		nucleic acid binding	p.Lys131Thr	A	C	7402	392
		reverse transcriptase family	p.Gln57His	A	C	5306	171
		monooxygenase activity	p.Val1752Leu	G	T	979	5254
		probable COP9 signalosome subunit 2	p.Arg1548Lys	G	A	2133	4643
	synonymous	N/A	p.Lys198Lys	G	A	4883	594

studies (Cryan et al. 2010; Palmer et al. 2018; Lorch et al. 2011; US Forest Service 2016; University of New Hampshire. 2017). Of the 60 strains with genome sequences in the archive, 16 of which had missing read(s) in at least one of those variant regions. All 16 genomes did not contain read information for three of the 23 variant sites located in three different scaffolds (#322, #1498, #1928) while the remaining 20 variant sites were found in at least one of the 16 genomes. These 16 genomes were excluded from Table 2.4. The remaining 44 were compared with our SNP variant set as described in Table 2.2. At these 23 variable sites, 12 of the 44 strains were identical to the US15 genome (Table 2.4). We found that only two samples (22884-4W and Pd_692102) contained one variant allele on scaffold 3235 that was shared with NB26 and PE8 (Table 2.2). The sample 22884-4W was isolated from an infected bat in Vermont (Table 2.4). Thus, most of the mutations identified here are novel, not reported in other sequenced genomes.

2.8 Discussion

The WNS epizootic in N. America is thought to have been initiated by the propagation and spread of a single clonal genotype of *P. destructans* (Ren et al. 2012; Rajkumar

TABLE 2.3: Results from enrichment analysis using Fisher's Exact Test. Significantly enriched genes ($p < 0.05$) from regions containing SNPs and the associated GO Terms annotation information. Genomic regions were significantly enriched in terms relevant to various cellular function, including metabolism and respiration pathways.

SNP Scaffold	**GO ID**	**GO Name**	**P-Value**	**FDR**
203, 6125, 720	GO:0015074	DNA integration	1.62E-07	2.02E-06
1316	GO:0042450	arginine biosynthetic process via ornithine	3.56E-03	5.85E-03
322	GO:0070469	respiratory chain	3.56E-03	5.85E-03
322, 592	GO:0016021	integral component of membrane	7.11E-03	1.13E-02
104, 1928	GO:0003677	DNA binding	3.66E-05	2.29E-04
0	GO:0016758	transferase activity, transferring hexosyl groups	3.56E-03	5.85E-03
720	GO:0008270	zinc ion binding	3.56E-03	5.85E-03
322	GO:0009916	alternative oxidase activity	3.56E-03	5.85E-03
41	GO:0008137	NADH dehydrogenase (ubiquinone) activity	3.56E-03	5.85E-03
1316	GO:0004056	argininosuccinate lyase activity	3.56E-03	5.85E-03
322	GO:0016787	hydrolase activity	1.06E-02	1.69E-02

et al. 2011; Leopardi et al. 2015). That genotype was among the many genotypes within its native ecosystem in Europe and the low virulence of these strains towards European bats was likely the result of their long-term co-evolution (Leopardi et al. 2015; Wibbelt et al. 2010). However, the situation differs in N. America where *P. destructans* is exploiting naïve hosts. Since the first detection of WNS in N. America over ten years ago, both phenotypic and genotypic changes have been reported among the N. America strains of this species (Khankhet et al. 2014; Trivedi et al. 2017). However, the broad geographic pattern of phenotypic changes and the potential genetic basis for the phenotypic diversity has not been investigated. Here we tested the hypothesis that the N. America environments have impacted the evolution of certain traits of the WNS pathogen since its introduction. We postulated that environmental pressures might have driven the evolution of phenotypic variation for some of the clonal descendants of the original genotype. Our analyses demonstrated that (i) phenotypic variability in the N. America population of *P. destructans* had a broad geographic pattern, (ii) differences in the responses of *P. destructans* arthroconidia to temperature stress have emerged among isolates, and (iii) several newly accumulated mutations may have contributed to the phenotypic variation among a subset of isolates. Below we discuss the relevance of

our results to previous studies and the implications of the results to the management of WNS and the conservation of bats in N. America.

2.8.1 Phenotypic Patterns in North America

The ability to generate and maintain phenotypic diversity within a population can enhance the survival of the population under environmental stress and improve the persistence of a population within novel environments (Pigliucci 2001). In N. America, the environmental conditions that *P. destructans* inhabits are highly heterogeneous, so far spanning 31 US States and five Canadian Provinces. Such heterogeneity could pose a significant challenge for the spread, reproduction, and survival of the pathogen, especially because the pathogen is psychrophilic and started as a single genotype in N. America. A previous study reported qualitative measures of phenotypic variation among strains of *P. destructans* in N. America (Khankhet et al. 2014). Our goal here was to quantitate phenotypic variations and investigate their geographic patterns in northeastern US and eastern Canada.

Overall, our results demonstrated a positive correlation between fungal colony area on artificial medium and relative geographic distance/coordinates from the epicenter of WNS in N. America. Isolates from more distant northern or eastern regions showed a greater variability and overall larger radial growth rates. In contrast, isolates from the southern expanse of the WNS range tend to have slower growth rates under the same lab condition (Figure. 2.2). Multiple environmental factors, such as changes in temperature, pH, or available nutrients, can trigger adaptive evolution in populations (Ernst 2000). Such a response has been demonstrated within *P. destructans*; when incubation temperature is increased from 12 °C to 15 °C, cultures exhibited faster growth rates (Verant et al. 2012). In addition, the same study demonstrated that growth rate of the establishing strain in New York State was higher than that of *P. destructans* from Europe (Verant et al. 2012). Taken together, these results suggest that the increasing

growth rate in certain geographical directions likely represents a significant adaptive change of this fungus in N. America. Furthermore, such adaptations may have included acclimatization to the array of environmental conditions such as the air temperature in most N. America regions (Figure. 2.3B). Increased growth rate for such strains in vitro may also increase their virulence and invasiveness on bats.

The production of pigments in pathogenic fungi is a common virulence factor, contributing resistance to both host and environmental stresses (Rosas and Casadevall 2001; Casadevall et al. 2003; Jahn et al. 1997). Within the northeastern range of *P. destructans*, the observed trend in colony surface pigment production mirrored that of colony growth rate. In contrast, the diffusion of pigments through agar was not significantly correlated with increased distance from the William's Hotel Mine (Figure. 2.2E & F). Interestingly, both measurements of colony pigmentation (colony surface excretions and the production and diffusion of pigments through substrates) have greater trait variances with increasing northern and eastern distances from early WNS isolates (Figure. 2.4). In addition, these two traits share a strong correlation and significant co-variation ($r = 0.5$, $p < 0.01$; Figure. 2.5). Although pigmentation at the top of colony and pigment diffusion through agar likely differ in function, these results suggest that their production and secretion in *P. destructans* may have been impacted by similar environmental conditions as WNS spreads into northeastern N. America. In this context, selective forces acting on *P. destructans* populations might have come from multiple stressors in the hibernacula environment, including other competing environmental microbes and interactions with bats. In addition, while the conditions for long-term persistence of *P. destructans* within the hibernacula are different from those outside of the hibernacula during the summer months, environmental factors from outside the hibernacula could also act as selective forces, contributing to differences in pigment production and secretion. A recent study showed that interactions with a partitivirus could influence phenotypes in *P. destructans* (Thapa et al. 2009). Indeed, multiple microbial species with antagonistic

activities against *P. destructans* within the cave environment have been isolated (Hamm et al. 2017). Similarly, N. America Myotis species have shown varying immune responses to *P. destructans* infections (Johnson et al. 2015), which may provide additional selective pressure on pigment production and secretion. The benefits of such adaptations to pigment production could influence the survival and reproduction rates of *P. destructans* both within and outside of N. America hibernacula, and potentially increase the probability of successful spread among niches.

The mechanism of WNS spread is among the most poorly understood aspects of the epizootic. The phenotypic variation observed here among strains and traits might be relevant to the patterns of spread and population adaptation over geographical ranges. The patterns of spread and adaptation of *P. destructans* in N. America could be explained by one of two competing hypotheses: (i) the spread of WNS has continued in stepwise fashion from the epicenter via clonal expansion, (ii) the spread of WNS is not stepwise and spread patterns are complex, involving multiple back and forth dispersals among hibernacula (Drees et al. 2017b). If the spread is a stepwise process, we should see increased accumulation of spontaneous mutations along geographic gradients and that different mutations were accumulated among different isolates as the population expanded to different directions. The phenotypic expectation of this stepwise process is that phenotypic trait values should diverge more as the distance of the population from the epicenter increases. While there is some evidence for the increased variance, there was no consistent pattern (Figure. 2.4). Our results suggest that the spread may not follow a strict stepwise or linear fashion over a temporal or geographical gradient. Rather, the spread likely involves multiple back and forth transmissions between hibernacula resulting in mixed phenotypic diversity within certain areas of the WNS epizootic. Recent genetic analyses of strains from N. America suggested evidence for widespread mixings and long-distance dispersals (Drees et al. 2017b; Trivedi et al. 2017), consistent with the second hypothesis and with what we observed here for phenotypic traits.

2.8.2 Sub-Optimal Temperatures and Environmental Stress

WNS has rapidly spread into N. America habitats, reaching the eastern Canadian Provinces and southern States after approximately 7 years, most recently appearing on the Western coast of the United States (Lorch et al. 2011). The dispersal over long distances requires tolerance across various climates and environments. The long-term persistence of this species in the presence of minimal nutrients and water has already been demonstrated (Hoyt et al. 2015b). Due to its psychrophilic nature, exposure to sub-optimal high temperatures likely represent a significant constraint on *P. destructans* spore viability (Johnson et al. 2015). By controlling exposure to sub-optimal temperatures, a threshold for *P. destructans* spore germination could be determined. Overall, we found that a 4 °C environment resulted in a higher germination rate of arthroconidia for a greater length of time than the 14 °C and 23 °C environments. The differential responses to these temperatures among strains from different environments are consistent with their adaptive significance. Specifically, we propose that such divergent responses may be related to coping with different environmental stresses and are associated with an increase in long-term persistence or spread potential of *P. destructans* in N. America, as was suggested by Drees et al. 2017b and Palmer et al. 2018. Here, we discuss the consequences of the differences in arthroconidia temperature tolerance in the context of the dispersal of WNS in N. America.

WNS was first reported in caves in New Brunswick, Nova Scotia, and Prince Edward Island (PE) as early as 2012-2013. The northern areas of the WNS distribution (New Brunswick, Nova Scotia, etc.) experience mean air temperatures of 5.49 °C (± 9.72) during year-round (Figure. 2.4A). Our low temperature treatment emulates a minimum level of temperature stress present in northern habitats for the majority of the winter months (November - March, -3.6 ± 4.7; Figure. 2.4A). After long-term exposure to this 4 °C, both derived isolates germinated significantly better compared to the isolate US15 from around the epicenter in N. America (Table 2.1). This result suggests that isolates

from these areas may have adapted to extend the lifespan of arthroconidia by entering a state of dormancy that can be activated in times of stress (Mysyakina et al. 2016). The activation of dormancy pathways was likely stimulated by the absence of proper nutrients, desiccation, and sub-optimal temperature. Cell dormancy under 4 °C is relevant in the context of the seasonal variation that occurs in many regions in N. America. Low temperatures around 4 °C could occur in early autumn (Figure. 2.4A) and last until early next summer. Being able to enter dormancy and maintain viability could offer a significant advantage to *P. destructans* populations in the long term.

In comparison to the northern reaches of this epizootic, the regions closer to the WNS epicenter (New York State) or the southern range of the distribution of our isolates (North Carolina), have higher average year-round air temperatures of 9.65 °C (± 8.13) and 17.12 °C (± 6.68) respectively (Figure. 2.4A). We induced heat stress in *P. destructans* by subjecting our spore populations to temperatures that exceeded the upper limit for growth (Mysyakina et al. 2016; Langwig et al. 2012; Verant et al. 2012). Compared to *P. destructans*, other species of the genus *Pseudogymnoascus* are found to be capable of growing at temperatures above 20 °C (Samson 1972). Different from the germination rate data for arthroconidia stored at 4 °C, arthroconidia of strain US15 maintained viability for a longer period of time at the 23 °C environment than all three derived isolates. These results suggest that a trade-off may have arisen since WNS has spread into novel environments, with arthroconidia gaining cold-temperature tolerance while losing resistance to heat stress.

We observed that storage time can have a greater impact than expected on the germination potential of arthroconidia. For example, the spore viability of isolates PE8 and US8 dropped significantly after 24 hours of storage at 23 °C. Interestingly, slightly prolonged exposure may result in unexpected increases in *P. destructans* germination. As demonstrated in other psychrophilic fungi, cold exposure can increase spore germination

rates (Juge et al. 2002). Consistent with those observations, the storage at 4 °C for 14 days resulted in significant increases in spore germination over the 7-day period. It should be noted that the activation of arthroconidia after prolonged dormancy likely depend on several factors including water availability, nutrients, temperature, and other biotic and abiotic factors (Wyatt et al. 2013). Taken together, this suggests that the viability of arthroconidia can be extended after storage under such cold temperatures.

Our result indicates that arthroconidia can survive up to three weeks at temperature of 23 °C. This result suggests that the surviving bats with WNS that exit winter hibernacula during the spring/summer months can carry viable arthroconidia with them (Ballmann et al. 2017; Bernard et al. 2017). However, other factors may influence the effectiveness of this dispersal, including solar radiation. In natural environments, solar radiation includes Ultraviolet radiation (UV) can negatively influence arthroconidia survival (Palmer et al. 2018). Furthermore, an estimated 10^6 cells of *P. destructans* are required to cause WNS (Lorch et al. 2011) and a successful dispersal event between hibernacula require not only appropriate temperatures but also other conditions that are conducive for *P. destructans* germination and growth. A realistic model for the spread of WNS should consider these factors.

2.8.3 Genetic Mutations and Adaptation

Adaptations provide some benefits to an organism's reproductive success under the sum of all environmental conditions (Fisher 2004). In their natural habitats, most fungi often experience rapidly changing conditions. Thus, having a robust system to cope with environmental changes could be highly beneficial. This study explored the potential relationships between the recently accumulated genetic variation within the N. America clonal population of *P. destructans* on possible adaptations to local conditions during the spread of WNS. Our analyses identified several putative variants related to the morphological/physiological variations found among the isolates. We specifically considered

regions relevant to regulation of growth, development, metabolism, and membrane integrity in the context of adaptation; areas with relevant enriched GO Terms represent potential targets for studying adaptive diversification in *P. destructans*. Interestingly, mutations within genes relevant to these areas have not been reported in other recently sequenced strains of *P. destructans* (Wyatt et al. 2013; Chibucos et al. 2013; Drees et al. 2016; Trivedi et al. 2017).

Of special note is the mutation in the homolog of velvet protein in *P. destructans*. Two recent studies identified that interactions between velvet proteins, a family of transcriptional regulator proteins, can have a large impact on fungal growth, secondary metabolism, and cell differentiation such as conidia germination/maturation, sporogenesis, and toxigenesis. In addition the velvet proteins are widespread in fungi (Reviewed in Bayram and Braus 2012; Ni and Yu 2007. The velvet proteins regulate development and defense pathways in fungi by modulating the expression of many genes (Ahmed et al. 2013). Compared to the early isolate close to the epicenter, US15, all three derived isolates that we sequenced shared the same missense mutation (Asp $\rightarrow$ Glu) at amino acid position 309 within the velvet protein. We considered this gene of particular interest as genetic changes in transcriptional regulators could influence an array of cell functions and contribute to phenotypic variations observed among the clonal descents of *P. destructans* in N. America. For example, interactions between regulators of genes in the velvet family have shown to impact conidia germination/maturation, stimulating dormancy pathways, trehalose biogenesis, or cell wall production (Park et al. 2012; Bayram et al. 2008; Sarikaya Bayram et al. 2010). If such mutation(s) occurred early on in the WNS epizootic, or was introduced to a specific region, they could have impacted disease spread and persistence (Palmer et al. 2018).

In the context of adaptation, improving metabolic functioning can convey obvious

benefits to a population's survival. In particular, the expansion of gene families pertaining to metabolic activity have been suggested as a factor driving transition to pathogenesis in other fungal pathogens (Gladieux et al. 2014). As in the Chytrid fungus (Batrachochytrium dendrobatidis), clonal spread and host shift were accompanied by duplication and expansion of protease genes (Joneson et al. 2011; Rosenblum et al. 2012). In this study, several mutations and regions with enriched GO Terms pose particular relevance to metabolism/catabolic activity (Tables 1 & 2). However, only one, a homolog of the hydroxyacid-oxoacid transhydrogenase, was impacted by a missense mutation (Arg → Leu). While its function in fungi is presently not known, this gene shows a sequence similarity ranges from 46-54% with the mammalian gene (Kardon et al. 2006) in the category of glycoside hydrolase family 61 and part of the lytic polysaccharide monooxygenases (LPMOs). LPMOs cleave polysaccharides by a novel oxidative mechanism (Levasseur et al. 2013) and certain LPMOs are found only in fungi, acting preferentially on cellulose (Beeson et al. 2015; Bennati-Granier et al. 2015). In the laboratory, *P. destructans* can grow in medium containing complex carbohydrates as the carbon and energy source. Thus, polysaccharides in the hibernacula could also be a significant carbon and energy source for *P. destructans* and the altered amino acid in the putative hydroxyacid-oxoacid transhydrogenase may represent an adaptation to the specific strains (Reynolds and Barton 2013).

The maintenance of cell membrane integrity makes intuitive sense when considering arthroconidia undergoing dispersal; such adaptations would be critical for the survival of all organisms. Increased membrane permeability or rigidity can result in cell death when faced with extreme temperatures (Gervais and Marañon 1995). As previously mentioned, mutations in the velvet protein in *P. destructans* could influence the regulation of trehalose, cell wall production, and spore dormancy pathways (Fillinger et al. 2001; Park et al. 2012) could all contribute to *P. destructans* survival under sub-optimal temperatures. In addition to this gene, one mutation found in the COP9 signalosome subunit

2 (CNS-2) is unique to PE8 and could be of importance for cold temperature tolerance (Table 2.2). Altered functioning of CNS-2 can cause a cascade of effects impacting components of cellular circadian rhythm development (He et al. 2005; Lakin-Thomas et al. 1990). Furthermore, this cascade of effects resulting from genetic changes can impact the formation of fungal hydrophobin in asexual conidia cells (Bell-Pedersen et al. 1992). Taken together, the mutations in COP9 may impact regulation of the development of certain cell features in filamentous fungi and possibly impact the maintenance of membrane integrity in *P. destructans*. The specificity of this mutation in PE8 may contribute to the differences observed between this isolate and others.

2.9 Conclusions and Perspectives

Invasive fungal pathogens bring significant concerns for the conservation and health of our ecosystems (Fisher et al. 2012; Fisher et al. 2016). Of the bat species infected with WNS, many hold an important position in the ecological space in N. America. For example, bats are predators of many insect pests. As bat populations decline, the ecosystem services that they provide to the agricultural industry could also disappear (Kunz et al. 2011). Here, we explored the phenotypic diversity, temperature-dependant spore germination, and novel genetic variations on the pathogen from different areas of the WNS epidemic. Our results suggest that temperature has likely played an important role in the geographic diversification of *P. destructans* during the spread of WNS. However, the influence of temperature is only one of many factors in the proliferation of *P. destructans* in the hibernacula environment; other factors such as relative humidity (Marroquin et al. 2017), nutrient availability (Raudabaugh and Miller 2013), and interactions with other microbes within the soil community likely also hold significant influences. Our results suggest that the genetic changes accumulated during the spread of WNS and the impact that they have on the survival and reproduction should be another factor in

our understanding of the transmission and spread of WNS. Additional studies involving experimental infections of bats or in vitro models of WNS infection are needed to determine how these genetic and morphological changes could have contributed to the expansion of WNS. Given the rapidly expanding distribution of WNS, a detailed understanding on these and other issues related to the growth, reproduction and dispersal of *P. destructans* are urgently needed in order to help control this disease.

2.10 Accession Numbers

Raw reads used for genomic analyses were submitted to the NCBI SRA database and can be found under the BioSample identifiers: SAMN09233324, SAMN09233325, SAMN09233326.

2.11 Acknowledgments

The following researchers contributed strains from Canada: Karen Vanderwolf, Drs. Donald McAlpine, Scott McBurney, David Overy, Durda Slavic. We thank Dr. Vishnu Chaturvedi for sharing his isolates from the US. The research presented here is supported by the Natural Sciences and Engineering Research Council of Canada (JX), McMaster Institute of Infectious Disease Research Fellowship (JA), and by Ontario Graduate Scholarship (AF).

2.12 Supplemental Material

2.12.1 *P. destructans* Isolates

Isolates originated from four Canadian Provinces: Ontario (11 isolates), New Brunswick (18 isolates), Nova Scotia (1 isolate), and Prince Edward Island (PE, 10 isolates) and six US States: New York (3 isolates), North Carolina (3 isolates), West Virginia (5 isolates), Ohio (1 isolate), Vermont (2 isolates), and Pennsylvania (1 isolate). Isolates from New

Brunswick were collected from live bats, arthropod species, and cave surface soils within seven hibernacula sites. The remaining isolates from Nova Scotia, Ontario, PE, and the US were from diseased bats due to WNS infections.

2.12.2 Spot densitometry

By measuring the light emission for each colony, the amount of colouration is estimated via Integrated-light Density Values (IDV), which provide data on the reflectiveness of the total colony. Here, darker cultures reflect less light than lighter colonies, where a value of 0 is assigned to white growth. To measure the extent of pigment secretion and diffusion into the agar medium we followed protocols described by Vogan et al. 2016. We first subtracted any interfering background noise from the solid agar media. The background IDV of the agar medium was used as a threshold for determining the edge of pigment diffusion on each plate. The area of pigment diffusion was then measured for each colony.

2.12.3 Sequencing

Raw reads were filtered using trimmomatic; adaptor sequences and regions with low quality scores were trimmed. Reads were corrected with a k-mer-based algorithm using SGA (Simpson and Durbin 2012), contigs were assembled with the IDBA-UD algorithm (Peng et al. 2012). At this point, mis-assembled regions were corrected and the final scaffolds were constructed. We then aligned the raw reads from all isolates to our de novo build using the Burrows-Wheeler Alignment MEM algorithm (V0.7.15; (Li and Durbin 2010), with shorter duplicate hits flagged as secondary alignments. We used PicardTools (V1.131; (Broad Institute 2015) to sort BAM files, remove PCR duplicates, and add read group identifiers. Lastly, we masked repetitive regions in the de novo assembly using RepeatMasker (V3.0; (Smit et al. n.d.).

Variant calling was conducted on concatenated BAM files using `Freebayes` V1.1.0 (Garrison and Marth 2012). We first excluded calls that lacked coverage and quality scores. Further quality-based filtering of variant calls was conducted with `bcftools` V1.3 (Li and Durbin 2010), with lenient parameters (QUAL & DP $>$ 20). With this final set, we performed sequence homology search of fungal protein database, mapping of GO terms, and functional annotation using the tools available on the Blast2GO platform (Conesa and Götz 2008). We then conducted an enrichment analysis using Fisher's Exact test to identify statistically significant enrichment within genes that contains variants. We investigated 30 loci that contained putative mutations based on genome sequence comparisons through locus-specific PCR and sequencing. The sequencing results identified a false positive rate of 30%, resulting in our final set of 23 confirmed mutations among the three isolates. In addition, the same sites were also investigated in the isolate US8, as its genome was not sequenced in the original Illumina MiSeq run.

Enrichment analysis determines the probability that the GO Terms within a given subset of genes, compared to a background set of genes, were assigned by chance. Using the built-in functions in Blast2GO, we compared the set of genes containing variants (Table 2.2) to all other genes that were assigned GO Terms. The results from Fisher's Exact Test were corrected for FDR, with a significance cut-off of < 0.05.

2.12.4 Statistical Analysis

We used a mixed-effects linear model to conduct a multivariate analysis of trait variance. Phenotype measures were scaled, with each trait having a mean of zero, and transformed prior to running of the multivariate mixed model. The resulting model followed the following design: $lmer(value \sim trait - 1 + trait - 1|isolate)$. This represents a model measuring the variance/covariances of traits among the random effect, the identity of isolates. By default, lmer also includes a term for residual variance (Bates et al. 2015).

We then computed a matrix of correlation p-values using `cor_pmat` (Wei and Simko 2017), with a significance threshold of 0.05.

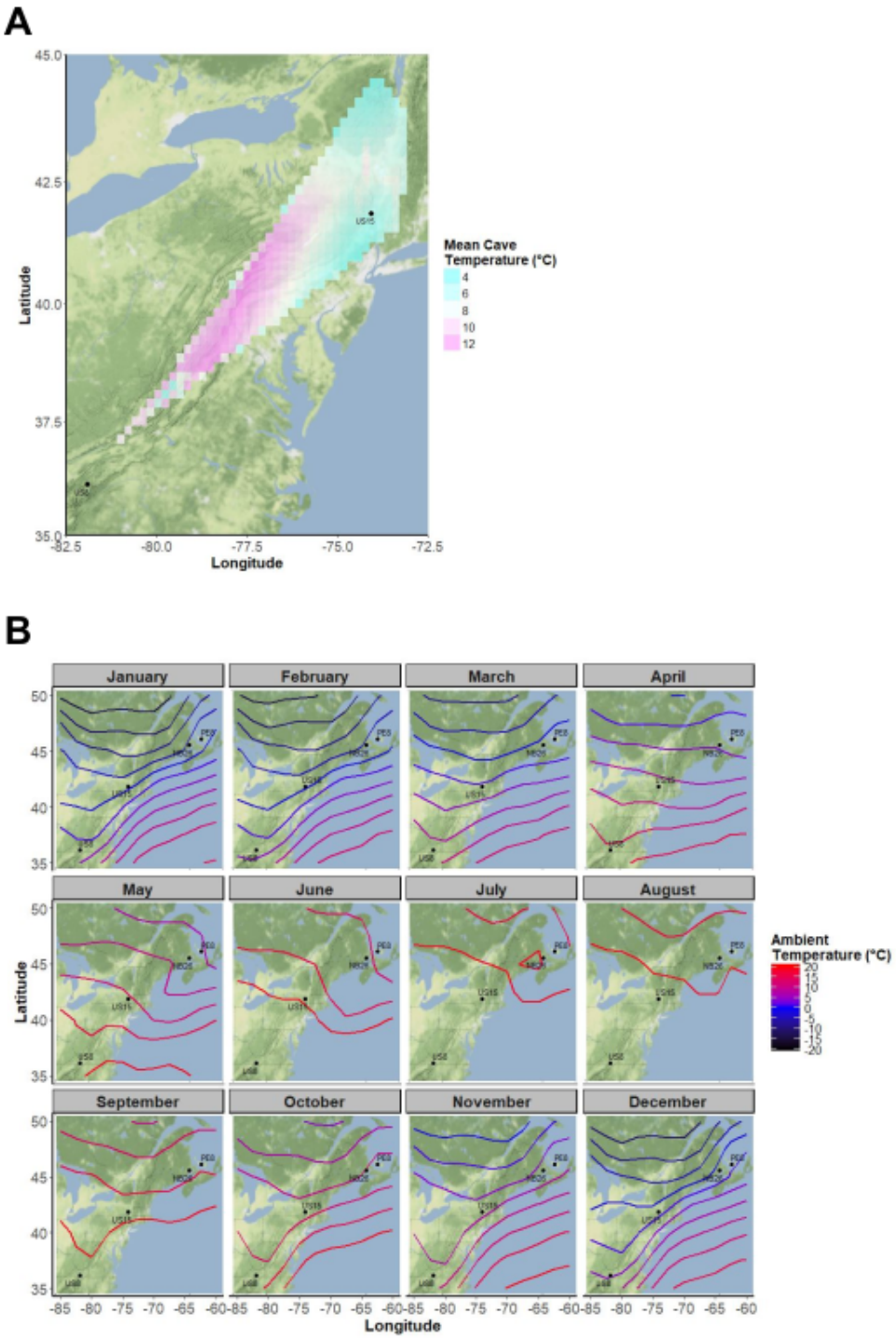

FIGURE 2.3: A) Measurements of cave temperatures were collected from Figure 18 A & B in Swezey and Garrity 2011. We used the data collected from WNS-infected sites to estimate the average cave conditions across the space spanning sampling areas, displayed here using a heat map. B) Records for monthly average air temperature was retrieved using `R` package `RNCEP` (Kemp et al. 2012). In this figure, the distance between contour lines represents 2 °C.

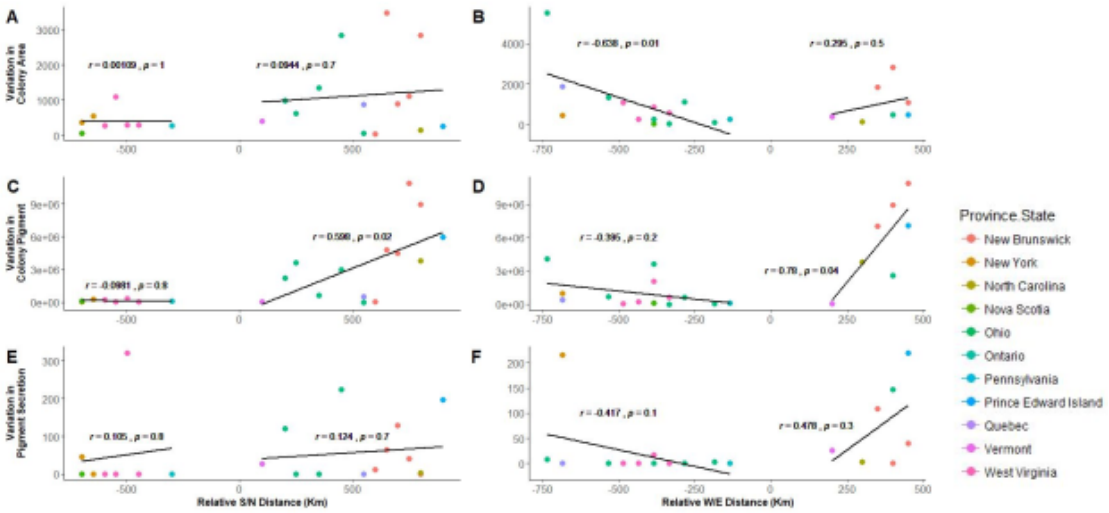

FIGURE 2.4: Measurements of *P. destructans* colony phenotypic traits at 14 °C after 28 days of growth. A: Variation of fungal colony area on agar plates along south/north (S/N) relative distance. B: Variation of fungal colony area on agar plates along west/east (W/E) relative distance. C: Variation of colony surface pigmentation along S/N relative distance. D: Variation of colony surface pigmentation along W/E relative distance. E: Variation in colony pigment diffusion along S/N relative distance. F: Variation in colony pigment diffusion along E/W relative distance.

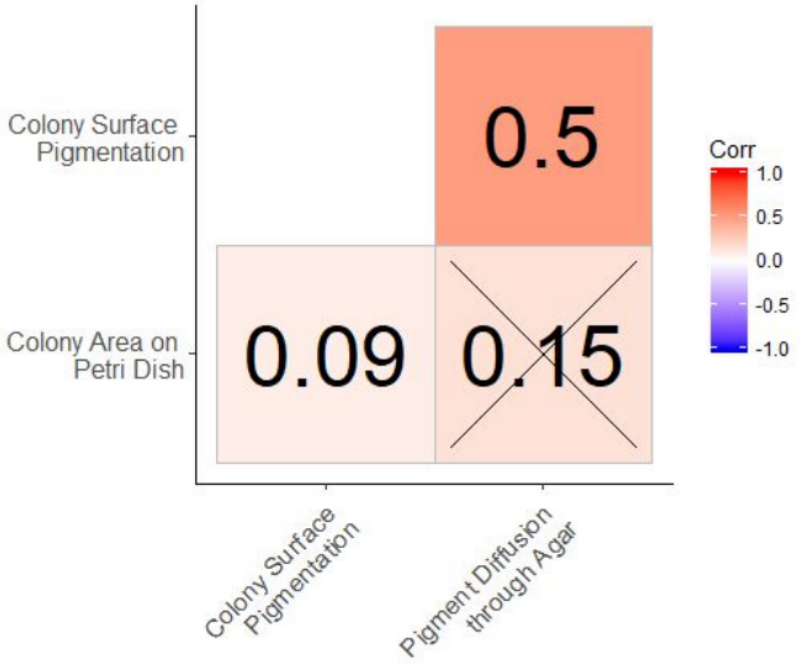

FIGURE 2.5: Results from multivariate linear mixed model demonstrate patterns of the correlation between pairs of traits. Labels and colours of squares represent correlation coefficients, while an "X" represents p-values greater than a significance level of 0.05. This figure was generated using the `R` package `ggcorrplot` (Wei and Simko 2017).

Table 2.4: Results from a genome comparison survey of *P. destructans* isolates based on data from our isolates and those retrieved from the Short Read Archive in NCBI. The retrieved reads were aligned to our de novo assembly and screened for the variants at our previously identified SNP sites. Base calls matching the reference genome are designated as "REF", while "ALT" indicates base calls that match mutations described in this paper. "N/A" indicates sequence information missing at the locus.

				Scaffold/Position									
Accession (SRR)	ID	Collection Date	Collection Location	4871	720	6034	355	1928	3235	1536	1498	2133	4883
				Reference/Alternative									
				T/G	C/T	G/T	G/A	T/C	C/T	T/A	T/C	G/A	G/A
SRR1952982	20631-21	2008	USA: New York, Williams Hotel	REF	REF	REF	REF	REF	REF	REF	REF	REF	REF
SRR6011474	20674-9	2008-03-18	USA: Vermont, Bennington County	REF	REF	REF	REF	REF	REF	REF	REF	REF	REF
SRR6011482	22884-4W	2010-01-27	USA: Vermont, Rutland County	REF	REF	REF	REF	N/A	ALT	REF	N/A	REF	REF
SRR6011480	22949-4	2010-03-05	USA: Maryland, Allegany County	REF	REF	REF	REF	REF	REF	REF	N/A	REF	REF
SRR6011488	W41203	2012-04-12	Canada: New Brunswick, Dorchester Mine	REF	REF	REF	REF	REF	REF	REF	N/A	REF	REF
SRR6011494	23877-1	2008-02-02	Near Rosendale NY	REF	REF	REF	REF	REF	REF	REF	REF	REF	REF
SRR6011470	22442-2	2011-09-22	USA:Grafton, MA	REF	REF	REF	REF	REF	REF	REF	N/A	REF	REF
SRR6011477	20682-10	2008-03-21	USA: Massachussetts, Berkshire County	REF	REF	REF	REF	REF	REF	REF	N/A	REF	REF
SRR5757331	Pd_52201	2012	N/A	REF	REF	REF	REF	REF	REF	REF	REF	REF	REF
SRR6011471	22429-8	2009-01-30	USA: West Virginia, Pendleton County	REF	REF	REF	REF	N/A	REF	REF	N/A	REF	REF
SRR5755626	Pd_681103	2012-04-22	N/A	REF	REF	REF	REF	REF	REF	REF	REF	REF	REF
SRR6011467	GU999986	2009-04-09	Germany: Thueringen	REF	REF	REF	REF	N/A	REF	REF	N/A	REF	REF
SRR5755631	Pd_692102	2013	N/A	REF	REF	REF	REF	REF	ALT	REF	REF	REF	REF
SRR5755630	Pd_H07218	2013	N/A	REF	REF	REF	REF	REF	REF	REF	REF	REF	REF
SRR5755633	Pd_M53205	2013	N/A	REF	REF	REF	REF	REF	REF	REF	REF	REF	REF
SRR5755618	Pd_UWMM.03	2013	N/A	REF	REF	REF	REF	N/A	REF	REF	REF	REF	REF
SRR5755620	Pd_X4702.13.1	2013	N/A	REF	REF	REF	REF	N/A	REF	REF	REF	REF	REF
SRR6011473	22948-1	2014-04-12	N/A	REF	REF	REF	REF	N/A	REF	REF	N/A	REF	REF
SRR5755623	Pd_UWMM.14	2014-04-12	N/A	REF	REF	REF	REF	N/A	REF	REF	REF	REF	REF
SRR6011466	20693-1	2008-03-21	USA: Massachussetts, Hampden County	REF	REF	REF	REF	N/A	REF	REF	REF	REF	REF
SRR5755627	Pd_102203	2015	N/A	REF	REF	REF	REF	N/A	REF	REF	REF	REF	REF
SRR5755624	Pd_WO2109	2015	N/A	REF	REF	REF	REF	N/A	REF	REF	REF	REF	REF
SRR6011478	22004-1	2008-04-01	USA: Connecticut, Litchfield County	REF	REF	REF	REF	REF	REF	REF	N/A	REF	REF
SRR6011475	22426-2	2009-01-27	USA: Connecticut, Litchfield County	REF	REF	REF	REF	REF	REF	REF	REF	REF	REF
SRR6011476	22469-1	2009-03-03	USA: Virginia, Giles, County	REF	REF	REF	REF	N/A	REF	REF	REF	REF	REF
SRR6011469	22504-1	2009-03-25	USA: Pennsylvania, Centre County	REF	REF	REF	REF	N/A	REF	REF	REF	REF	REF
SRR6011479	22930-2	2010-02-08	USA: Tennessee, Sullivan County	REF	REF	REF	REF	N/A	REF	REF	N/A	REF	REF
SRR6011472	22971-3	2010-03-10	Canada: Ontario, Kirkland Lake	REF	REF	REF	REF	REF	REF	REF	REF	REF	REF
SRR6011483	22972-2W	2010-03-15	Canada: Ontario	REF	REF	REF	REF	REF	REF	REF	N/A	REF	REF
SRR6011484	22997-1	2010-04-08	USA: Tennessee, Fentress County	REF	REF	REF	REF	REF	REF	REF	N/A	REF	REF
SRR6011493	23414-1W	2011-01-13	USA: Indiana, Washington County	REF	REF	REF	REF	REF	REF	REF	REF	REF	REF
SRR6011491	23444-1	2011-02-09	USA: Tennessee, Montgomery County	REF	REF	REF	REF	REF	REF	REF	REF	REF	REF
SRR6011490	23455-1	2011-02-16	USA: Virginia, Wise County	REF	REF	REF	REF	REF	REF	REF	N/A	REF	REF
SRR6011495	23874-1	2011-12-12	USA: Maine, Hancock County	REF	REF	REF	REF	REF	REF	REF	N/A	REF	REF
SRR6011489	23897-2	2012-03-19	USA: Missouri, Lincoln County	REF	REF	REF	REF	REF	REF	REF	N/A	REF	REF
SRR6011468	GU350433	2009-04-01	Switzerland: Aargau	REF	REF	REF	REF	N/A	REF	REF	N/A	REF	REF
SRR6011465	GU350434	2009-03-29	Hungary: Kislod	REF	REF	REF	REF	N/A	REF	REF	N/A	REF	REF
SRR5755625	Pd_671202	N/A	N/A	REF	REF	REF	REF	REF	REF	REF	REF	REF	REF
SRR5755629	Pd_European	N/A	N/A	REF	REF	REF	REF	REF	REF	REF	REF	REF	REF
SRR5755634	Pd_N. American	N/A	Illinois	REF	REF	REF	REF	REF	REF	REF	REF	REF	REF
SRR5755619	Pd_UWMM.13	N/A	N/A	REF	REF	REF	REF	REF	REF	REF	N/A	REF	REF
SRR5755622	Pd_X4148.13	N/A	West Virginia	REF	REF	REF	REF	REF	REF	REF	N/A	REF	REF
SRR5755621	Pd_X4702.13.2	N/A	N/A	REF	REF	REF	REF	REF	REF	REF	REF	REF	REF

Chapter 3

Anthropogenic Activity Influences Connectivity between North American Populations of the White-Nose Syndrome Pathogen, *Pseudogymnoascus destructans*

3.1 Preface

The work within this chapter is centered on a central question: what factors influence the transmission of *Pseudogymnoascus destructans* (*P. destructans*) and spread of White-Nose Syndrome (WNS) in North America? To address this, we draw from two different but complementary approaches: 1) classical tests of population genetic criteria for consistent with clonality and 2) more recently developed statistical approaches using genomic information to further understanding the genetic connectivity of *P. destructans* isolates in WNS. This work has been submitted to FEMS Microbial Ecology.

3.2 Abstract

WNS is an ongoing fungal epizootic caused by epidermal infections of the fungus, *P. destructans*, affecting multiple bat species in North America (N. America) and is now considered the deadliest disease affecting any non-human wildlife mammal species in history. Emerging early in 2006 in New York State, WNS has spread to 33 US States and seven Canadian Provinces. Since then, clonal isolates of *P. destructans* have accumulated mutations, with evidence for local adaptation in N. America. Using microsatellite and single nucleotide polymorphism markers, we investigated the population structure and genetic relationships among *P. destructans* isolates from across infected regions in N. America to understand its pattern of spread, and to test hypotheses about factors that contribute to *P. destructans* transmission. We found limited support for genetic isolation of *P. destructans* populations by geographic distance, and instead identified evidence for frequent transfers of *P. destructans* between regions. Interestingly, allelic association tests revealed evidence for recombination in the N. America *P. destructans* population. Our landscape genetic analyses revealed that *P. destructans* population structure was significantly influenced by anthropogenic impacts on the landscape. Our results have important implications for understanding the mechanism(s) of WNS spread.

3.3 Introduction

White-Nose Syndrome (WNS) is an epidermal infection of hibernating North America (N. America) bats caused by the fungal pathogen *Pseudogymnoascus destructans* (*P. destructans*) (formerly *Geomyces destructans*, (Gargas et al. 2009). Infections are characterized by the presence of white mycelial growth on the muzzle or wing tissues of bats, leading to the formation of ulcers and the erosion of epithelial tissues (Meteyer et al. 2009). The N. America *P. destructans* population likely originated from a single European *P. destructans* migrant strain (Leopardi et al. 2015; Palmer et al. 2014).

The European *P. destructans* population is known to infect local bat species but has no known associated mortality (Puechmaille et al. 2011a; Warnecke et al. 2012). Since the first recorded case in N. America bats in 2006, WNS has caused the deaths of millions of bats involving multiple species (Froschauer and Coleman 2012). Coupled with the increasing bat deaths is the expanding geographic range of WNS in N. America, which is now found in 38 US States and seven Canadian Provinces, including the west coast of N. America (Heffernan 2017; Lorch et al. 2016). Despite the drastic declines in bat populations, relatively little is known about how *P. destructans* and WNS have spread among geographic regions. Because the disease is caused by a recently introduced strain, there is limited genetic variation in the N. America *P. destructans* population (Drees et al. 2017b; Trivedi et al. 2017). Consequently, it has been difficult to identify the routes of spread of the pathogen.

Early investigations into genetic structure of *P. destructans* populations showed results consistent with clonal spread of a single genotype in N. America (Ren et al. 2012; Rajkumar et al. 2011; Khankhet et al. 2014). If the pathogen were spread in a step-wise fashion from the center of outbreak origin in New York, we should expect a relationship between the amount of accumulated mutation during the spread of *P. destructans* and the geographic distance from the center. However, recent studies have failed to identify large-scale geographic or temporal structure in the N. America *P. destructans* population (Drees et al. 2017b). For example, the *P. destructans* isolate from Washington State was more closely related to the earliest known isolate from the epicenter in New York state than some other isolates from within New York are to the original isolate (Trivedi et al. 2017). However, such a result could be due to chance events in sampling where the genetic relationships between specific isolates may not be representative of the whole populations, and consequently causing misinterpretations of how *P. destructans* has been transmitted between bats and their hibernacula. Alternatively, the spread of

P. destructans and WNS may not follow a strictly stepwise model of outward expansion from the epicenter, but rather a more complex process, with both forward and backward migrations between infected regions. In addition, secondary introductions of *P. destructans* genotypes between hibernacula could also influence genetic variation and complicate population structure, making the patterns of genetic variations inconsistent with the stepwise model of clonal expansion. The introduction of foreign genotypes into N. America could further complicate the population structure and genetic variation. This is especially true if the additional introduced strain(s) from Eurasia have a complementary mating type (MAT1-1) to that of *P. destructans* isolates in N. America, which could significantly contribute to generating genotypic and phenotypic diversity of *P. destructans* (Halkett et al. 2005; Arnaud-Haond et al. 2007).

Much about the timing (i.e. seasonal or yearly rates of transfer) and route of *P. destructans* spread in N. America remains unknown. Broadly speaking, *P. destructans* could be spread by three methods: airborne spores, host bats, and human factors. First, fungal spores are known to be capable of air dispersal for up to thousands of kilometers by wind and air currents (Aylor 1990; Rieux et al. 2014). Aerosolized *P. destructans* propagules have been detected both inside and outside of hibernacula (Kokurewicz et al. 2016). However, given the psychrophilic nature and extreme sensitivity to high temperature and radiation of *P. destructans* (Palmer et al. 2018; Forsythe et al. 2018; Campbell et al. 2020), the role of wind-aided dispersal between hibernacula may be limited (Hayes 2012). Secondly, *P. destructans* spread could be mediated by infected hosts. The distance covered by N. America bat species can sometimes extend upwards of 500 km within a season (Norquay et al. 2013). Indeed, the early estimated rate for the expansion of WNS was about 300 km each year (Foley et al. 2011). However, with the high bat mortality rates (upwards of 90%) associated with *P. destructans* infection, often few bats could survive and remain within most hibernacula impacted by WNS. The third scenario concerns the spread of *P. destructans* through human activity. Indeed, human-mediated

transmission of *P. destructans* was the most likely cause for *P. destructans* spread from Europe to N. America (Reynolds and Barton 2013), and it could have continued to contribute to the dispersal of *P. destructans* between caves in N. America (Ballmann et al. 2017). These three mechanisms are not mutually exclusive and all three could have contributed to the dispersal of WNS, with differing levels of contributions among different geographic regions. Identifying the dominant mechanism(s) could help develop targeted WNS control and prevention strategies for different regions.

Both the *P. destructans* pathogen and host bats live in highly variable environments across the diverse landscape in N. America. Understanding how landscape features influence the spread of *P. destructans* is an important component of assessing the risk of further spread for zoonotic infections. In this study, we employed microsatellite markers and genomic variants to assess the genetic relationships among *P. destructans* isolates and populations, and to identify the potential patterns of dispersal that may exist among the locations sampled across the WNS distribution range in N. America. Specifically, we compare the potential influences of landscape features with the null model that geographic distance was the main contributor to genetic distance between isolates. Here, the landscape features that we analyzed include geographical, environmental, or anthropogenic factors. The relationships of these environmental variables with genotype distributions of *P. destructans* strains across the landscape can also help infer the presence/absence of barriers to *P. destructans* spread and inform conservation strategies for N. America bats.

3.4 Methods

3.4.1 Strain Information

The strains analyzed in this study came from two sources: (i) those from published literature that contained genome sequences and/or microsatellite genotype information and

(ii) our own strains described in an earlier study (Khankhet et al. 2014). Briefly, our own samples were collected from hibernacula between 2008-2013; the majority were isolated from live bats, cave associated arthropods, or hibernaculum walls. A few were collected from deceased bats confirmed to have died of WNS. All samples were cultured on nutrient agar media at 14 °C and purified through sub-culturing at the hyphal tip of mycelial growth. These purified cultures matured for one month on Sabouraud Dextrose Agar (SDA) before DNA was extracted using a standard cetyl-trimethylammonium bromide (CTAB) and phenol-chloroform protocol typical for filamentous fungal cultures (Katz and Cheetham 2009). Complete strain information is presented in Supplementary Data 1.

3.4.2 Multilocus Genotyping and Bioinformatic Analyses

For microsatellite genotyping of our own strains, we chose the nine most polymorphic microsatellite loci from the panel developed by Drees et al. 2017b. We genotyped 108 isolates using a multiplex PCR method, consisting of three reactions with each reaction containing three sets of primers. In each reaction, each of the three primer sets contained either a HEX, TET, or FAM fluorophore to allow scoring for all three fragments in each reaction. The multiplexed PCR recipe included: 6 µl of 2× GoTaq Green MasterMix (Promega: Madison, Wisconsin), 3 µl nuclease-free water, 0.5 µl of 10 µmol forward primer (total of 1.5 µl for a reaction amplifying three loci), 1 µl of 10 µmol reverse primer (total of 3 µl for a reaction amplifying three loci), and 1 µl of template DNA. PCR products were diluted 10X prior to fragment analysis. All samples were run by Mobix Lab at McMaster University using a GeneAmp PCR SYSTEM 9700 machine (ThermoFisher: Waltham, Massachusetts). The resulting fragment sizes were binned using the Microsatellite Plugin (V1.4, Biomatters Ltd) for Geneious (2018.11.4), based on the known fragment sizes of isolates in Drees et al. 2017b as references.

To further understand the potential geographic patterns of genetic variation in *P. destructans* populations, we analyzed single nucleotide polymorphisms from 41 published genome sequences from the Short Read Archive on NCBI, plus the genomes of three newly sequenced strains (Forsythe et al. 2018). The three new genomes were obtained from strains originating from hibernacula in the Canadian Maritimes and were sequenced on an Illumina MiSeq platform with paired-end libraries. All genomic reads were aligned to the NHWC 20631-21 reference genome (Drees et al. 2016) using the Burrows-Wheeler Alignment (BWA) mem algorithm (V0.7.15; (Li and Durbin 2010). We sorted BAM files, removed PCR duplicates, and added read group identifiers using `PicardTools` (V1.131; (Broad Institute 2015). Single Nucleotide Polymorphism (SNP) variants were called from our sample cohort using HaplotypeCaller in gVCF mode (GATK: V4.1.2) at a minimum calling threshold of 20. Variants within repeat-rich regions were discarded after aligning back to the reference genome using `NUCmer` (V3.23; (Delcher et al. 2003). Missing calls in our multi-sample VCF were resolved using alignment information in each BAM using `FixVcfMissingGenotypes` in `jvarkit` (Lindenbaum 2015). We excluded variants within our re-sequenced sample of the reference genome and variants with low quality (QUAL $>$ 1000) and depth (DP $>$ 10). The final set of variants included 131 SNPs among 45 N. America *P. destructans* strains (see results below). We added annotations and prediction of effects of SNPs using `SnpEff` (Cingolani et al. 2012).

3.4.3 Population Genetic Analyses

We calculated several population genetic statistics using our microsatellite and SNP datasets. All population genetic statistics were generated using the `R` package `poppr` (Kamvar et al. 2014). Our microsatellite dataset consists of 139 isolates, including 108 *P. destructans* isolates we genotyped in this study, plus 31 N. America and 5 European isolates (those with geographical coordinates available) initially genotyped by Drees et al. 2017b. For the SNP dataset, we excluded SNP loci if greater than 5% of isolates had

no REF/ALT call. If we identified multiple isolates from the same hibernaculum having the same multilocus genotype, only one of the clonal isolates was used in subsequent population and landscape analyses.

The patterns of allelic relationships among loci were measured using the index of association tests standardized by the number of loci used ($\overline{r}D$). The null hypothesis for index of association measures is that there is random association among alleles at different loci. Statistical significance was derived by comparing the observed index of association to a null distribution (assuming random recombination) over 999 permutations. After a randomization test on a shuffled dataset, simulated p-values below 0.05 indicates that the null hypothesis of random recombination should be rejected. To further reveal which pairs of loci might show evidence of recombination, we also measured linkage disequilibrium (LD) between all pairs of loci.

The proportion of pairwise loci that were phylogenetically incompatible, also known as the four-gamete test (Hudson and Kaplan 1985), was determined using Multilocus (V1.3; Agapow and Burt 2001). In short, the four-gamete test considers all possible combinations of alleles between two loci. Loci are assumed to be phylogenetically compatible if there is no evidence of homoplasy or recombination. We considered the results of a four-gamete test against a null distribution of 999 permutations of a shuffled dataset. We used SNP loci to determine genomic regions where potential breakpoints from recombination exist using FGTpartitioner (Chafin 2019). Lastly, we conducted ϕ tests for recombination in both datasets using `SplitsTree4` (V4.13.1) (Huson and Bryant 2006). Population genetic structure was estimated using the `STRUCTURE` (V2.3.4) and `fastSTRUCTURE` (V2.7) (Raj et al. 2014) for microsatellite and SNP datasets, respectively, obtained from N. America isolates and European isolates.

3.4.4 Landscape Genetics

To analyze how landscape features might be associated with genetic relationships among isolates, we first generated genetic distance metrics from our SNP and microsatellite datasets using the first two principal components based on individual-level allele usage (Kierepka and Latch 2015). We followed the best practices for resistance surface optimization using the `all_comb` function in `ResistanceGA` (Peterman 2018). Resistance surfaces were created using the `commuteDistance` algorithm in gdistance (Etten 2017). Optimized resistance surfaces were used in a series of Maximum Likihood Population Effects mixed-effects models (MLPE), using the function `MLPE.lmm` (Peterman 2018). We considered multiple hypotheses to test the patterns of genetic distance between our sampled sites: (i) Isolation by Distance (IBD) which proposes that gene flow is a function of the Euclidean distance among populations; (ii) Isolation by Environment (IBE) which states that a higher level of gene flow should occur among locations with similar climate; (iii) Isolation by Resistance (IBR) which proposes that gene flow is a function of the resistance distance; and (iv) a null model which assumes the absence of any geographic structure. To evaluate the relative support of the competing models, we assessed each model's fit using the Akaike information criterion (AIC), and conducted bootstrapping replications by subsampling response and distance matrices, then fitting them back to the MLPE model. The percentage of bootstrap replications in which each IBD, IBE, or IBR model was the best-fitting determines the level of support for each model.

To test the different models, we collected rasters of climate, elevation, anthropogenic impact, and wind conductance across the landscape covering regions where *P. destructans* samples were collected. We combined 19 bio-climatic variables (`worldclim.org`, variables "bio1-19") into a single surface using raster principal component analysis in `RStoolbox` (Leutner and Horning 2017) in order to reduce the amount of multicollinearity between variables. Elevation data were obtained from `R` package `elevatr` (Hollister

and Shah 2017). We collected raster layers of anthropogenic impact from the Commission for Environmental Cooperation (CEC) which estimates the impact of human activity across the landscape with an index of human influence; a measure which encapsulates land-use, light pollution, and human density, among others, to gauge the degree of disturbance across the landscape. We generated a raster surface of wind conductance using monthly averages of wind speed and direction with `rWind` (Fernández-López and Schliep 2019). All variables were aggregated to a resolution of $\sim$ 20 arc minutes ($\sim 26km$) prior to optimization.

Lastly, we estimated effective migration rates based on genetic distances using the Estimated Effective Migration Surfaces (`EEMS`) software package (Petkova et al. 2016). This method visualizes the influence of IBD across geographic space and creates estimates of effective migration rates by interpolation. Complementary to our MLPE approach using resistance surfaces, `EEMS` creates effective migration surfaces across space without incorporating environmental variables. We conducted three independent simulations of 200 demes with 1 million burn-in Markov chain Monte Carlo steps over 2 million iterations. Estimated migration surfaces were created from averaging the results of all simulation replicates using the `rEEMSplots` package (Petkova et al. 2016).

3.5 Results

3.5.1 Genetic Relationships Among N. America *P. destructans*

In this study we genotyped 108 N. America *P. destructans* isolates using primers targeting nine microsatellite loci (Supplementary Data 1). These isolates belonged to 42 multilocus genotypes multilocus genotype (MLG). We present these results in combination with the MLG data from Drees et al. 2017b to provide a greater context for the genetic relationships among *P. destructans* isolates in N. America (after clonal correction, N = 134, MLGs = 59; Figure 3.1). Within this combined dataset, we found an

overall high allelic diversity (Simpson's Diversity; $\lambda = 0.98$), and well over half the MLGs were exclusive to a single isolate. However, 35 isolates distributed among caves in New Brunswick, Prince Edward Island, New York, Ontario, Québec, and Vermont belonged to a single microsatellite genotype (Table 3.1). Aside from this dominant genotype, 12 other genotypes are also shared by two or more isolates, often from multiple US States/Canadian Provinces.

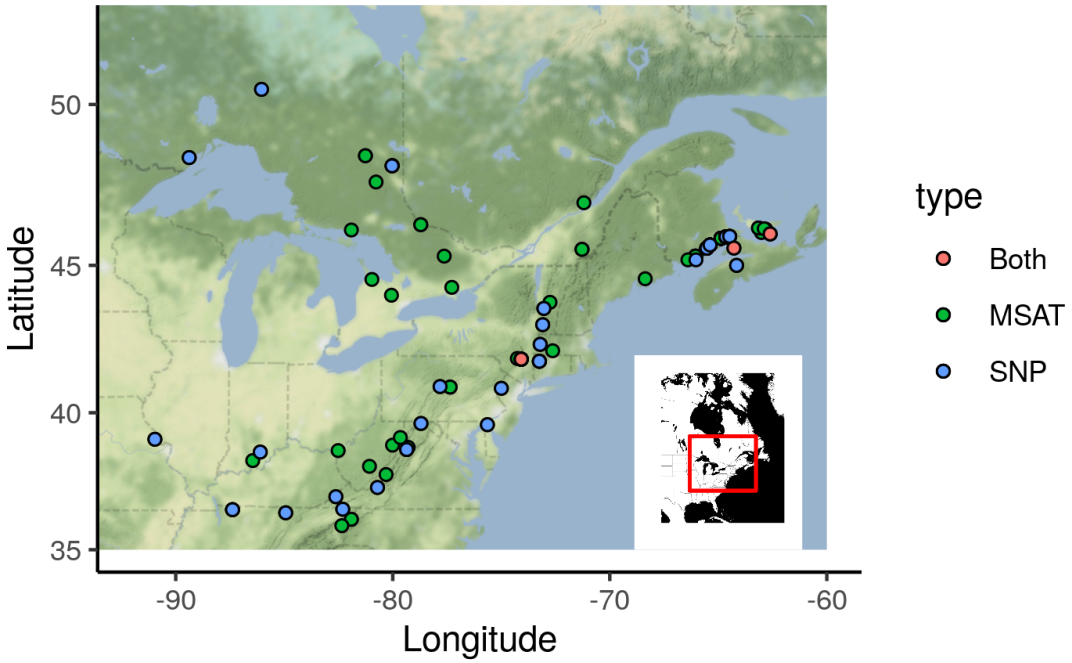

FIGURE 3.1: Map of sampling locations with isolates genotyped using SNPs (blue), microsatellites (green), or both (red).

TABLE 3.1: Shared microsatellite genotypes present in multiple caves across North America. The isolates reported here for each genotype have been clone-corrected to exclude clonal individuals from the same sampling site.

MLG Code	**Number of Isolates**	**Province/State, Country**	**Site**
MLG.9	3	New Brunswick, Canada	Glebe Mine
			Markhamville Mine
			White Cave
MLG.11	3	New Brunswick, Canada	Glebe Mine
			Howes Cave
MLG.13	2	New Brunswick, Canada	Glebe Mine
			White Cave
MLG.15	2	West Virginia, USA	Pendleton
			Tucker
MLG.16	2	Nova Scotia, Canada	Falmouth
		New York, USA	Williams Hotel Mine
MLG.25	4	Not Available	Not Available
		North Carolina, USA	Yancey
		Ontario, Canada	Not Available
MLG.33	2	Tennessee, USA	Not Available
		Tennessee, USA	Not Available
MLG.35	2	New Brunswick, Canada	Dorchester Mine
		Prince Edward Island, Canada	Uigg
MLG.40	8	Connecticut, USA	Not Available
		Delaware, USA	Not Available
		Massachusetts, USA	Not Available
		Missouri, USA	Not Available
		Tennessee, USA	Not Available

		Virginia, USA	Not Available
		Not Available	Not Available
MLG.47	7	New Brunswick, Canada	Markhamville Mine
			Not Available
		Not Available	Not Available
MLG.69	2	New Brunswick, Canada	Berryton Cave
			Harbells Cave
MLG.72	7	New Brunswick, Canada	Berryton Cave
			White Cave
		Prince Edward Island, USA	Rocky Point
			Vernon Bridge
MLG.73	3	New Brunswick, Canada	Berryton Cave
			Harbells Cave
			White Cave
MLG.75	6	New Brunswick, Canada	Berryton Cave
			Dorchester Mine
			Markhamville Mine
			White Cave
		Ontario, Canada	Not Available
MLG.80	2	Indiana, USA	Not Available
		West Virginia, USA	Not Available
MLG.82	4	New Brunswick, Canada	Berryton Cave
			Dorchester Mine
			Markhamville Mine
		Prince Edward Island, USA	Murray River
		New Brunswick, Canada	Berryton Cave
			Dorchester Mine

			Glebe Mine
			Harbells Cave
			Markhamville Mine
			White Cave
		North Carolina, USA	Avery
		New York, USA	Williams Hotel Mine
			Not Available
			Not Available
		Ontario, Canada	Not Available
			Not Available
			Not Available
		Prince Edward Island, Canada	Rocky Point
		Québec, Canada	Not Available
		Virginia, USA	Greely Mine
MLG.84	3	Ontario, Canada	Not Available
		Not Available	Not Available
MLG.87	6	New Brunswick, Canada	Berryton Cave
			Glebe Mine
			Harbells Cave
			Markhamville Mine
			White Cave

Complementary to the nine microsatellite marker data, we also analyzed the genome sequences of 41 N. America *P. destructans* strains. A total of 54 SNPs were identified and these SNPs resolved the 41 strains into 40 SNP genotypes. Two isolates from Glebe and Markhamville Mine in New Brunswick shared an identical SNP genotype. As we observed within microsatellite genotypes, SNP diversity was high ($\lambda = 0.966$, Table

3.2) compared to previous observations in the N. America populations ($\lambda = 0.69$) (Drees et al. 2017b). All SNPs reported here were unique to N. America and have not been found within European *P. destructans* genomes.

3.5.2 LD /Recombination Tests

Standardized index of association ($\bar{r}D$) values are often used in tests of LD and are compared to a null distribution of $\bar{r}D$ values, representing linkage equilibrium (LD) as with random recombination in the genome. If the observed is significantly different from the null distribution, the null hypothesis of LD would be rejected and the observed $\bar{r}D$ would be consistent with LD . After censoring clonal isolates, analyses of microsatellite ($\bar{r}D = 0.02$, p = 0.22) and SNP genotypes ($\bar{r}D = 0.006$, p = 0.23) failed to reject the null hypothesis. These tests of index of association were also performed in a hierarchical manner, to identify patterns of linkage between pairs of loci (Table 3.2). With further partitioning, $\bar{r}D$ showed patterns of association not significantly different from LD in most loci combinations of microsatellite (72%) and SNPs (94%). Only ten of the 36 microsatellite pairs were inconsistent with LD (Figure 3.2A); whereas 83 of the 1 431 SNP pairs (∼6% of all combinations) were not in LD (Figure 3.2B). These results demonstrate that most loci are in LD within the N. America *P. destructans* population.

The above index of association and LD tests used random recombination as the null hypothesis to generate the expected genotype counts. We also investigated whether loci pairs are incompatible with strict clonal reproduction in the N. America *P. destructans* population using the four-gamete test. Overall, 50% of microsatellite loci were phylogenetically incompatible (Figure 3.3A, $p < 0.01$). However, phylogenetic incompatibility was not evenly distributed, as combinations of alleles between some loci (i.e. Pd1/Pd11/Pd19 and Pd7/Pd13) have higher proportions of compatible alleles (50-12.5%, respectively) compared to others ($p < 0.01$; Figure 3.3A). Approximately 75% of all SNP loci combinations were consistent with phylogenetic compatibility, though

TABLE 3.2: Microsatellite genotypes and population genetic metrics from 139 isolates presented in this study. All metrics were clone-corrected at the Province/State level.

Region	**Country**	**State/Province**	**N**	**MLG**	λ†	**Hexp**‡	$\bar{r}D$	$\bar{r}D$ **p-value**
North America	Canada	New Brunswick	23	23	0.957	0.38	0.065	0.65
		Nova Scotia	1	1	0	-	-	-
		Ontario	11	11	0.91	0.32	-0.013	0.87
		Prince Edward Island	6	6	0.83	0.24	-0.069	0.88
		Québec	2	2	0.5	0.22	-	-
		Total	97 (not clone-corrected)	36	0.97	0.38	0.02	0.89
	USA	Connecticut	1	1	0	-	-	-
		Delaware	1	1	0	-	-	-
		Indiana	2	2	0.5	0.22	-	-
		Massachusetts	2	2	0.5	0.33	-	-
		MD	1	1	0	-	-	-
		ME	1	1	0	-	-	-
		Missouri	1	1	0	-	-	-
		North Carolina	3	3	0.67	0.33	-8.3E-17	0.78
		NJ	1	1	0	-	-	-
		New York	5	5	0.8	0.41	0.12	0.12
		OH	1	1	0	-	-	-
		PA	2	2	0.5	0.67	-	-
		Tennessee	3	3	0.67	0.22	-8.3E-17	0.77
		Virginia	3	3	0.67	0.37	0.4	0.16
		VT	2	2	0.5	0.44	-	-
		West Virginia	5	5	0.8	0.4	0.12	0.1
		Total	37 (not clone-corrected)	26	0.96	0.46	0.04	0.03
	Total		134 (not clone-corrected)	59	0.98	0.46	0.03	0.16
Europe	**Total**		5	5	0.8	0.51	0.08	0.27

there was limited statistical support for these results compared to a null distribution ($p > 0.05$; Figure 3.3B).

A neighbour-network with N. America *P. destructans* isolates showed the prevalence of closed loops which indicates incongruence with a perfect monophyletic tree (Figure 3.4), consistent with recombination and the presence of recombinant lineages in the population. However, ϕ tests for recombination conducted on these collections are not consistent with frequent recombination (SNPs $\phi = 0.138$, $p = 0.9$). Whereas, with the inclusion of European strains in these tests, ϕ is consistent with frequent recombination (SNPs $\phi = 0.122$, $p < 0.01$). Four Gamete Test (FGT) loci suggest the presence of four breakpoint events in NA *P. destructans* since introduction, compared to the 402 FGT breakpoints estimated from EU loci in the *P. destructans* genome (Figure 3.5). Taken together, our results indicate unambiguous evidence for recombination in the N. America *P. destructans* population.

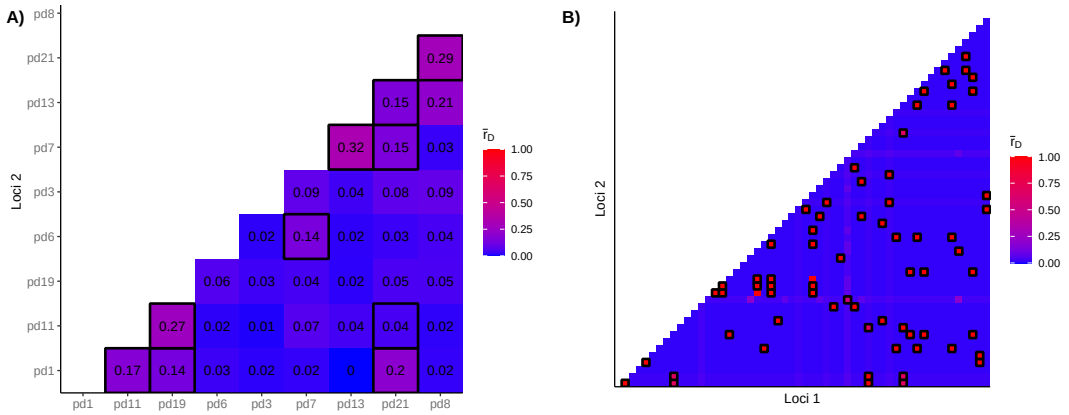

FIGURE 3.2: Pairwise comparison of standardized index of association tests $\bar{r}D$. Squares of the heatmap outlined in black are combination of loci where $\bar{r}D$ p-value < 0.05, consistence with null-expectations under clonality. Microsatellite (A) SNP (B) datasets with greater than 5% of samples missing calls were dropped.

3.5.3 Population Structure

To visualize the population structure of *P. destructans* in N. America, we created unrooted phylogenies using N. America strains genotyped by microsatellite or SNPs. As revealed by microsatellite genotype information, common genotypes (i.e. MLG 83) and genotype clusters often include isolates from multiple locations, including around the epicenter of the WNS distribution (Figure 3.4). While we detected a statistically significant positive correlation between geographic distance and genetic distance based on microsatellite genotypes, that correlation was very weak (r^2 = 0.05, p > 0.01; Figure 3.6A). Furthermore, there was no correlation between geographic distance and genetic distance based on SNPs (r^2 = -0.002, p = 0.9; Figure 3.6B). These results are consistent with frequent gene flows between geographic populations and inconsistent with the step-wise expansion model.

Using `STRUCTURE`, we identified the optimal number of clusters (k=2) for N. America and European *P. destructans*. Interestingly, the two genotyping methods used here revealed differences in the assignment of isolates to either cluster. Based on microsatellite

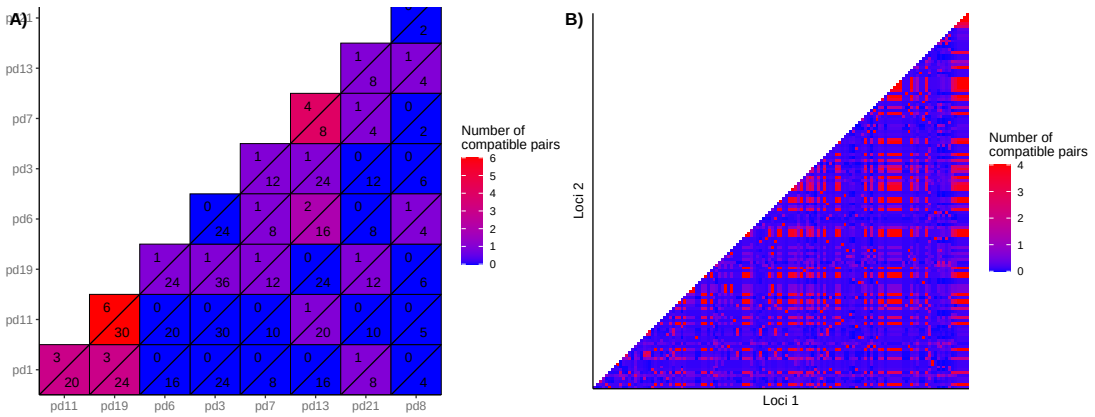

FIGURE 3.3: Pairwise comparison of bi-allelic loci where the presence of more than three allele combinations results in phylogenetic incompatibility. Within our microsatellite dataset (A) the numerator shows the number of pairs that are compatible, while the denominator lists the total number of allelic combinations between the loci. (B) SNP loci with greater than 5% of samples missing calls were dropped.

genotyping, the majority of USA isolates and all European isolates were assigned to one cluster separated from the other cluster that contained mostly Canadian and some US isolates (Figure 3.7A). In comparison, based on SNP markers, all isolates from Canada and US strains formed a cluster that also contained two isolates from Europe (Germany and Switzerland) while the other cluster contained only European isolates (Figure 3.7B).

3.5.4 Landscape Genetics

We examined the potential influence of multiple landscape factors on the patterns of *P. destructans* genetic distance in microsatellite (MSAT) and SNP datasets. We measured model performance across several sets of models to test hypotheses of IBD, IBE, and IBR. The summary results of these tests are presented in Table 3.3. Interestingly, the model selection results differed between MSAT and SNP datasets (Table 3.3). Patterns of genetic distance between individuals in the MSAT dataset can be largely explained by resistance to human impacted landscape, i.e. the IBR-Human Influence model (AICc = 1221.26, bootstrap = 88.9%, Table 3.3). Overall, we found that there

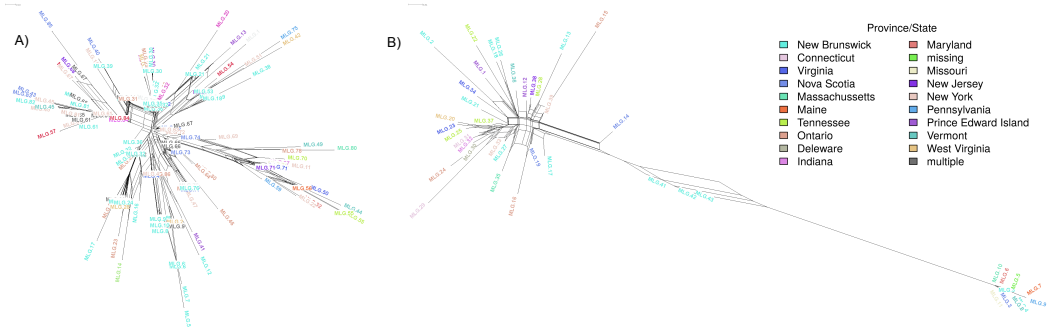

FIGURE 3.4: Neighbor-net network constructed using SplitsTree using (A) 9 microsatellite loci and (B) 53 SNP loci. Parallel edges in this network indicate incongruence with a perfect monophyletic tree.

was greater support for this model than the IBD, IBE, and other IBR models. Furthermore, these isolates demonstrate that genetic distance increases with greater resistance (commuter distance) across human impacted landscapes (slope = 0.16, t-value = 10.6). These results suggest that anthropogenic factors and their effects on landscape (land use, population density, etc.) have prominent effects on *P. destructans* spread.

Among the isolates genotyped using SNPs, the MLPE model with the highest bootstrap support is IBD (51.3%), followed by IBR - Human influence (22.7%), and IBE (21%; Table 3.3). Although these results suggest IBD as an important driver of genetic distance patterns in *P. destructans*, the relationship between genetic and geographic distance is relatively weak (slope = -0.002, t-value = -0.01). Furthermore, models suggesting isolation via human influence on the landscape consistently had the lowest average AICs and highest average marginal r^2 scores compared to all other models tested (Table 3.3). As the SNP genetic distance increases with resistance to human influence across the landscape (slope = 0.34, t-value = 1.26), some influence of IBR on *P. destructans* populations may persist.

We estimated effective migration surfaces across the landscape for an area roughly $2x10^6 \text{km}^2$ in size, comparable to 1/6 of the total area of the United States. Figure 3.8 shows areas of high/low estimated migration rates between locations sampled in both

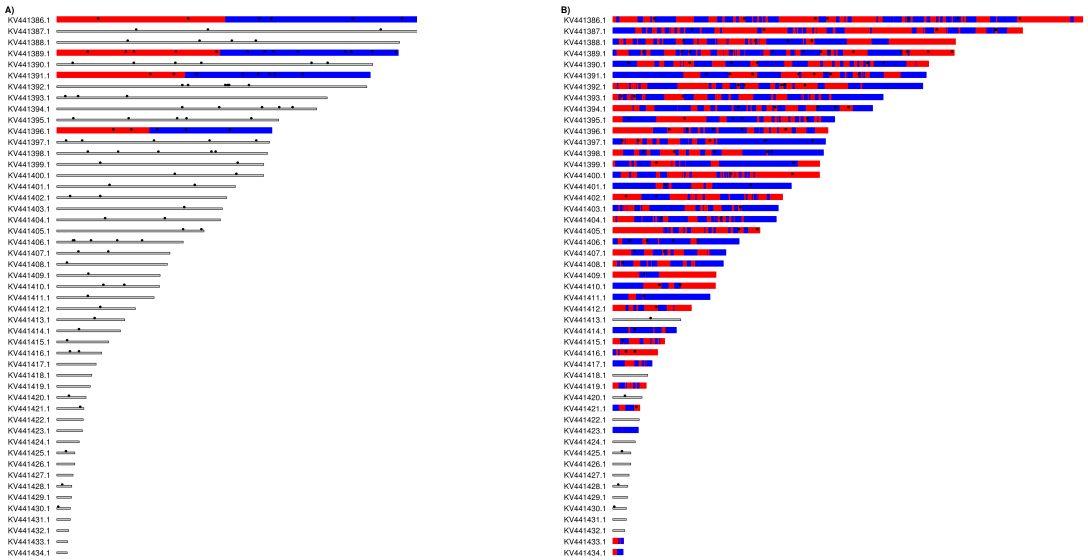

FIGURE 3.5: The estimated genomic locations of recombination breakpoints based on four-gamete test criteria Using SNPs from A) North American and B) European samples. Contigs from *P. destructans* reference genome. Gene coding regions in green. Contiguous regions alternate between red and blue at estimated FGT break points. Black points are SNP locations.

SNP and MSAT. Consistent between these datasets is a large section of the distribution with low rates of migration, extending in a south-west/north-east direction (Figures 3.8A & 3.8B). As the estimated migration rates are lower than what would be anticipated under IBD, this suggests reduced gene flow between these areas of the WNS distribution. Flanked by this region are parts of the distribution that have comparably higher estimated rates of migration, greater than expected under the null hypothesis of IBD (Figures 3.8A & 3.8B). Taken together, estimated migration surfaces for both the SNP and MSAT datasets suggest a disconnect between the south west and north east corners of the distribution.

3.6 Discussion

This study investigated the population genetic structure of *P. destructans* in N. America and the potential landscape factors influencing the patterns of population genetic

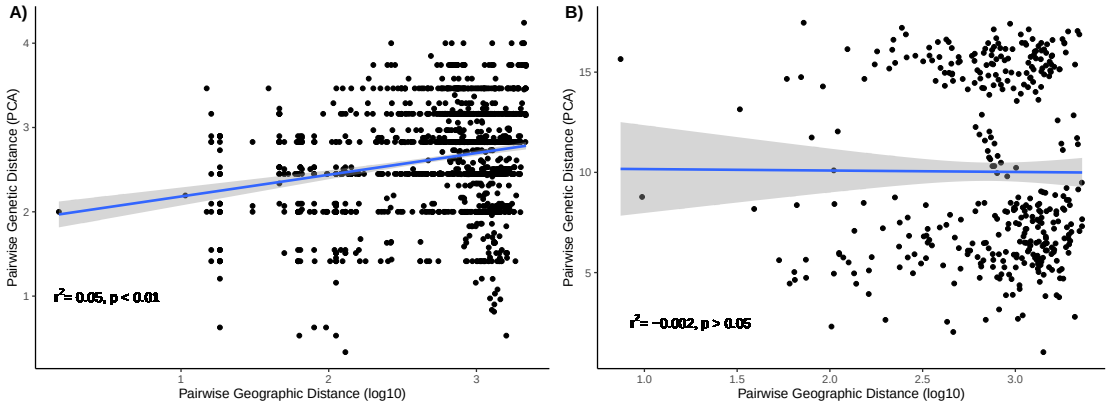

FIGURE 3.6: Correlation between genetic distance of (A) microsatellites and (B) SNPs and log10 geographical distance of all pairwise combinations of isolates.

variations. Using microsatellite markers and whole-genome sequence data, we found substantial allelic diversity, including novel alleles not reported in prior studies with these markers (Drees et al. 2017b; Drees et al. 2017a). In addition, we found N. America *P. destructans* populations are inconsistent with the expectations of strict clonality. We built upon similar recent studies by including a collection of isolates from regions not previously investigated (Drees et al. 2017b; Trivedi et al. 2017). Our analyses revealed limited signals of population genetic structure based on a standard population genetic approach. Our analyses identified connectivity of *P. destructans* isolates strongly influenced by climate and human impacts on landscapes in N. America. Below we discuss the factors influencing the genetic diversity of *P. destructans* across the landscape.

3.6.1 Multilocus Genetic Variation

In clonal microbial pathogens, the rapid generation of novel MLGs via mutation can help overcome selective pressures and niche heterogeneity challenges (Monis et al. 2009; Campbell and Carter 2006; Narra and Ochman 2006). For a recently introduced pathogen that primarily reproduces asexually, we expect the population to harbor low genotype

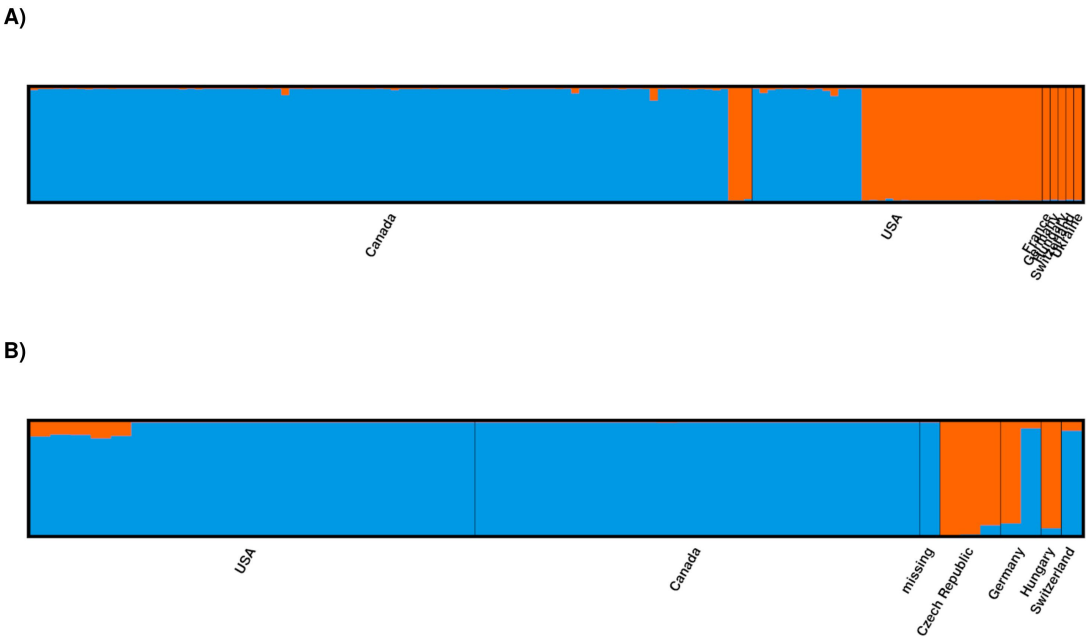

FIGURE 3.7: Visualization of `STRUCTURE` results in a "distruct", showing the individual membership to each population for isolates genotyped with A) microsatellite loci (134 North American isolates and 7 European isolates) and B) SNPs (44 North American isolates and 8 European isolates).

diversity (Raboin et al. 2007; Hovmøller et al. 2008). In comparison, a population capable of both asexual and sexual reproduction would have higher genotype diversity, with evidence of loci in LD and phylogenetically incompatible loci (Attanayake et al. 2014; Sibley and Ajioka 2008). Our analyses based on both MSAT and SNP genotypes are inconsistent with strict asexual reproduction in the N. America *P. destructans* population (Figures 2 & 3). The occurrence of hyphal fusion between members of the same mating type is not uncommon within clonal populations, as parasexual recombination can be a major force of evolution among asexual fungi, causing increased genetic diversity and the emergence of new pathotypes (Read and Roca 2006). Many other species of Ascomycota maintain cellular machinery necessary for the parasexual life cycle (Glass et al. 2000). Although mitotic recombination has been described within other *Pseudogymnoascus* genera (Leushkin et al. 2015), more evidence is needed to distinguish the

TABLE 3.3: Assessment of environmental variables contributing to *P. destructans* genotype distributions across landscape. Using a maximum likelihood population effects mixed-model, we measured the effects of various environmental variables/resistance surfaces to predict changes in pairwise genetic differences (PCA scores) generated from microsatellite or SNP alleles. AICc: adjusted Akaike information criterion; weight; marginal R^2 values of the fitted MLPE model. LL: log likelihood; Percent Top: the percentage of times each model was the best-fit model in over 1000 bootstrap replications.

	Variable(s)	**Mean AICc**	**Mean weight**	**Mean marginal R^2**	**Mean LL**	**Percent Top**	**k**
MSAT	Human Influence	1217.11	0.56	0.08	-604.01	90.5	4
	Climate X Human Influence	1221.43	0.07	0.08	-605.07	0	7
	Wind X Human Influence	1221.53	0.07	0.08	-605.12	0	7
	Climate	1222.17	0.06	0.06	-606.55	0.1	4
	Elevation X Human Influence	1221.64	0.06	0.07	-605.17	0	7
	Wind	1223.34	0.12	0.06	-607.13	9.4	4
	Climate X Elevation	1224.69	0.02	0.06	-606.7	0	7
	Climate X Wind	1225.9	0.02	0.06	-607.3	0	7
	Climate X Elevation X Human Influence	1227.26	0	0.07	-606.08	0	10
	Distance	1227.83	0.01	0.05	-609.76	0	2
	Elevation X Wind	1227.97	0	0.05	-608.34	0	7
	Elevation	1228.45	0.01	0.05	-609.68	0	4
	Climate X Elevation X Wind	1228.86	0	0.06	-606.88	0	10
	Climate X Wind X Human Influence	1228.93	0	0.05	-606.92	0	10
	Elevation X Wind X Human Influence	1229.25	0	0.06	-607.08	0	10
	Climate X Elevation X Wind X Human Influence	1234.15	0	0.07	-606.57	0	13
SNP	Distance	1211.72	0.25	0	-601.52	46.3	2
	Climate	1212.3	0.21	0.02	-600.9	23.7	4
	Human Influence	1212.09	0.24	0.01	-600.8	25	4
	Elevation	1213.18	0.13	0.01	-601.34	4.9	4
	Wind	1213.42	0.11	0	-601.46	0.1	4
	Climate X Human Influence	1218.24	0.01	0.02	-600.81	0	7
	Climate X Wind	1218.57	0.01	0.01	-600.98	0	7
	Wind X Human Influence	1218.4	0.01	0.01	-600.89	0	7
	Climate X Elevation	1218.58	0.01	0.01	-600.98	0	7
	Elevation X Human Influence	1218.43	0.01	0.01	-600.91	0	7
	Elevation X Wind	1219.38	0.01	0	-601.38	0	7
	Climate X Elevation X Human Influence	1231.92	0	0.01	-600.96	0	10
	Climate X Elevation X Wind	1232.13	0	0.01	-601.07	0	10
	Elevation X Wind X Human Influence	1231.96	0	0.01	-600.98	0	10
	Climate X Wind X Human Influence	1232.18	0	0.01	-601.09	0	10
	Climate X Elevation X Wind X Human Influence	1262.07	0	0.01	-601.04	0	13

mechanisms responsible for the allelic patterns observed in this study.

Evidence of recombination has been reported in several seemingly asexual fungal populations where only a single mating type was present (e.g. Hiremath and Lehtoma 2006). A recent study by Sharma et al. 2019 also suggested evidence of recombination based on sequences from multiple loci in a collection of global *P. destructans* strains. However, they compared their data to only the null model of random recombination. With relatively limited sample size, it might be difficult to reject the null model. In contrast, our analyses compared the data to both the strictly asexual reproduction model and the random recombination model with a large sample size. Thus, we believe that

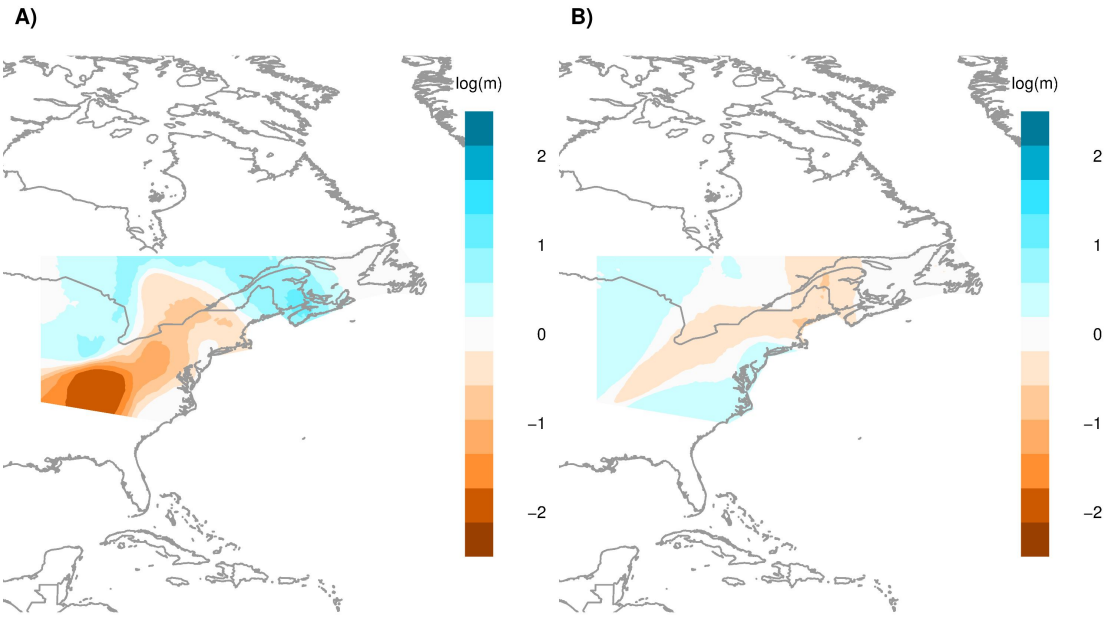

FIGURE 3.8: Estimated effective migration surfaces (EEMS) plot for *P. destructans* based on (A) SNP and (B) MSAT markers. Considering a maximum of 200 demes across the landscape, `EEMS` generates posterior mean migration rates (log10), indicating areas which have a higher (blue) or lower (orange) rate of migration (shown in blue) than expected under isolation by distance (IBD).

our results provide much more robust support for recombination in the N. America *P. destructans* population.

Sexual reproductive events between complementary mating types might be common within the ancestral range of *P. destructans* (Europe), as different mating types have been found to co-occur in the same ecological niche (Palmer et al. 2014). However, only one mating type (MAT1-1) has been reported in the N. America *P. destructans* population (Table 3.4) (Palmer et al. 2014). As a result, recombination in the N. America *P. destructans* population unlikely arose through traditional heterosexual mating. Instead, both same-sex mating and parasexuality, as reported for other fungi (Ene and Bennett 2014), could have contributed to recombination in the N. America *P. destructans* population. Alternatively, there could be multiple introduction events of strains of

the same mating type from Europe where recombination is likely common (Dilmaghani et al. 2012). Our `STRUCTURE` output profiles based on both MSAT and SNP data (Figure 3.3) are consistent with the potential of secondary introductions and recombination after secondary introductions.

TABLE 3.4: Summary of microsatellite locus information.

Locus	**Contig (Accession)**	**Number of Alleles**	**1-D**
Pd1	KV441387	4	0.34
Pd11	KV441394	4	0.31
P19	KV441397	5	0.22
Pd3	KV441391	3	0.3
Pd6	KV441390	6	0.33
Pd7	KV441406	1	-
Pd8	KV441398	2	2
Pd13	KV441393	1	-
Pd21	KV441412	1	-
	Mean	3	8

The two types of genotype data provided complementary insights into the structure of *P. destructans* in N. America, but several inconsistencies do exist. For example, SNPs were useful in distinguishing European isolates of *P. destructans*, identifying those more closely related to N. America strains (Figure 3.7B). In addition, patterns of inferred migration differed slightly between the two genotyping methods (Figure 3.8). Some differences were likely due to the different sample sizes and distributions of the analyzed isolates by the two genotyping methods. Here, more locations were sampled at a higher depth using MSAT markers than the SNPs while very few isolates were genotyped using both methods. In addition, due to the different mutational processes for the two types of markers, models explaining population structure based on MSAT markers may be more useful for revealing fine-scale genetic structure while SNP results are more suited for large-scale and long-term inferences.

Indeed, previous studies have suggested that the rate of mutation in microsatellite loci is significantly higher than nucleotide substitutions. Consequently, homoplasy will

likely be less common for SNP markers than for MSAT markers. Here, homoplasy refers to a MSAT allele or a SNP shared by different strains due to parallel mutational events but not present in their common ancestor. Homoplasy could contribute to LD and phylogenetic incompatibility. While the true rate of homoplasy for either type of marker is unknown in the N. America *P. destructans* population, if present at a significant rate, we expect that the number of phylogenetically incompatible pairs of loci should be higher for loci with a higher number of alleles per locus. However, there is limited statistical support for this hypothesis (Figure 3.4 & Supplementary Data 1), suggesting that homoplasy is unlikely to be the major cause of phylogenetic incompatibility and the observed evidence for recombination. Furthermore, we did not find any evidence for the assayed MSAT markers or the SNPs being in regions of mutational hotspots. For example, we found that none of the SNPs were distributed close to the 1kb region flanking microsatellite markers based on our whole-genome analyses.

3.6.2 Factors Contributing to *P. destructans* Population Structure

The spread of *P. destructans* in N. America was initially believed to be due to clonal expansion (Rajkumar et al. 2011). As such, we would expect *P. destructans* to accumulate genetic diversity as it spread from the epicenter of the outbreak. Overall, we found statistically significant support for a correlation between MSAT genetic distance and geographic distance within N. America. However, the correlation coefficient was very weak (r^2=0.05) and many isolates with identical genotypes were shared across sampling sites (Figure 3.6; Table 3.2). Indeed, almost half of the isolates genotyped using MSAT markers belong to a single genotype (MLG 83) and this genotype was distributed across several Canadian Provinces/US States (Figure 3.4 & Table 3.2). Furthermore, there was no correlation between SNP-based genetic distance and geographical distance among isolates (Figure 3.6). Taken together, this suggests that gene flow is frequent between sites within regions impacted by WNS.

Our interpretation of *P. destructans* population structure suggests little to no correlation with genetic distance (Figure 3.4 & Table 3.3). As the impact of infections varies depending on species characteristics (Langwig et al. 2012), the spread of WNS is consistent with the genetic structure of some bat species (Miller-Butterworth et al. 2014; Burns et al. 2014) but inconsistent with others (Davy et al. 2015). Indeed, the effect of geographic distance on *P. destructans* population structure may be limited (Miller-Butterworth et al. 2014; Vonhof et al. 2015) as long-distance dispersal events push the expansion front and back-transmission fills in behind (Wilder et al. 2011; Thogmartin et al. 2012).

Climatic patterns influence bat population structure via the seasonal regulation of migration behaviours, impacting when and where hosts congregate in social groups (Biek and Real 2010; Warnecke et al. 2012). Migration of N. America Myotis between winter and summer roosts is crucial to understanding the patterns of WNS transmission (Park et al. 2000; Smith and McWilliams 2016; Jonasson 2017; Pettit and O'Keefe 2017; Miller-Butterworth et al. 2014; Reynolds et al. 2015; Krauel et al. 2018; Taylor et al. 2011). Regional similarities in climate appear to be important in regulating the timing of seasonal migrations which may correspond to minimizing energy expenditure (Adams and Hayes 2008; Popa-Lisseanu and Voigt 2009) or prey availability (Meyer et al. 2016). We report no substantial influence of seasonal variations in climate on the connectivity between *P. destructans* strains (Table 3.3). Yet, estimated migration rates between sampled locations appear to be consistent with landscape resistance to climate (Figure 3.8B & Figure 3.9A); this may indicate that additional climatic measures (or other variables that vary with climate) could be included to better explain population structure.

Variation in landscape topography or climate is an important driver of the phylogeographic patterns found in a wide variety of taxa (Shafer et al. 2010). For instance, in

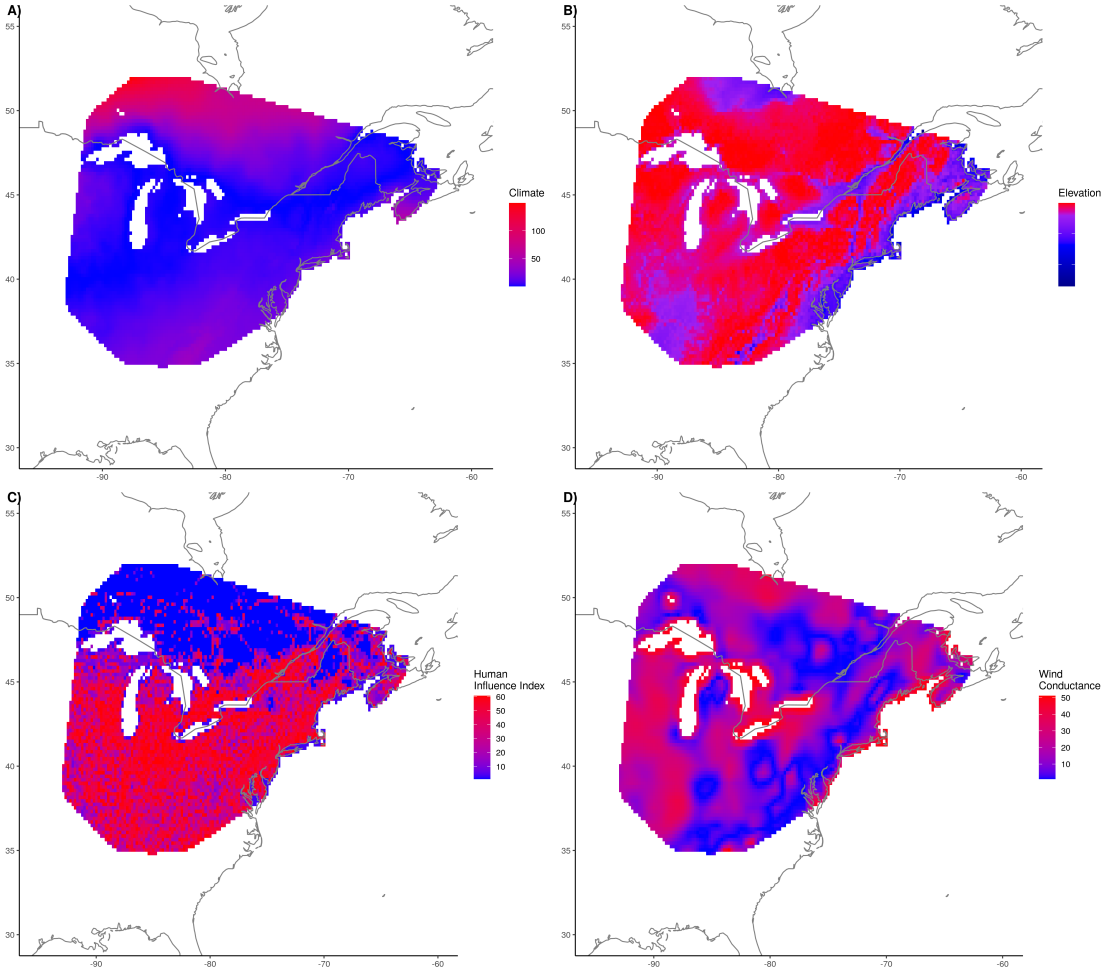

FIGURE 3.9: Optimized surfaces for A) climate, B) elevation, C) human influence index, and D) wind conductance.

Eastern United States and Canada, the Appalachians present a major geological feature that overlaps with bat migratory routes (Reynolds and Barton 2013). The high plateau and extending mountain range of the Allegheny Front escarpment may act as a barrier to gene flow, as colonies of little brown bats located on the western side of the Appalachian high plateau were infected with WNS 1–2 years later than colonies in central or eastern Pennsylvania (Miller-Butterworth et al. 2014; Heffernan 2017). While this feature of the landscape definitely has a local impact on bat populations, we find no influence of altitude on the overall structure of *P. destructans* populations (Table 3.3). Similarly,

while wind dispersal is a common mechanism of passive dispersal for many fungal species (Rieux et al. 2014; Hovmøller et al. 2008), we find no influence of wind currents on the genetic patterns between *P. destructans* isolates (Table 3.3).

Variation in climate across the landscape could potentially impact the survival of *P. destructans* propagules (Forsythe et al. 2018; Campbell et al. 2020) in environmental reservoirs during the summer months. Recent detection of *P. destructans* on free-flying bats during the summer months (Ballmann et al. 2017; Carpenter et al. 2016) suggests that cells of this fungus can persist on bats for some time. In comparison, positive detection of *P. destructans* appears to be much more common on the skin of European bats (Bandouchova et al. 2015; Pikula et al. 2017). As such, either the persistence of *P. destructans* over the summer months or the seasonal shedding and recolonization of the skin microbiome from the environment could enable WNS transmission in N. America. As bat activity ceases at temperatures $\leq 10\,^{\circ}\mathrm{C}$ (*Range-Wide Indiana Bat Summer Survey Guidelines* 2018), dormant *P. destructans* cells could then propagate when conditions are favorable (Langwig et al. 2012; Marroquin et al. 2017; Lilley et al. 2018).

Human activities could potentially influence the transmission of WNS, by directly facilitating the transmission of *P. destructans* between caves (Leopardi et al. 2015; Reynolds and Barton 2013). Although commonly isolated from the sediments of caves impacted by WNS (Lorch et al. 2013), *P. destructans* does not appear to be commonly picked up by cave visitors (Morisak 2018; Ballmann et al. 2017) and the frequency of human visits to rural caves is unknown. Instead, indirect influences on transmission may be impacted by the consequences of urbanization/land use (Mathews et al. 2015; Cryan 2011).

Our results suggest that areas with high anthropogenic impacts have lower connectivity between locations with regards to *P. destructans* genotypes. Compared to forested

areas, species richness and relative abundance of bats is lower in urban areas (Avila-Flores and Fenton 2005; Jung and Kalko 2011). At higher latitudes of the WNS distribution, the degree of human impact on the landscape drops off quickly 3.9. Region migration of bats occurs in all directions, not just latitudinally (Davis and Hitchcock 1965). For instance, the hibernation ecology impacts the distance that some species migrate between seasons. Species that spend hibernation in alone often travel longer distances to reach warmer hibernacula in the south while species that hibernate in clusters are less susceptible to the temperatures at northern hibernacula in the winter. Species like *Perimyotis subflavus* migrate longer distances as solitary species (Briggler and Prather 2003) compared to species that hibernate in clusters, and reduce the amount of energy needed to survive winter at northern latitudes (Boyles et al. 2008). The differing migration strategies that result in longer migration distances and long distance dispersal of *P. destructans*. This may also serve as an explanation for why these regions may remain well connected 3.8.

Although some insectivorous bats do remain in large urban environments (Dixon 2012; Duchamp and Swihart 2008), some Vespertilionidae may have a higher preference for natural areas than urban areas in N. America (Jung and Threlfall 2016). With a higher degree of urbanization and fragmentation of suitable habitat, population sizes are decreased (Sendor and Simon 2003; Papadatou et al. 2011). As such, high levels of urban development seem to restrict the frequency and length of migration events, posing as a barrier to dispersal (Jung and Threlfall 2016). If bat migrations encounter resistance from anthropogenic change to the landscape, then by extension, they can impact the genetic structure of *P. destructans*.

The breadth of sampling for WNS may be limited, as the understanding of where particular environmental sources and sinks exist could be further developed. Much of the least populated areas are less likely to be surveyed as those near city centers. As our

analyses suggest higher rates of migration that span areas with lesser human influence, where resistance to migration (and connectivity of *P. destructans* strains) is relaxed (Figure 3.8), more thorough sampling of these areas could reveal the impact of human activity on the spread of *P. destructans*.

3.7 Conclusion

The increasing prevalence of fungal epidemics emphasizes the importance of understanding how fungal pathogens spread and invade new ecological niches (Seyedmousavi et al. 2018). Rapid and effective genotyping methods are essential for monitoring wildlife diseases, especially WNS, as the high mobility of host species and airborne nature of pathogens themselves present significant challenges in tracking pathogen transmission. In recent years, high-throughput DNA sequencing technologies have improved the accuracy of genetic variation estimates, providing abundant SNPs often with greater discriminating power compared to a few microsatellite markers in most studies (Santure et al. 2010; Helyar et al. 2011; Fischer et al. 2017). In this study, we have found that these genetic markers can provide complementary information for inferences about *P. destructans* population structure. Both types of genotype data showed deviations from the null expectations of strict clonality in N. America. In addition, we find that the N. America *P. destructans* population could not strictly be explained a stepping-stone model, involving IBD scenarios of dispersal. Instead, N. America population structure of *P. destructans* has been influenced by anthropogenic impacts across the landscape and IBD and IBE may play secondary roles.

More complex models incorporating seasonal changes across the landscape, including more robust estimates of *P. destructans* prevalence in environments, and measurement of fungal loads on free-flying bats are needed to better understand the population structure of *P. destructans* in N. America.

3.8 Acknowledgements

We are grateful for Drs. Donald F. McAlpine, Scott McBurney, and David P. Overy for their contributions of *P. destructans* isolates to our research. This research was supported by the Natural Sciences and Engineering Research Council of Canada and by the Ontario Graduate Scholarship.

3.9 Data Accessibility Statement

The data that support the findings of this study are openly available in Dryad (Sampling locations, microsatellite data, and VCF: Dryad doi:https://doi.org/10.5061/dryad.n2z34tmtc) and NCBI SRA (Illumina paired-end reads for 4 novel *P. destructans* strains: PRJNA633856)

Chapter 4

Copy number variations reveal cryptic population structure within North America and evidence of genomic adaptation in global *Pseudogymnoascus destructans* populations

4.1 Preface

This chapter is part of a larger effort to describe the extent of genetic diversity in an invasive clonal population. The analyses conducted here are one method that we have employed to track spread of *Pseudogymnoascus destructans (P. destructans)* in North America. Other types of genomic variation (i.e. structural variations, transposable

elements) are not included in this thesis, but will be the subject of additional manuscripts in the future.

4.2 Abstract

In the present study we characterize the abundance, location, and functional association of genomic copy number variation (CNV)s from a collection of *P. destructans* strains from North America, Europe, and Asia. In addition, we have included a collection of Single Nucleotide Polymorphism (SNP)s to assess the utility of CNVs in resolving clonal population structure, and to identify signals of selection of *P. destructans* in the novel North American environments from multiple genomic sources. The occurrence of beneficial mutations that provide some adaptive advantage will increase in frequency, or be lost by genetic drift. With the increase in frequency of a beneficial mutation, the standing genetic variation in neighboring regions will be affected. As a result, the level of variability in surrounding sites will be reduced, the level of linkage disequilibrium (LD) increased, and the pattern of allele frequencies will be skewed. Using these criteria, we measured signatures of selection in the *P. destructans* genome. In this manuscript, we describe the accumulation of genomic diversity and adaptations within clonal lineages of *P. destructans*, which have potentially contributed to the rapid expansion in the novel environment.

4.3 Introduction

White-Nose Syndrome (WNS) is an epidermal infection of North American bat species, caused by the fungal pathogen, *Pseudogymnoascus destructans* (*P. destructans*) (Gargas et al. 2009). WNS is characterized by the presence of white mycelial growth on the muzzle or wing tissues of bats, leading to the formation of ulcers and the erosion of epithelial tissues (Meteyer et al. 2009). As a recent invasive pathogen in North America,

P. destructans is believed to have originated in Europe, where infections on bats are common but mortality as a result of this infection has never been recorded (Puechmaille et al. 2011a). In contrast, WNS has caused millions of deaths in North American bat populations since it was first detected in New York State in 2006 (Blehert et al. 2009). During this time, WNS has expanded rapidly throughout most of eastern North America, with reports of this fungus in 35 US States and 7 Canadian Provinces, recently reaching the west coast of North America (Heffernan 2017; Lindner et al. 2011).

Current evidence suggests that the spread of *P. destructans* was initiated from a single point of introduction in North America (Khankhet et al. 2014; Rajkumar et al. 2011; Ren et al. 2012). The rapid spread of WNS is consistent with the Novel Pathogen Hypothesis, in which a recently introduced pathogen may experience ecological release, relieved from the selective pressures from their hosts or competition from other species in their native environment (Rachowicz et al. 2005). Introduced pathogens are able to spread rapidly throughout the novel environment as host populations commonly lack the necessary immune response/factors to deal with infection. In the case of WNS, *P. destructans* populations in Europe have likely maintained a long-standing host-pathogen relationship with local bats, which are somewhat resistant to the detrimental effects of infection. This relationship may have enabled the rapid spread of *P. destructans* and the exploitation of naïve hosts in North America (Warnecke et al. 2012).

Preliminary genetic surveys of *P. destructans* have described the accumulation of mutations since WNS was introduced into North America, from a single point of introduction some 14 years ago (Drees et al. 2017a; Trivedi et al. 2017; Forsythe et al. 2018). Yet, the genetic background of the invading *P. destructans* population(s) are not well understood. Since undergoing a clear population bottleneck event, the invasion of *P. destructans* into North American niches must have overcome a number of different barriers typical of invasive fungal pathogens (Reviewed in Gladieux et al. 2015). For example,

a large clonal population can accumulate beneficial mutations quickly. The beneficial mutations may include base substitutions, insertions/deletions, chromosomal structure changes, and copy number variations. Such mutations can enable rapid adaptation of clonal organisms in the absence of outcrossing.

For most organisms, their migrations into new ecological niches may be substantially different, with new stressors/competitors not seen in their original niches. For *P. destructans*, its original niche in Europe as well as in North America is the soil environment. Its transition from a primary soil microbe to a fungal pathogen of bat species has likely occurred over a long period of time in its home range in Europe. This transition has left signatures on its genome. Specifically, the *P. destructans* genome has reduced metabolic capacity (Raudabaugh and Miller 2013) and Ultraviolet radiation (UV) stress tolerance (Palmer et al. 2018) relative to other *Pseudogymnoascus* species. In addition, *P. destructans* has reduced functions that are relevant for life in the soil environment (Reynolds and Barton 2014), which have likely been lost as a consequence of the long-standing association with host bats. Furthermore, the bats in North America are different from those in Europe, and with their niches and stressors likely different as well. Indeed, it has been suggested that within the short time since *P. destructans* arrived in North America, its capacity for nutrient acquisition from soil has been reduced (Thapa et al. 2009), with a possible tradeoff in coping with temperature stress (Forsythe et al. 2018; Campbell et al. 2020).

Within the fungal kingdom, the expansion and loss of gene families have been commonly associated with ecological niche specializations, reflecting ecological shifts (Baroncelli et al. 2016; Lespinet et al. 2002; Soanes et al. 2008). Indeed, genome sequence analyses have shown that copy number variation (CNV)s for genes encoding secreted proteins, nutrient transporters, and enzymes are often associated with ecological niche specializations and adaptations (Duplessis et al. 2011; Joneson et al. 2011; Martinez

et al. 2004; Ohm et al. 2012; Xu et al. 2007). In addition, duplications of pathogenicity-related genes can occur quickly during the spread and proliferation of infections (Lind et al. 2017; Steenwyk et al. 2016) as well as in response to environmental stressors such as when exposed to antifungal drugs (Chow et al. 2012). As such, CNVs are emerging as informative genotyping markers for studying the genetics of natural fungal populations. For example, gene duplications/deletions are commonly found when comparing closely related species and even clonal lineages within individual species (Lauer et al. 2018). CNVs have been reported to impact phenotypic expression in various ways (Sjödin and Jakobsson 2012). In fungi, CNVs have been associated with phenotypic variation and adaptation (Gibbons et al. 2012; Steenwyk and Rokas 2018; Steenwyk and Rokas 2017). Notably, CNV mutation rates are often higher than those of Single Nucleotide Polymorphism (SNP)s (Zhang et al. 2009; Redon et al. 2006; Dorant et al. 2020), which make them informative markers for tracking the evolution of expanding pathogen populations. Yet, to date, CNVs have not been utilized to describe population dynamics of *P. destructans* populations.

CNVs are thought to be generally deleterious and subject to purifying selection and, thus, affect coding sequences less frequently than noncoding sequences (Katju and Bergthorsson 2013; Emerson et al. 2008). Deletion CNVs can lead to loss of function, whereas duplication CNVs affecting entire protein-coding genes can be deleterious if they affect dosage-sensitive genes (Zhang et al. 2009; Katju and Bergthorsson 2013). Through measuring the CNVs in clonal isolates of *P. destructans* we can observe the influence of this type of genomic variation on the genetic diversity and population structure during the rapid expansion of WNS in a novel environment. We hypothesize that the genetic diversity in *P. destructans* population in North America due to CNVs has been influenced by both the recent contraction (population bottleneck) and subsequent expansion into a novel environment. Based on the assumptions for a clonal population operating without opportunities for outcrossing, we expect CNVs to be more frequent than SNPs,

but with lower CNV genotype richness than in the European/Asian *P. destructans*.

In the present study we characterize the abundance, location, and functional association of genomic CNVs from a collection of *P. destructans* strains from North America, Europe, and Asia. In addition, we have included a collection of SNPs to assess the utility of CNVs in resolving clonal population structure, and to identify signals of selection of *P. destructans* in the novel North American environments from multiple genomic sources. The occurrence of beneficial mutations that provide some adaptive advantage will increase in frequency, or be lost by genetic drift. With the increase in frequency of a beneficial mutation, the standing genetic variation in neighboring regions will be affected. As a result, the level of variability in surrounding sites will be reduced, the level of linkage disequilibrium (LD) increased, and the pattern of allele frequencies will be skewed. Using these criteria, we measured signatures of selection in the *P. destructans* genome. Our analyses present CNVs as a useful tool in monitoring the spread and diversification of a clonal pathogen in nature, and reveal potential insights to patterns of mutational accumulation and adaptation of *P. destructans*.

4.4 Methods

4.4.1 Sequence processing, CNV calling

We retrieved raw reads of *P. destructans* isolates from the NCBI Short Read Archive using SRA toolkit (https://github.com/ncbi/sra-tools). Reads were first trimmed using `trimmomatic` (V0.39; Bolger et al. 2014) based on quality thresholds (LEADING:3 TRAILING:3 MINLEN:36) before mapping to the NHWC 20631-21 reference genome (Drees et al. 2016). For read-depth-based copy number calling, we used a sensitive mapping procedure with `-very-sensitive-local` parameters in `bowtie2` (Longmead and Salzberg 2012). To control for the innate differences between sequencing runs, alignments were down-sampled to an average of 20X coverage using `samtools`. We called

CNVs using `Control-FREEC` (Boeva et al. 2012), which GC-normalizes read depth prior to estimating integer copy number relative to the reference genome at 500bp windows. We retained only the CNV calls with statistical support after a Wilcoxon Rank Sum test ($p < 0.05$), and those that overlapped with gene coding regions. Here, the copy number variation refers to presence/absence of variation relative to the reference genome; a CN of 0 may be the result of a gain in the reference genome relative to the query and thus does not necessarily suggest that a complete gene deletion in the query genome has occurred. Likewise, a gene gain and loss event refers to a substantial difference between the sample and the reference genome (+1/-1, respectively). We compared the frequency of cumulative gene copy gain/loss events between North America and European/Asian populations using a series of t-tests.

In order to determine genomic hotspots for CNVs, we computed Polymorphic index content (PIC) at 500bp windows. Similarly, we measured the variant fixation index (V_{ST}) of CNVs between different populations of *P. destructans* from multiple continents. We permuted V_{ST} over 1000 permutations and determined 95% confidence intervals, following a similar protocol described by Rinker et al. 2019.

4.4.2 CNV Gene Ontology

Enrichment analysis determines the probability that gene ontology terms are enriched within a given subset of genes, compared to the genomic background. We carried out gene set enrichment using topGO (Alexa and Rahnenfuhrer 2010), comparing the set of genes containing CNV to all other genes that were assigned Gene Ontology (GO) Terms in the *P. destructans* reference genome. We combined existing annotation information from previous studies (Drees et al. 2016; Palmer et al. 2018) to provide insights on genes coding for secreted proteins, secondary metabolites, CAZymes or proteases. The results from Fisher's Exact Test were corrected using a False Discovery Rate (FDR).

4.4.3 SNP Genotyping

We called SNPs relative to the *P. destructans* reference genome present in samples from the CNV pipeline. We employed a different read mapping approach with our trimmed reads, using Burrows-Wheeler Alignment (BWA) `mem` (V0.7.15; Li and Durbin 2010. In preparation for SNP calling, we sorted BAM files, removed PCR duplicates, and added read group identifiers using `PicardTools` (V1.131; (Broad Institute 2015). SNP variants were called from our sample cohort using `HaplotypeCaller` in `gVCF` mode (`GATK`: V4.1.2 (Poplin et al. 2017)) at a minimum calling threshold of 20. Variants within repeat-rich regions were discarded after aligning back to the reference genome using `NUCmer` (V3.23; (Delcher et al. 2003). Missing calls in our multi-sample VCF were resolved using alignment information in each BAM using `FixVcfMissingGenotypes` in `jvarkit` (Lindenbaum 2015). We excluded variants within our re-sequenced sample of the reference genome and variants with low quality (QUAL $>$ 1000) and depth (DP $>$ 10). The final set of variants included 131 SNPs among 45 North American *P. destructans* strains (See Results below). We added annotations and prediction of effects of SNPs using `SnpEff` (Cingolani et al. 2012).

4.4.4 Multidimensional Scaling and Clustering

We categorized CNV clusters based on the cumulative number of full/partial gene copy gains/loss events within isolates from a given region. To visualize clusters of CNV genotypes, we created a matrix of gene copy loss/gains events and tested for the optimal number of clusters using a multidimensional scaling approach with the `R` package `mclust` (Scrucca et al. 2016), which uses a finite mixture estimation via iterative expectation maximization steps for a range of k components and the best model is selected using the Bayesian Information Criterion (BIC). We compared our results with SNP genotypes by invoking the same approach on a matrix of allele usage in our samples. The results of clustering were visualized using the `R` package `factoextra`

(github.com/kassambara/factoextra).

4.4.5 Measuring Signatures of Selection

In order to characterize the patterns of selective pressure in *P. destructans*, we measured the ratio of non-synonymous/synonymous substitutions (dN/dS), between isolates from different regions of the WNS global distribution using `snpgenie` (Nelson et al. 2015). Using molecular evolution codon models at a sliding window of 8 codons, $dN/dS < 1$ indicates purifying selection, $dN/dS > 1$ suggests positive selection and $dN/dS = 1$ relaxed selection or neutral evolution. Estimates of dN/dS were permuted over 999 replicates to determine statistical adherence.

To detect signatures of a selective sweep, we ran SNP genotypes using `RAiSD` (Alachiotis and Pavlidis 2018). `RAiSD` measures three separate statistics involved with a selective sweep (site frequency spectrum, LD, and genetic diversity) and calculates the composite μ statistic in sliding-windows along a chromosome/contig. We selected regions with μ values above the 99.95% threshold as putative regions involved with a selective sweep for further investigation.

4.5 Results

4.5.1 Genome-Wide Copy Number Variations

In total, we characterized the whole-genome CNV profiles of 57 strains from North America (n=45), Europe (n=9), and Asia (n=3). In order to determine the overall influence of CNVs on the genetic diversity between clonal strains and between global populations, we used a number of different approaches. We found that, on average, the frequency of CNV events was higher in European/Asian *P. destructans* compared to the North American population ($p < 0.01$; Figure 4.1). We summarized the CNV profiles of each sample by considering the cumulative number of gene copy gain/loss events that

overlap completely/partially with gene coding regions. In general, occurrences of full gene copy gains are less frequent than gene copy loss events in North America ($p < 0.01$), which is also evident in European and Asian isolates (Figure 4.2). Full gene gains and losses as well as partial gene gain events are less common in North American strains than in strains from other regions ($p < 0.05$).

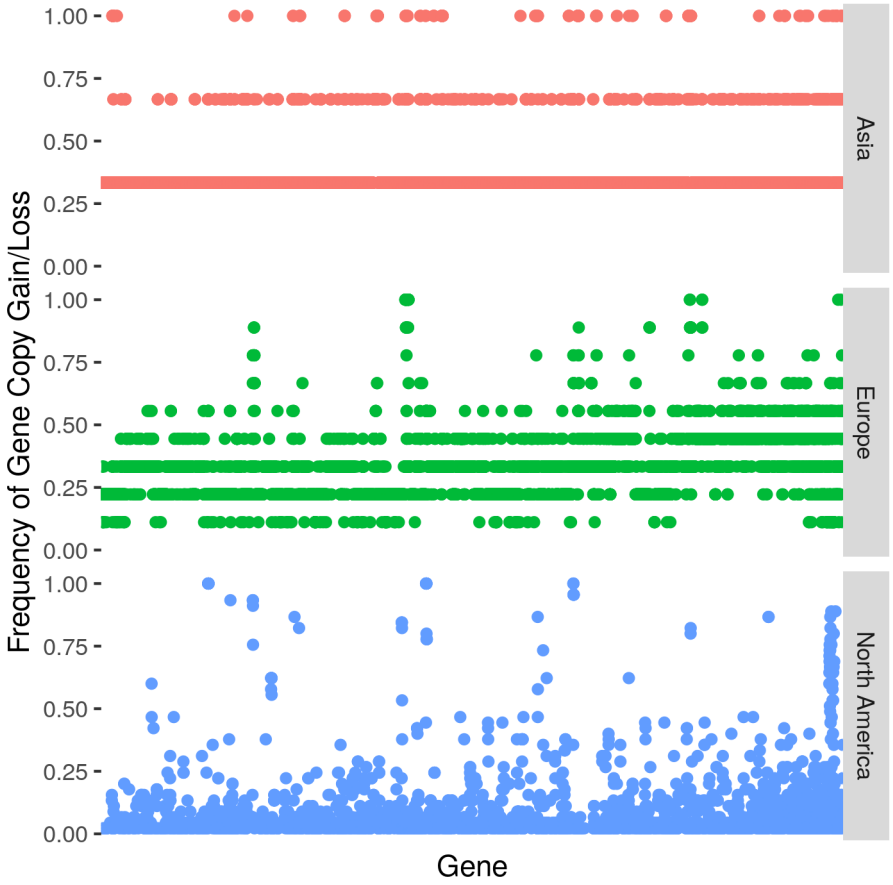

FIGURE 4.1: Frequency of gene copy gain/loss events in *P. destructans* isolates from Asia (n=3), Europe (n=9), and North America (n=45).

As the vast majority of North American *P. destructans* genomes have a low frequency of CNVs (average PIC = 0.15), we extracted the genes with the most variation in CN genotypes by only considering genes within the top 1% of PIC values. We found 68 genes within the top 1% of PIC genes, several of which have metabolic function, or are

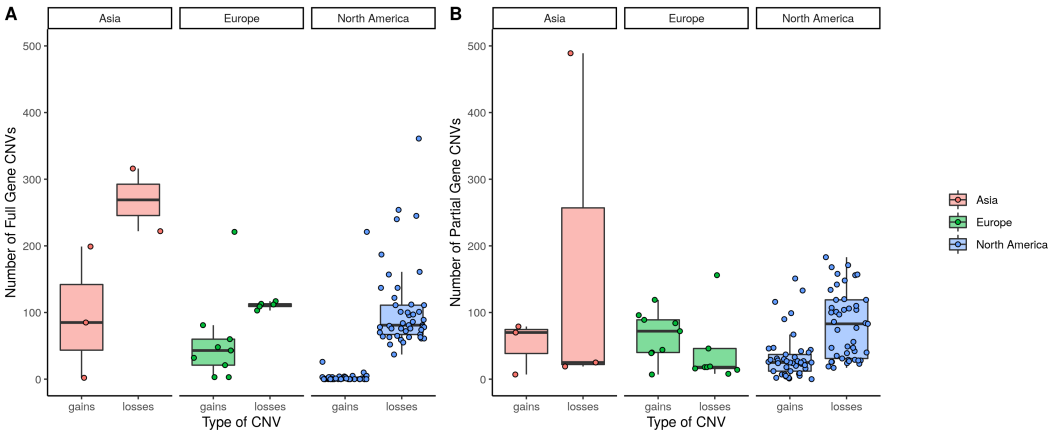

FIGURE 4.2: Distribution of cumulative gene copy gain/loss events (A) fully spanning gene regions, and (B) partially spanning gene regions.

within the predicted secondary metabolite gene clusters (Table 4.5). For example, the most CN-variable gene (PIC = 0.75) is an acid degradation gene present within the ferri-chrome biosynthetic cluster (Table 4.5). In one large contiguous region of the genome, we find consistently elevated CNVs in a collection of isolates from Delaware, New Brunswick, New York, Nova Scotia, Ontario, and Prince Edward Island (Figure 4.10). In particular, there are 15 genes, including hydrolase, zinc finger, DNA binding and transcription factors, which all have increased CNVs. Interestingly, the same isolates contain a 29.78kb contiguous region showing gene copy losses. This region contains 8 genes (Figure 4.1); among them are the 18S rRNA biogenesis protein (RCL1), 39S ribosomal protein (YmL44), and Pimeloyl-ACP methyl ester carboxylesterase (MhpC).

In order to determine if the CNVs have associated functions, we conducted gene set enrichment tests using Fisher's Exact Test. We found no significant enrichment for genes impacted by gene copy loss or partial copy gains in North American *P. destructans* genomes. However, since the introduction of WNS genes with full copy gains are enriched in ATP binding, zinc ion binding, carbohydrate metabolic processes, cell cortex, and microtubule organization (Figure 4.2). In particular, copy number gains within hydrolase activity genes are significantly enriched. Almost all of the 16 significantly

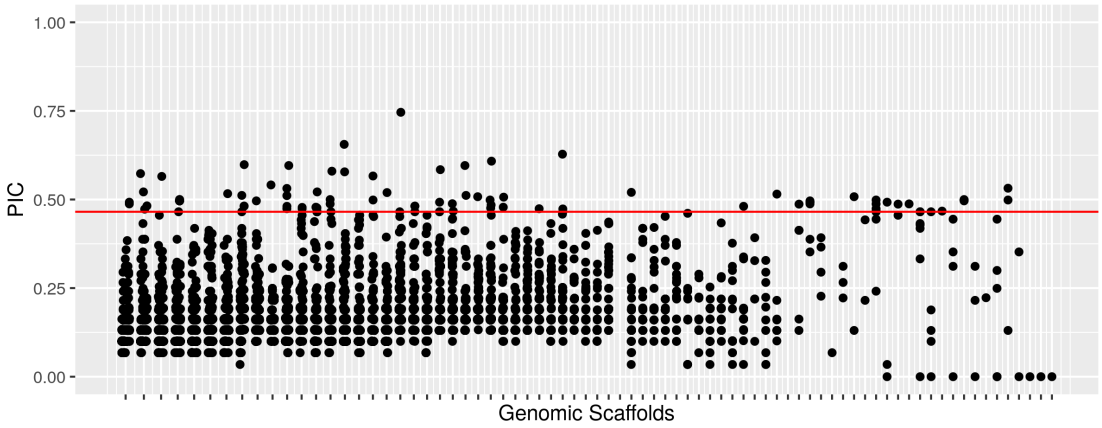

FIGURE 4.3: Polymorphic index content (PIC) Manhattan plot for all *P. destructans* samples (including European and Asian). Red line denotes top 0.1% CN variable sites.

enriched hydrolase genes have predicted activity for hydrolyzing O-glycosyl compounds, a specific class of carbohydrate active enzyme (CAZymes), involved in the breakdown and utilization of carbohydrate sources. In addition to enrichment of genes with enzymatic functions, genes involved with chromosomal structure maintenance were significantly associated with copy number gains. Specifically, we found enrichment of various core histone proteins (H2A/H2B/H3/H4) and enrichment of proteins within the core centromere; relative to the reference genome, with all North American strains having higher copy numbers than the few European isolates we compared here.

4.5.2 Contribution of Copy Number Variation to Population Structure

Our analyses revealed that gene copy number changes contributed to the global population structure of *P. destructans*. Here we briefly describe the influence of genes with CNVs in differentiating the geographic populations using a permuted V_{ST} score. In total, 14% of genes impacted by CNVs within the *P. destructans* genome have high confidence in separating populations ($V_{ST} > 99\%$ CI). Most of the genes with high V_{ST} ($> 95\%$ CI) have increased gene copy number compared to European isolates, which are

TABLE 4.1: Annotation information of genes within a region of contiguous gene copy reduction on the *P. destructans* genome contig KV441389.1

GENE_ID	SCAFFOLD	length	description	EggNog	InterPro.Domains	GO.terms
VC83_02189	KV441389.1	406	18S rRNA biogenesis protein RCL1	ENOG410PH5X: RNA-3'-phosphate cyclase family protein	IPR000228: RNA 3'-terminal phosphate cyclase; IPR013791: RNA 3'-terminal phosphate cyclase, insert domain; IPR013792: RNA 3'-terminal phosphate cyclase/enolpyruvate transferase, alpha/beta; IPR016443: RNA 3'-terminal phosphate cyclase type 2; IPR023797: RNA 3'-terminal phosphate cyclase domain	GO:0005730 nucleolus; GO:0003824 catalytic activity; GO:0006396 RNA processing; GO:0042254 ribosome biogenesis
VC83_02190	KV441389.1	106	hypothetical protein	ENOG410PQWA: mitochondrial 54S ribosomal protein YmL44	IPR019716: Ribosomal protein L53, mitochondrial	
VC83_02191	KV441389.1	413	hypothetical protein	ENOG410PMMI: protein transport membrane glycoprotein Sec20	IPR005606: Sec20	
VC83_02192	KV441389.1	428	hypothetical protein	ENOG410PI68: Demethylates proteins that have been reversibly carboxymethylated (By similarity)	IPR000073: Alpha/beta hydrolase fold-1; IPR016812: Protein phosphatase methylesterase, eukaryotic; IPR029058: Alpha/Beta hydrolase fold	GO:0052689 carboxylic ester hydrolase activity; GO:0006482 protein demethylation
VC83_02193	KV441389.1	447	hypothetical protein	ENOG410PHE1: integral membrane protein	IPR019431: Protein of unknown function DUF2417; IPR029058: Alpha/Beta hydrolase fold	
VC83_02194	KV441389.1	378	hypothetical protein	ENOG410PH5Y: replication factor C subunit	IPR008921: DNA polymerase III, clamp loader complex, gamma/delta/delta subunit, C-terminal; IPR013748: Replication factor C, C-terminal; IPR027417: P-loop containing nucleoside triphosphate hydrolase	GO:0003677 DNA binding; GO:0006260 DNA replication
VC83_02195	KV441389.1	276	hypothetical protein		IPR013715: Domain of unknown function DUF1746	
VC83_02196	KV441389.1	794	hypothetical protein		IPR001330: PFTB repeat; IPR002365: Terpene synthase, conserved site; IPR008930: Terpenoid cyclases/protein prenyltransferase alpha-alpha toroid; IPR018333: Squalene cyclase; IPR032696: Squalene cyclase, C-terminal; IPR032697: Squalene cyclase, N-terminal	GO:0016866 intramolecular transferase activity; GO:0003824 catalytic activity

TABLE 4.2: Results of of gene set enrichment show significantly over-represented Gene Ontology Terms from genes with increased copy number in North America

	GO ID	Term	Annotated	Significant	Expected	p-value
Cellular Components	GO:0000786	nucleosome	26	7	2.41	0.0074
	GO:0000775	chromosome, centromeric region	17	5	1.58	0.0235
	GO:0005871	kinesin complex	3	2	0.28	0.0241
Molecular Function	GO:0004075	biotin carboxylase activity	2	2	0.23	0.014
	GO:0005507	copper ion binding	2	2	0.23	0.014
	GO:0008479	queuine tRNA-ribosyltransferase activity	2	2	0.23	0.014
	GO:0008408	3'-5' exonuclease activity	3	2	0.35	0.038
	GO:0000155	phosphorelay sensor kinase activity	3	2	0.35	0.038
	GO:0003676	nucleic acid binding	247	32	29	0.039
	GO:0004553	hydrolase activity, hydrolyzing O-glycos...	81	16	9.51	0.041

common in most North American strains (Figure 4.4). For example, one large contiguous 188.59kb region containing 19 genes consistently showed increased copy number in North American strains over Eurasian strains, separating those two geographic populations ($V_{ST} > 0.1$) (Figure 4.3). These genes are involved in metabolism and ion binding: dynamin central domain, SET domain, AAA+ ATPase domain, Protein kinase domain; Zinc finger (C2H2); and acetyl-CoA hydrolase, Dihydroorotate dehydrogenase, Kinesin light chain, and Phosphotransferase enzyme family.

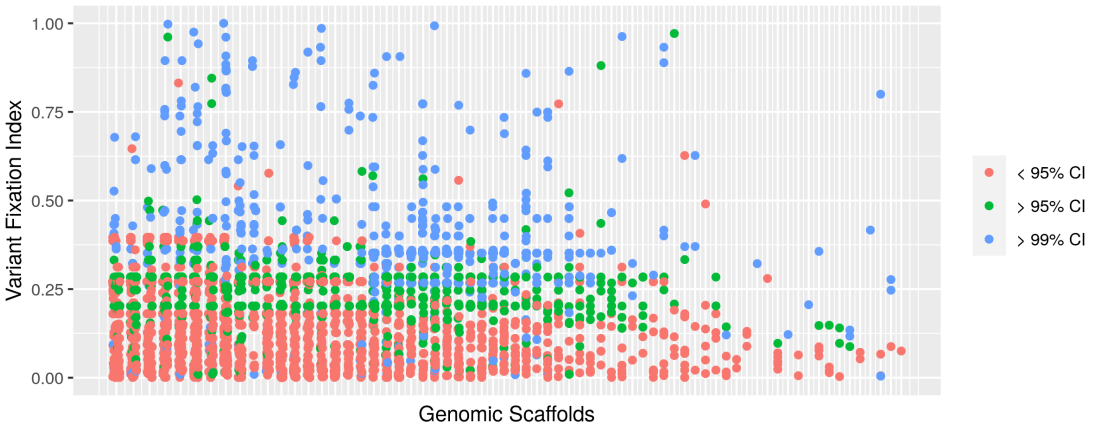

FIGURE 4.4: Manhattan plot of variant fixation index (V_{ST}) values of genes impacted by CNVs that discriminate isolates between North America, Europe, and Asia. Thresholds of 95% and 99% were determined through permutation of V_{ST} values over 1000 iterations.

Table 4.3: Annotation information for genes with widespread copy number gains and high V_{ST} values within *P. destructans* isolates in North America.

GeneID	length	EggNog	InterPro.Domains	GO.terms	V_{ST}
VC83_03918	546	ENOG410PH2C: DYNc	IPR000375: Dynamin central domain; IPR020850: GTPase effector domain; IPR022812: Dynamin superfamily; IPR027417: P-loop containing nucleoside triphosphate hydrolase; IPR030381: Dynamin-type guanine nucleotide-binding (G) domain	GO:0005525 GTP binding	0.88
VC83_03919	242		IPR022812: Dynamin superfamily; IPR027417: P-loop containing nucleoside triphosphate hydrolase		0.82
VC83_03920	412		IPR001214: SET domain	GO:0005515 protein binding	0.8129786
VC83_03921	243				0.96
VC83_03922	772	ENOG410PWJM: ATPase family associated with various cellular activities (AAA)	IPR003593: AAA+ ATPase domain; IPR003959: ATPase, AAA-type, core; IPR027417: P-loop containing nucleoside triphosphate hydrolase	GO:0005524 ATP binding	0.91
VC83_03923	427				0.82
VC83_03924	244	ENOG410Q038: NA	IPR000719: Protein kinase domain; IPR008266: Tyrosine-protein kinase, active site; IPR011009: Protein kinase-like domain	GO:0005524 ATP binding; GO:0004672 protein kinase activity; GO:0006468 protein phosphorylation	0.82
VC83_03929	282		IPR007087: Zinc finger, C2H2; IPR013087: Zinc finger C2H2-type/integrase DNA-binding domain	GO:0046872 metal ion binding; GO:0003676 nucleic acid binding	0.8657407
VC83_03930	534	ENOG410PNU7: conserved hypothetical protein	IPR022198: Protein of unknown function DUF3723		0.87
VC83_03931	230	ENOG410PNU7: conserved hypothetical protein	IPR022198: Protein of unknown function DUF3723		0.87
VC83_03951	528	ENOG410PIR1: acetyl-CoA hydrolase	IPR003702: Acetyl-CoA hydrolase/transferase; IPR026888: Acetyl-CoA hydrolase/transferase C-terminal domain	GO:0003824 catalytic activity; GO:0006084 acetyl-CoA metabolic process	0.18
VC83_03952	249	ENOG410PIPI: conserved hypothetical protein	IPR011009: Protein kinase-like domain		0.67

VC83_03953 116		IPR002110: Ankyrin repeat; IPR020683: Ankyrin repeat-containing domain	GO:0005515 protein binding	0.67
VC83_03954 190		IPR000182: GNAT domain; IPR016181: Acyl-CoA N-acyltransferase; IPR020683: Ankyrin repeat-containing domain	GO:0008080 N-acetyltransferase activity	0.81
VC83_03955 229	ENOG410PFTF: Dihydroorotate dehydrogenase	IPR005720: Dihydroorotate dehydrogenase domain; IPR013785: Aldolase-type TIM barrel	GO:0005737 cytoplasm; GO:0016627 oxidoreductase activity, acting on the CH-CH group of donors; GO:0003824 catalytic activity; GO:0055114 oxidation-reduction process	0.81
VC83_03956 186	ENOG410PFTF: Dihydroorotate dehydrogenase	IPR005720: Dihydroorotate dehydrogenase domain; IPR013785: Aldolase-type TIM barrel	GO:0005737 cytoplasm; GO:0016627 oxidoreductase activity, acting on the CH-CH group of donors; GO:0003824 catalytic activity; GO:0055114 oxidation-reduction process	0.81
VC83_03957 143				0.8657407
VC83_03958 916	ENOG410PJH8: Kinesin light chain	IPR011990: Tetratricopeptide-like helical domain; IPR013026: Tetratricopeptide repeat-containing domain; IPR019734: Tetratricopeptide repeat; IPR027417: P-loop containing nucleoside triphosphate hydrolase; IPR029058: Alpha/Beta hydrolase fold	GO:0005515 protein binding	0.81
VC83_03959 511	ENOG410PWEH: Phosphotransferase enzyme family	IPR002575: Aminoglycoside phosphotransferase; IPR011009: Protein kinase-like domain		0.81

Using a gene copy number presence/absence matrix, we assigned *P. destructans* isolates to CNV clusters based on a multi-dimensional scaling (MDS) approach (Figure 4.5). These clusters designate the 57 *P. destructans* strains into eight different clusters, two of which are shared between the continents, three are unique to North America, two unique to Europe, and one in Asia. Two of these clusters (Clusters 1 & 2) consist of *P. destructans* strains from different continents. Interestingly, we find that the earliest known *P. destructans* isolate (New York State) is assigned to the same cluster as the majority of the European isolates (Czech Republic, Hungary, Germany, Switzerland, Ukraine), and a single isolate from Asia (Mongolia) (Figure 4.5C).

The 4 CNV Clusters in North America are made up of collections of isolates that are not specific to a single area of the WNS distribution. However, these clusters do show distinct differences in copy number profile relative to the reference strain (Figure 4.6). There are very few full gene copy gain events that span full gene CDS in North American *P. destructans*, and most differences between NA clusters and the ancestral EU cluster draw from the cumulative number of full gene copy gains and partial gene copy losses (Figure 4.6). For instance, the isolates belonging to Cluster 1 (Delaware, New Brunswick, New York, Nova Scotia, Ontario, and PEI) have a higher occurrence of cumulative gene copy loss relative to the ancestral European cluster (Figure 4.6). The two remaining clusters in NA (Clusters 5 & 6) are very similar in number of gene loss events (Figure 4.6). Ultimately, the assignment of CNV Clusters shows distinction between the clonal isolates within North America. Principal components of the MDS clusters demonstrate the similarity in CNV profiles between Clusters 1 & 2, which are more closely related to other EU/Asian clusters, compared to Clusters 5 & 6.

To assess the discriminatory power of CNV Clusters, we also analyzed a collection of 89 967 high quality SNPs within *P. destructans* isolates from Asia, Europe, and North America. The vast majority of these mutations are present within Asian/European

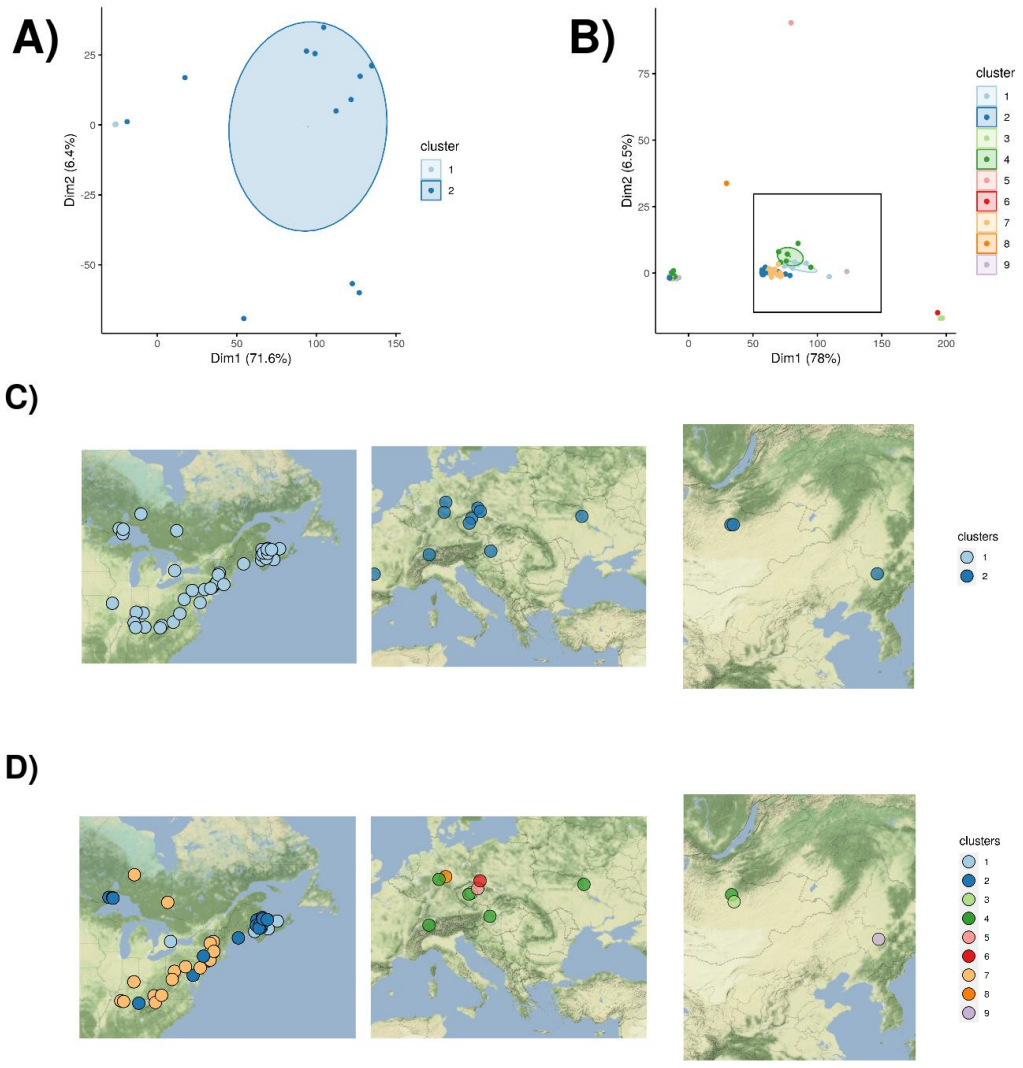

FIGURE 4.5: The results of multidimensional scaling constructed from (A) the copy number profiles from a random sample of 4 000 genomic loci and (B) alleles from a random sample of 4 000 SNP loci. The geographic placement of these clusters is shown for (C) CNVs and (D) SNPs.

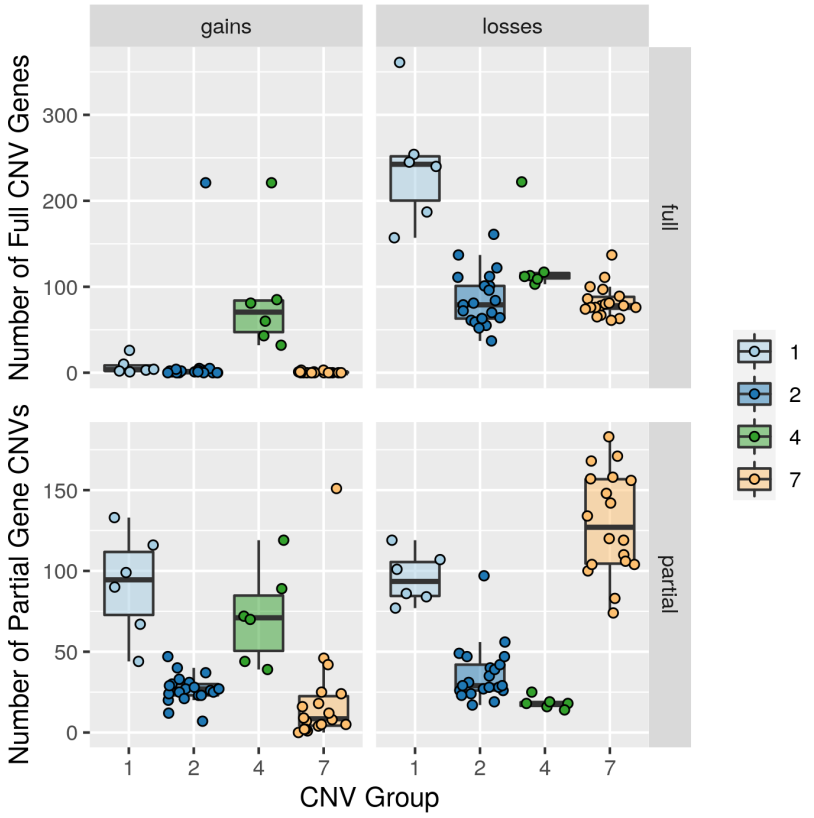

FIGURE 4.6: Distribution of the total number of genes showing copy number variants (presence/absence). The Y-axis shows the number of genes in each of the categories. Only North American and EU clusters with ancestral isolates were included here.

P. destructans populations, and only 131 SNPs are found within North America Using an identical MDS approach, we are able to clearly distinguish 2 SNP clusters present within this collection of global isolates. All North America isolates belong to a single cluster, including the reference strain NHWC 20631-21. This cluster is distinct from all other European and Asian *P. destructans* samples (Figure 4.5D).

4.5.3 Genomic Regions of Impacted by Selection

We compare the impact of mutations on codon usage and the impact of potential selective sweep(s) on nucleotide diversity in order to determine signals of directional selection/neutral evolution on *P. destructans* in North America. The site frequency spectrum

of CNVs demonstrates that while most CNVs are rare in North America, the frequency of very common CNVs are higher than what is expected under a neutral model (Figure 4.7A). The site frequency distribution of SNPs shows a similar skew towards higher allele frequencies, for which the majority of SNPs represent non-synonymous mutations (Figure 4.7B). Together, these suggest that directional selection may be operating within North America.

The magnitude of the impact of selection was investigated further by computing genome-wide dN/dS ratios. The regional differences in non-synonymous to synonymous substitution ratios reveals that signals of purifying selection ($dN/dS < 1$) are common between North American and European genomes. A total of 251 genes under purifying selection ($p < 0.05$) and 9 genes under positive selection that are statistically supported (Figure 4.8; $p < 0.05$). Of the genes under purifying selection, 10 have mutations that have occurred since the introduction of *P. destructans* into North America. Two key genes have SNPs present in almost all North American isolates: Retinoic acid induced 16-like protein, and the Von Willebrand/RING finger domain protein. In contrast, all genes impacted by positive selection are either represented by mutations that are only present in European strains, which suggests their accumulation occurred either very early during the spread of WNS within North America or prior to first introduction. In total, nine genes are impacted by positive selection between the North American and European populations. Two of the nine genes are an RNA binding protein and the DNA repair protein RAD50.

We surveyed *P. destructans* genomes for signatures of a selective sweep(s), and we identified regions of the genome that have been impacted by selective sweeps. The mutations within these regions are ubiquitous within North American isolates due to the population bottleneck event with the introduction. We used `RAiSD` to produce a composite score of selective sweep signals. Based on the 99.95% threshold of μ statistic,

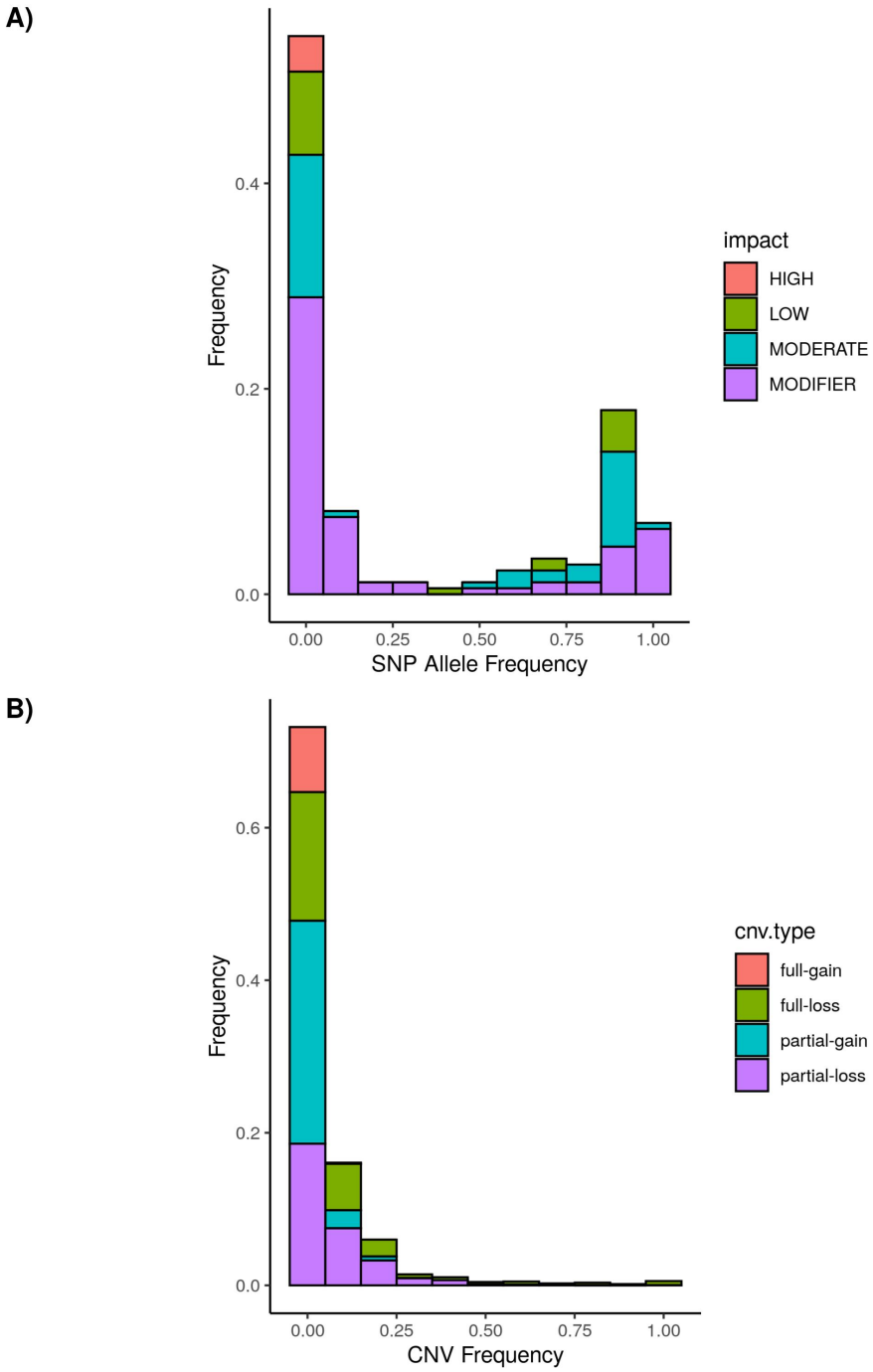

FIGURE 4.7: Site frequency spectrum of (A) SNP alleles and (B) CNVs alleles in *P. destructans* genomes. The stacked coloured bars represent either (A) the predicted impact of SNPs on gene function or (B) the span and type of CNV on the impacted gene.

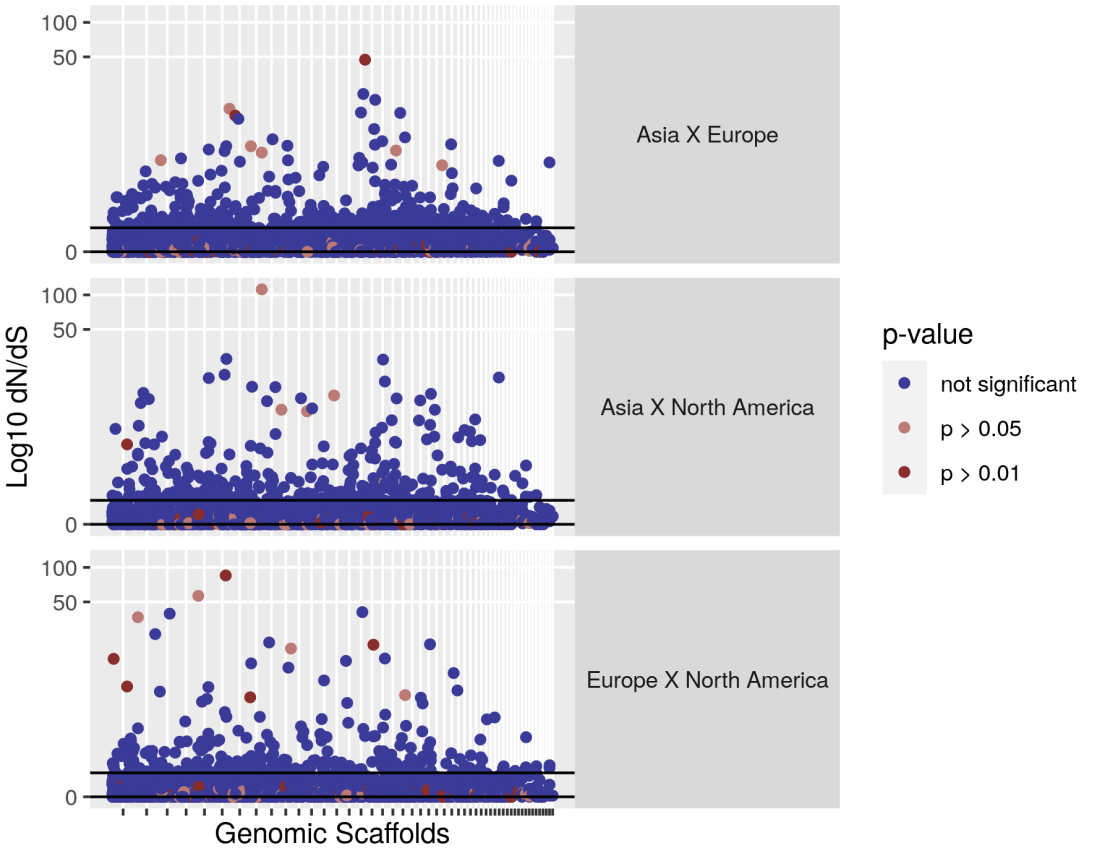

FIGURE 4.8: The ratio of non-synonymous/synonymous substitutions (dN/dS) between isolates from different regions of the WNS global distribution. Estimates of dN/dS were permuted over 999 replicates to determine statistical adherence. Above an equal dN/dS ratio (a threshold of 1 shown here with a solid black line) suggests positive selection, and below this threshold suggests purifying selection is occurring.

we identified 14 regions involved in putative selective sweep events (Figure 4.9). The strongest signal of a selective sweep is from a large ~86.4kb region containing 18 genes related to oxidoreductase, zinc ion binding, adenylylsulfate kinase, and ATP synthase. The remaining regions with lower μ statistic scores consisted of genes with oxidoreductase processes, ion binding/transport, membrane components, and genes for structural maintenance of chromosomes (Figure 4.9).

Table 4.4: Annotation information for regions impacted by a recent selective selective sweep event, identified based on the 99.95% threshold for the composite μ statistic generated by `RAiSD`. LD = localized pattern of LD. LSV = Local Site Variation

Scaffolds	Annotations	Start	End	LSV	LD	μ statistic
KV441386.1	fumarase fum1, structural maintenance of chromosomes protein (SMC5)	428354	480808	2.472	5.52	1.463E-10
KV441387.1		853700	884306	1.742	7.018	1.311E-10
KV441387.1		853712	884310	1.742	7.35	1.372E-10
KV441387.1	protein transport protein bet1	853716	884956	1.778	7.683	1.465E-10
KV441387.1		853719	885001	1.78	13.75	2.625E-10
KV441387.1		853723	885640	1.817	9.583	1.866E-10
KV441387.1	mitochondrial import inner membrane translocase subunit tim54	1424692	1434293	0.5465	27.27	1.598E-10
KV441387.1		1433675	1444051	0.5906	22	1.393E-10
KV441390.1		1050790	1096265	2.771	4.691	1.393E-10
KV441390.1		1051034	1096272	2.756	6.196	1.831E-10
KV441390.1		1051418	1096313	2.735	11.28	3.308E-10
KV441390.1		1051812	1096349	2.713	10.81	3.145E-10
KV441390.1		1051849	1096350	2.711	6.933	2.015E-10
KV441390.1		1055603	1096363	2.483	6.622	1.763E-10
KV441390.1		1055824	1096403	2.472	6.622	1.755E-10
KV441390.1		1056857	1096404	2.409	6.311	1.63E-10
KV441390.1	oxidoreductase activity	1069869	1096503	1.623	7.929	1.379E-10
KV441390.1		1069885	1096697	1.634	7.464	1.307E-10
KV441390.1		1097191	1130121	2.006	6.85	1.473E-10
KV441390.1		1097229	1133635	2.218	7.364	1.751E-10
KV441390.1		1097244	1133721	2.222	7.875	1.876E-10
KV441390.1		1097247	1136449	2.388	8.346	2.137E-10
KV441390.1		1097266	1136486	2.389	8.857	2.269E-10
KV441390.1		1097297	1136623	2.396	9.367	2.406E-10
KV441390.1		1097299	1136927	2.414	9.367	2.424E-10
KV441390.1		1097347	1137179	2.427	4.979	1.295E-10
KV441391.1	protein dimerization activity	1194841	1231099	2.215	5.952	1.414E-10
KV441394.1	p21 protein (Cdc42 Rac)-activated kinase, oxidoreductase, protein kinase, DNA binding/recombination/integration	34068	64855	1.494	10.42	1.669E-10
KV441394.1	iron ion transmembrane transport	1050977	1080030	1.41	8.571	1.296E-10

KV441397.1	transmembrane transport	766113	829342	2.852	4.458	1.363E-10
KV441400.1	GAR1 (H/ACA snoRNP pseudouridylase subunit), THS1 (threonyl-tRNA synthetase), TORC2 complex	311654	339454	1.466	10.42	1.637E-10
KV441403.1	protein heterodimerization activity, ATPase activity	81750	126887	2.007	6.595	1.419E-10
KV441403.1		81770	127426	2.031	6.905	1.503E-10
KV441408.1	protein phosporylation, DNA binding, Fmp27 (mitochondrial?)	138468	187959	3.621	3.869	1.502E-10
KV441408.1		138476	188271	3.643	3.846	1.502E-10
KV441408.1		138483	188619	3.668	4.006	1.575E-10
KV441411.1	FAD binding/oxidoreductase process, N-acetyltransferase activity	403552	441167	1.613	11.41	1.973E-10
KV441411.1		403555	441168	1.613	10.97	1.897E-10
KV441411.1		403712	441172	1.606	7.792	1.342E-10
KV441417.1	GO_component: GO:0016020 - membrane [Evidence IEA]; GO_function: GO:0016773 - phosphotransferase activity, alcohol group as acceptor [Evidence IEA]; GO_function: GO:0005524 - ATP binding [Evidence IEA]"	41704	64292	2.912	4.7	1.467E-10

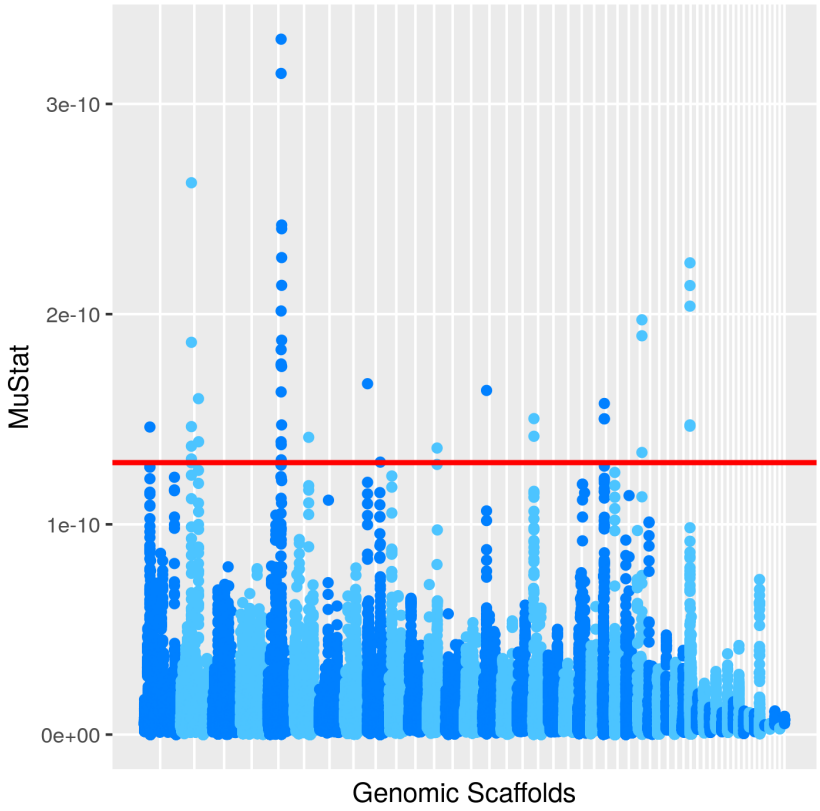

FIGURE 4.9: Manhattan plot of the composite μ statistic calculated using SNPs within European/North American *P. destructans* isolates. Red horizontal line indicates a 99.95% threshold for the μ statistic.

4.6 Discussion

Using genome sequence and annotation information, we investigated the patterns of SNPs and CNVs within a collection of clonal isolates of *P. destructans* in North America. In addition, we compared the genetic variations in the North American *P. destructans* population with those from Eurasia. Our analyses allowed for identification of genomic regions that have been impacted by selection since the introduction of *P. destructans* into North America. Compared to the ancestral population in Eurasia, the introduction bottleneck event has limited the genetic diversity of the North American population. However, mutations have been accumulating in these clonal lineages in North America.

Alongside SNPs, CNVs can be a significant source of genetic variation and accelerate adaptation. This study describes the patterns of CNVs and how they may have contributed to adaptation in the North American *P. destructans* population.

4.6.1 The Accumulation of CNVs in North America

We identified a number of regions within the *P. destructans* genomes with high variation in gene copy gain/loss events relative to the reference strain (top 1% of PIC genes Figure 4.3). One highly variable region is likely responsible for most of the variation we observed among *P. destructans* isolates in North America (Figure 4.10). Regions with a high rate of CNV may cause the formation of multiple CNV lineages, which could compete with each other during adaptive evolution, resulting in clonal interference (Ohm et al. 2012; Park et al. 2008; MacPherson et al. 2006). As CNVs are commonly manifested in regions spanning multiple neighbouring genes (Felenbok et al. 2001), these regions are likely inherited together even in sexual populations. In clonal organisms, genomic regions rich in CNVs may reflect changes that are specific to distinct clonal lineages.

Table 4.5: Annotation information for highly polymorphic genes (PIC > 99%) with consistent higher copy numbers within North America *P. destructans* isolates.

Locus Tag	Length	EggNog	InterPro Domains	GO Terms	Mean Copy Number
VC83_01059	119		IPR013842: GTP-binding protein LepA, C-terminal		1.67
VC83_01647	391		IPR001878: Zinc finger, CCHC-type; IPR032567: LDOC1-related	GO:0008270 zinc ion binding; GO:0003676 nucleic acid binding	1.71
VC83_04073	674	ENOG410PHGF: MFS sugar transporter	IPR003663: Sugar/inositol transporter; IPR005828: Major facilitator, sugar transporter-like; IPR020846: Major facilitator superfamily domain	GO:0016020 membrane; GO:0016021 integral component of membrane; GO:0022857 transmembrane transporter activity; GO:0022891 substrate-specific transmembrane transporter activity; GO:0055085 transmembrane transport	2.4
VC83_05166	392	ENOG410PGEP: Alpha beta hydrolase	IPR000073: Alpha/beta hydrolase fold-1; IPR022742: Serine aminopeptidase, S33; IPR029058: Alpha/Beta hydrolase fold		1.57
VC83_05353	546		IPR017877: Myb-like domain		1.29
VC83_06077	568	ENOG410PFIF: Threonine dehydratase	IPR000634: Serine/threonine dehydratase, pyridoxal-phosphate-binding site; IPR001721: ACT-like domain; IPR001926: Tryptophan synthase beta subunit-like PLP-dependent enzyme; IPR005787: Threonine dehydratase, biosynthetic	GO:0030170 pyridoxal phosphate binding; GO:0004794 L-threonine ammonia-lyase activity; GO:0006520 cellular amino acid metabolic process; GO:0009097 isoleucine biosynthetic process	1.73
VC83_06796	589		IPR001107: Band 7 domain; IPR001597: Aromatic amino acid beta-eliminating lyase/threonine aldolase; IPR001972: Stomatin family; IPR015421: Pyridoxal phosphate-dependent transferase, major region, subdomain 1; IPR015422: Pyridoxal phosphate-dependent transferase, major region, subdomain 2; IPR015424: Pyridoxal phosphate-dependent transferase	GO:0016020 membrane; GO:0016829 lyase activity; GO:0003824 catalytic activity; GO:0006520 cellular amino acid metabolic process	2.05
VC83_07009	672	ENOG410PFWM: Transcriptional regulatory protein pro1	IPR001138: Zn(2)-C6 fungal-type DNA-binding domain; IPR021858: Protein of unknown function DUF3468	GO:0005634 nucleus; GO:0008270 zinc ion binding; GO:0000981 RNA polymerase II transcription factor activity, sequence-specific DNA binding; GO:0006355 regulation of transcription, DNA-templated	1.28

VC83_07257	749	ENOG410PJAG: CP2 transcription factor	IPR007604: CP2 transcription factor		1.33
VC83_07592	1115	ENOG410QEFM: NACHT domain	IPR001680: WD40 repeat; IPR007111: NACHT nucleoside triphosphatase; IPR015943: WD40/YVTN repeat-like-containing domain; IPR017986: WD40-repeat-containing domain; IPR018391: Pyrrolo-quinoline quinone beta-propeller repeat; IPR019775: WD40 repeat, conserved site; IPR020472: G-protein beta WD-40 repeat; IPR027417: P-loop containing nucleoside triphosphate hydrolase	GO:0005515 protein binding	1.21
VC83_07864	337	ENOG410PKBZ: Protein N-terminal amidase	IPR003010: Carbon-nitrogen hydrolase	GO:0016810 hydrolase activity, acting on carbon-nitrogen (but not peptide) bonds; GO:0006807 nitrogen compound metabolic process	2.18
VC83_08277	520	ENOG410PIV6: Transcription factor	IPR002112: Transcription factor Jun; IPR004827: Basic-leucine zipper domain; IPR020956: Transcription factor Aft1, osmotic stress domain; IPR021755: Transcription factor Aft1, HRA domain; IPR021756: Transcription factor Aft1, HRR domain	GO:0003677 DNA binding; GO:0043565 sequence-specific DNA binding; GO:0003700 transcription factor activity, sequence-specific DNA binding; GO:0006355 regulation of transcription, DNA-templated	1.57
VC83_08365	665		IPR024436: Domain of unknown function DUF3824		1.2
VC83_08499	296		IPR013078: Histidine phosphatase superfamily, clade-1; IPR029033: Histidine phosphatase superfamily		2.89
VC83_08799	410	ENOG410PI0B: UBX domain-containing protein	IPR001012: UBX domain; IPR009060: UBA-like; IPR012989: SEP domain; IPR029071: Ubiquitin-related domain	GO:0005515 protein binding	2
VC83_08838	642	ENOG410QE8U: Zn-finger in Ran binding protein and others	IPR000504: RNA recognition motif domain; IPR001876: Zinc finger, RanBP2-type; IPR012337: Ribonuclease H-like domain; IPR012677: Nucleotide-binding alpha-beta plait domain; IPR013520: Exonuclease, RNase T/DNA polymerase III	GO:0008270 zinc ion binding; GO:0000166 nucleotide binding; GO:0003676 nucleic acid binding	1.21

VC83_09414	451	ENOG410PFDM: casein kinase	IPR000719: Protein kinase domain; IPR002290: Serine/threonine/dual specificity protein kinase, catalytic domain; IPR008271: Serine/threonine-protein kinase, active site; IPR011009: Protein kinase-like domain; IPR017441: Protein kinase, ATP binding site	GO:0005524 ATP binding; GO:0004672 protein kinase activity; GO:0006468 protein phosphorylation	1.2
VC83_09491	1689	ENOG410PV6B: DNA helicase	IPR001650: Helicase, C-terminal; IPR011991: Winged helix-turn-helix DNA-binding domain; IPR014001: Helicase superfamily 1/2, ATP-binding domain; IPR022698: Protein of unknown function DUF3505; IPR027417: P-loop containing nucleoside triphosphate hydrolase		1.47

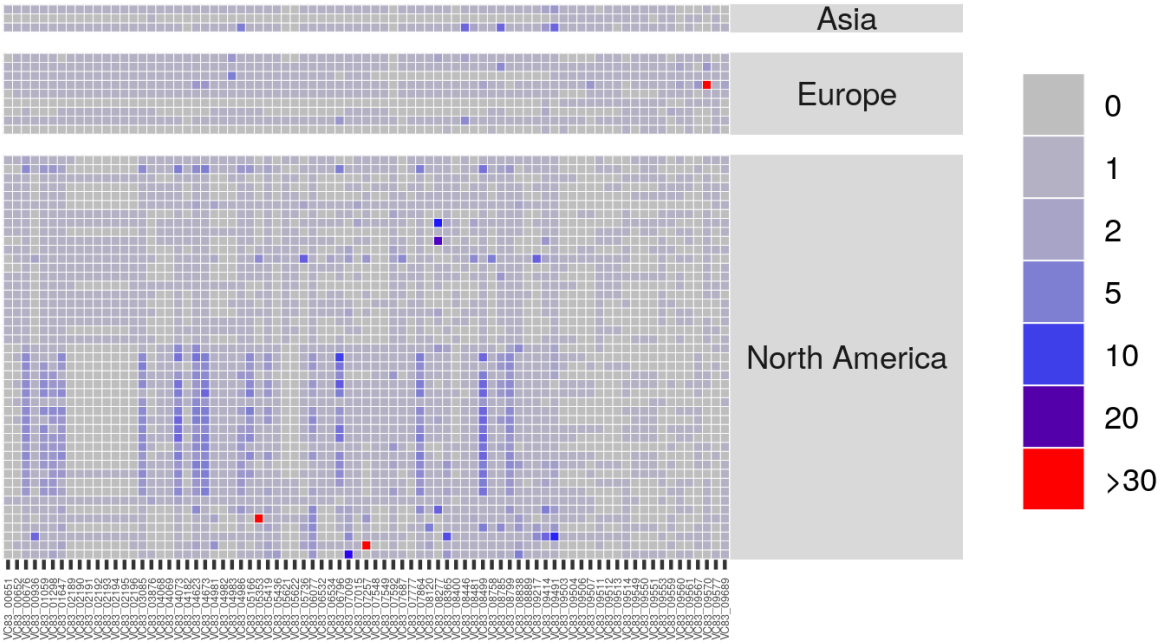

FIGURE 4.10: Contiguous region on genomic scaffold KV441389.1 consisting of multiple genes with CNVs within the top 1% of PIC scores. Text annotations are InterProt IDs.

Table 4.6: Annotation information (Interprot IDs) for the genes shown within Figure 4.10, the contiguous region on genomic scaffold KV441389.1 within the top 1% of highly polymorphic genes.

GENE_ID	InterPro Domains	Average CNV
VC83_00651	IPR011701: Major facilitator superfamily; IPR020846: Major facilitator superfamily domain	0.42
VC83_00652	IPR001128: Cytochrome P450; IPR002401: Cytochrome P450, E-class, group I; IPR017972: Cytochrome P450, conserved site	0.56
VC83_00676		1.75
VC83_00936	IPR001138: Zn(2)-C6 fungal-type DNA-binding domain; IPR007219: Transcription factor domain, fungi	0.72
VC83_01059	IPR013842: GTP-binding protein LepA, C-terminal	1.46
VC83_01298		1.42
VC83_01647	IPR001878: Zinc finger, CCHC-type; IPR032567: LDOC1-related	1.49
VC83_02189	IPR000228: RNA 3'-terminal phosphate cyclase; IPR013791: RNA 3'-terminal phosphate cyclase, insert domain; IPR013792: RNA 3'-terminal phosphate cyclase/enolpyruvate transferase, alpha/beta; IPR016443: RNA 3'-terminal phosphate cyclase type 2; IPR023797: RNA 3'-terminal phosphate cyclase domain	0.49
VC83_02190	IPR019716: Ribosomal protein L53, mitochondrial	0.46
VC83_02191	IPR005606: Sec20	0.46
VC83_02192	IPR000073: Alpha/beta hydrolase fold-1; IPR016812: Protein phosphatase methylesterase, eukaryotic; IPR029058: Alpha/Beta hydrolase fold	0.46
VC83_02193	IPR019431: Protein of unknown function DUF2417; IPR029058: Alpha/Beta hydrolase fold	0.46
VC83_02194	IPR008921: DNA polymerase III, clamp loader complex, gamma/delta/delta subunit, C-terminal; IPR013748: Replication factor C, C-terminal; IPR027417: P-loop containing nucleoside triphosphate hydrolase	0.46
VC83_02195	IPR013715: Domain of unknown function DUF1746	0.46
VC83_02196	IPR001330: PFTB repeat; IPR002365: Terpene synthase, conserved site; IPR008930: Terpenoid cyclases/protein prenyltransferase alpha-alpha toroid; IPR018333: Squalene cyclase; IPR032696: Squalene cyclase, C-terminal; IPR032697: Squalene cyclase, N-terminal	0.51
VC83_03085		1.70
VC83_03876		0.58
VC83_04068	IPR000408: Regulator of chromosome condensation, RCC1; IPR009091: Regulator of chromosome condensation 1/beta-lactamase-inhibitor protein II	0.60
VC83_04069	IPR008207: Signal transduction histidine kinase, phosphotransfer (Hpt) domain	0.60
VC83_04073	IPR003663: Sugar/inositol transporter; IPR005828: Major facilitator, sugar transporter-like; IPR020846: Major facilitator superfamily domain	2.04
VC83_04182		0.54
VC83_04623		1.96
VC83_04673		2.07
VC83_04981		0.75
VC83_04982	IPR002921: Fungal lipase-like domain; IPR029058: Alpha/Beta hydrolase fold	0.61

VC83_04983	IPR001789: Signal transduction response regulator, receiver domain; IPR003594: Histidine kinase-like ATPase, C-terminal domain; IPR003661: Signal transduction histidine kinase, dimerisation/phosphoacceptor domain; IPR004358: Signal transduction histidine kinase-related protein, C-terminal; IPR005467: Histidine kinase domain; IPR011006: CheY-like superfamily	0.78
VC83_04986		1.41
VC83_05166	IPR000073: Alpha/beta hydrolase fold-1; IPR022742: Serine aminopeptidase, S33; IPR029058: Alpha/Beta hydrolase fold	1.39
VC83_05353	IPR017877: Myb-like domain	1.18
VC83_05419		1.28
VC83_05436		0.63
VC83_05621		0.51
VC83_05622	IPR001849: Pleckstrin homology domain; IPR011993: PH domain-like	0.42
VC83_05736	IPR007087: Zinc finger, C2H2; IPR007219: Transcription factor domain, fungi; IPR013087: Zinc finger C2H2-type/integrase DNA-binding domain; IPR015880: Zinc finger, C2H2-like	0.70
VC83_06077	IPR000634: Serine/threonine dehydratase, pyridoxal-phosphate-binding site; IPR001721: ACT-like domain; IPR001926: Tryptophan synthase beta subunit-like PLP-dependent enzyme; IPR005787: Threonine dehydratase, biosynthetic	1.51
VC83_06532		0.61
VC83_06534		0.67
VC83_06796	IPR001107: Band 7 domain; IPR001597: Aromatic amino acid beta-eliminating lyase/threonine aldolase; IPR001972: Stomatin family; IPR015421: Pyridoxal phosphate-dependent transferase, major region, subdomain 1; IPR015422: Pyridoxal phosphate-dependent transferase, major region, subdomain 2; IPR015424: Pyridoxal phosphate-dependent transferase	1.77
VC83_07009	IPR001138: Zn(2)-C6 fungal-type DNA-binding domain; IPR021858: Protein of unknown function DUF3468	1.17
VC83_07015		0.68
VC83_07257	IPR007604: CP2 transcription factor	1.21
VC83_07548	IPR001623: DnaJ domain	0.60
VC83_07549	IPR001452: SH3 domain; IPR007223: Peroxin 13, N-terminal; IPR011511: Variant SH3 domain	0.60
VC83_07592	IPR001680: WD40 repeat; IPR007111: NACHT nucleoside triphosphatase; IPR015943: WD40/YVTN repeat-like-containing domain; IPR017986: WD40-repeat-containing domain; IPR018391: Pyrrolo-quinoline quinone beta-propeller repeat; IPR019775: WD40 repeat, conserved site; IPR020472: G-protein beta WD-40 repeat; IPR027417: P-loop containing nucleoside triphosphate hydrolase	0.97
VC83_07687		0.72
VC83_07777	IPR027973: Protein of unknown function DUF4602	0.56
VC83_07864	IPR003010: Carbon-nitrogen hydrolase	1.84
VC83_08120	IPR001138: Zn(2)-C6 fungal-type DNA-binding domain; IPR002409: Aflatoxin biosynthesis regulatory protein; IPR007219: Transcription factor domain, fungi	0.72
VC83_08277	IPR002112: Transcription factor Jun; IPR004827: Basic-leucine zipper domain; IPR020956: Transcription factor Aft1, osmotic stress domain; IPR021755: Transcription factor Aft1, HRA domain; IPR021756: Transcription factor Aft1, HRR domain	1.38
VC83_08365	IPR024436: Domain of unknown function DUF3824	1.08

VC83_08400		0.53
VC83_08446	IPR001128: Cytochrome P450; IPR002401: Cytochrome P450, E-class, group I; IPR017972: Cytochrome P450, conserved site	0.89
VC83_08481		0.83
VC83_08499	IPR013078: Histidine phosphatase superfamily, clade-1; IPR029033: Histidine phosphatase superfamily	2.42
VC83_08758	IPR003590: Leucine-rich repeat, ribonuclease inhibitor subtype; IPR032675: Leucine-rich repeat domain, L domain-like	0.75
VC83_08785		1.36
VC83_08799	IPR001012: UBX domain; IPR009060: UBA-like; IPR012989: SEP domain; IPR029071: Ubiquitin-related domain	1.68
VC83_08838	IPR000504: RNA recognition motif domain; IPR001876: Zinc finger, RanBP2-type; IPR012337: Ribonuclease H-like domain; IPR012677: Nucleotide-binding alpha-beta plait domain; IPR013520: Exonuclease, RNase T/DNA polymerase III	1.08
VC83_08889	IPR018565: Kinetochore subunit NKP2	0.61
VC83_09217		0.84
VC83_09414	IPR000719: Protein kinase domain; IPR002290: Serine/threonine/dual specificity protein kinase, catalytic domain; IPR008271: Serine/threonine-protein kinase, active site; IPR011009: Protein kinase-like domain; IPR017441: Protein kinase, ATP binding site	1.18
VC83_09491	IPR001650: Helicase, C-terminal; IPR011991: Winged helix-turn-helix DNA-binding domain; IPR014001: Helicase superfamily 1/2, ATP-binding domain; IPR022698: Protein of unknown function DUF3505; IPR027417: P-loop containing nucleoside triphosphate hydrolase	1.46
VC83_09503	IPR003959: ATPase, AAA-type, core; IPR003960: ATPase, AAA-type, conserved site; IPR027417: P-loop containing nucleoside triphosphate hydrolase	0.47
VC83_09504		0.42
VC83_09506	IPR002327: Cytochrome c, class IA/ IB; IPR009056: Cytochrome c-like domain	0.39
VC83_09507		0.39
VC83_09511	IPR013883: Transcription factor Iwr1	0.54
VC83_09512		0.44
VC83_09513	IPR012336: Thioredoxin-like fold	0.42
VC83_09514	IPR001878: Zinc finger, CCHC-type	0.56
VC83_09549		0.49
VC83_09550		0.53
VC83_09551		0.54
VC83_09553		0.56
VC83_09559	IPR002213: UDP-glucuronosyl/UDP-glucosyltransferase; IPR003903: Ubiquitin interacting motif; IPR004276: Glycosyltransferase family 28, N-terminal domain	0.39
VC83_09560		0.53
VC83_09561	IPR001958: Tetracycline resistance protein TetA/multidrug resistance protein MdtG; IPR011701: Major facilitator superfamily; IPR020846: Major facilitator superfamily domain	0.47
VC83_09567		0.39
VC83_09570		4.37

VC83_09577	IPR001878: Zinc finger, CCHC-type	0.42
VC83_09689	NA	0.65

Most of the genes in the *P. destructans* genome did not show evidence of CNVs for the North American samples. Of the genomic regions with significant CNVs in North America, on average 82.9% represent gene copy losses and 17.1% are gene copy gains. Most CNVs are exclusive to one or few isolates only, with a low average gene copy number across the genome. Furthermore, the type of CNV, partially/fully spanning gene CDS, differs in frequency between different populations (Figure 4.2). Among these isolates, we found fewer gene copy gains than gene copy losses within the North American *P. destructans* population. Gene copy losses may indicate that gene CNVs are hypervariable in the *P. destructans* genome, and that there is substantial selective pressure acting on the *P. destructans* genome since introduction into a novel environment. As such, decreases in gene copies spanning both partial and full gene CDS can have consequences for gene function and can contribute to adaptation (Fidalgo et al. 2006; Katju and Lynch 2003; Qian and Zhang 2014).

The enriched genes are preferentially grouped to zinc-ion binding (Figure 4.2). A high diversity of zinc finger transcription factors are present in many fungal species (Park et al. 2008). This class of proteins act as key regulators of multiple cellular and developmental processes (Reviewed in MacPherson et al. 2006), including carbon (Felenbok et al. 2001) and amino acid metabolism (Kohlhaw 2003), and nitrogen utilization (Davis et al. 1996). Interestingly, zinc-ions are particularly important in the maintenance of multiple pathways for fungal pathogenesis (Reviewed in Staats et al. 2013). The mediation of zinc uptake or storage via membrane transporters or zinc-binding proteins in zinc-depleting conditions are known to lead to reduced fungal growth (Lulloff et al. 2004). Among the enriched zinc-binding protein genes, alcohol dehydrogenase (Adh1) is abundant in *P. destructans*. In zinc-limiting conditions, such as that of the host environment, zinc storage pathways via zinc-dependent alcohol dehydrogenases are down-regulated (Eide 2009). Many different kinds of cellular stress can occur under zinc deprivation. Pathogenic species can modulate zinc storage in response to a diverse set of

stimuli from the host and external environment (Park et al. 2013). During *P. destructans* pathogenesis, increasing gene copies of zinc binding proteins may be beneficial for coping with zinc deprivation and cellular stress.

Previous studies have demonstrated the association of fungal pathogenesis with expansion in gene families with catalytic potential such as hydrolases, secreted proteins, and carbohydrate recognition/binding (Powell et al. 2008). Genes with increased copy number in North American isolates are significantly enriched in several categories compared to some European *P. destructans* strains (Figure 4.2). The majority of these hydrolase genes belong to a single CAZyme family GH18, with targeted activity to the degradation of chitinase for nutritional needs (Reviewed in Hartl et al. 2012). As the usage of environmental chitin sources by *P. destructans* appears to be limited (Raudabaugh and Miller 2013; Reynolds and Barton 2014), their role may instead be in autolysis and recycling of the fungal mycelia (Reeder et al. 2017). *P. destructans* only has approximately 1/3 of the total CAZyme genes present in other *Pseudogymnoascus* species, which has likely influenced *P. destructans*'s ability to utilize certain carbohydrate sources (Palmer et al. 2018). Copy number increases of genes within carbon metabolic pathways would be consistent with rapid adaptation within *P. destructans* to increase acquisition of organic carbon from the environment. Initially, *P. destructans* might have lost multiple CAZyme pathways necessary for living in soil/sediments, as they were no longer required in its pathogenic lifestyle. Carbon sources can modulate cell wall structure and virulence in fungal pathogens (Ene et al. 2012a; Ene et al. 2012b), so changes in cell wall remodeling could be due to changes in metabolic pathways that accompany the shift from abiotic to infectious niches. It is possible that changes in cell wall structures are caused by changes in metabolic function during infection, rather than direct adaptation to the host.

4.6.2 The Contribution of CNVs to Population Structure in North America

Differences in CNVs among populations can be the result of selection favoring mutations that are advantageous in a particular environment. We identified multiple CNV clusters within North America which are based on substantial differentiation in CNV of genes. There is little variation within these North American clusters compared to those consisting of isolates from Europe/Asia. All CNV clusters unique to North America are more closely related to the cluster containing the closest related European strain than to other European clusters (Figure 4.5B). In comparison, the clusters assigned using SNP genotypes are not as informative as CNV profiles and cannot distinguish lineages within North America or between European/Asian strains. As CNVs can accumulate at a rate higher than SNPs (Zhang et al. 2009; Redon et al. 2006; Dorant et al. 2020), these results demonstrate the utility of CNVs in tracking clonal structure in *P. destructans* populations.

We found no correlation between the rate of gene copy gain/loss events and the distance separating hibernacula in North America (Figure 4.11). In addition, cumulative gene copy gain/loss events between CNV lineages differ between lineages with low variation within each cluster (Figure 4.6). Specific CNV events may have contributed to adaptation processes enabling greater spread/persistence through the environment. For example, members of CNV Cluster 6 have increased gene copies within the hypervariable region on scaffold KV441389. These variations may have resulted in clonal interference between lineages, provided that the selective advantage/disadvantage influences the fate of respective clonal lineages. Taken together, the wide distribution of clusters throughout North America, suggest that *P. destructans* CNV lineages may have diverged early on during the spread of WNS.

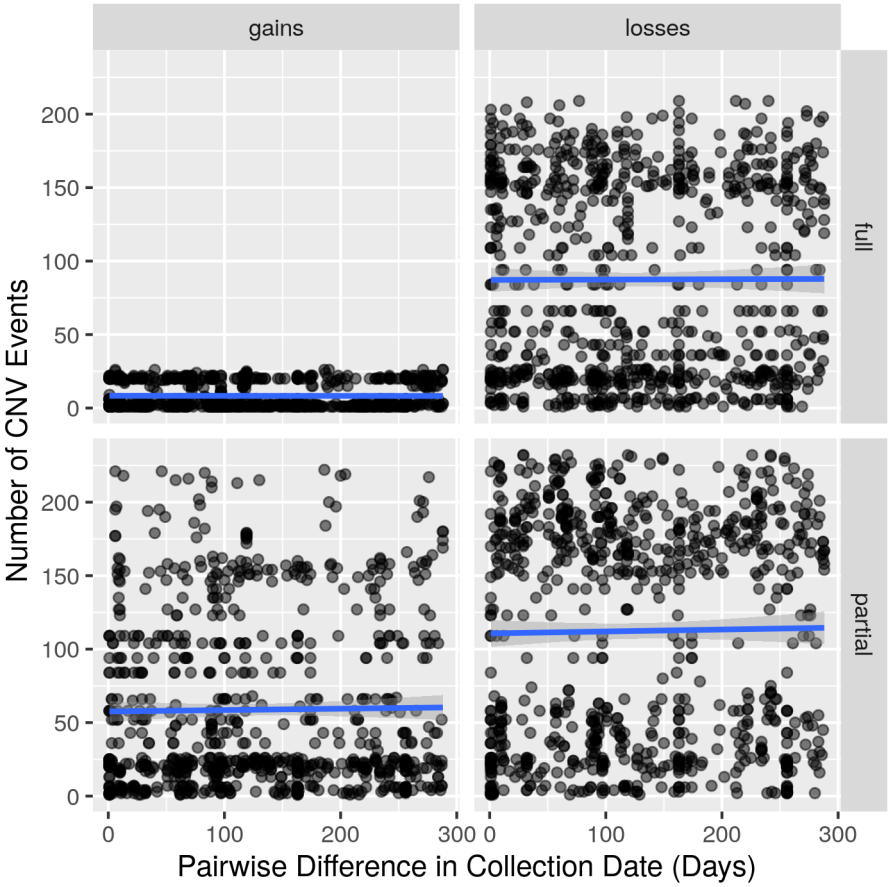

FIGURE 4.11: Pairwise total of gene gain/loss as represented by CNV regions that partially or completely span gene sequences. Here we show the correlation between the difference in gene copy gain/loss events with the pairwise difference in sample dates between *P. destructans* isolates in North America.

4.6.3 The Impacts of Positive and Purifying Selection on *P. destructans*

Signatures of positive selection within the *P. destructans* genome may represent the occurrence of a relatively recent selective sweep event(s) in the ancestral population. All members of the invasive clonal lineage in North America carry mutations within several genes under positive selection. Interestingly, one of these genes is the DNA repair protein RAD50, which is involved in DNA double-strand break repair, telomere

maintenance and meiotic recombination (Reviewed in Goldman et al. 2002). Despite the high sensitivity of *P. destructans* to UV stress and the loss of other genes within the DNA repair pathway compared to *Pseudogymnoascus* allies (Palmer et al. 2018), the regulation of RAD50 may provide advantages by maintaining genome integrity.

Signatures of positive selection were likely present prior to the introduction of WNS to North America. As the earliest known isolate, reference strain NHWC 20631-21 was sampled from an infected bat from Williams Hotel Mine, NY in 2008 (Drees et al. 2016). Mutations that occurred prior to the introduction could be considered as putative targets for pre-adaptation, in which invasive populations represent a subset of the ancestral population that have adapted to enable/promote proliferation and spread within the novel environment. Pre-adaptation has been proposed to explain the spread of other fungal pathogens, leading to the successful establishment outside of their native range or into novel or extreme environments (Gostinčar et al. 2009; Robert and Casadevall 2009). The founding population of invasive *P. destructans* may have been sufficiently robust, enabling persistence across a wider range of environmental conditions without obligate adaptation to local conditions.

Compared to the genes under selection identified using dN/dS ratios, `RAiSD` incorporates more information into deciding where regions of positive selection exist in the genome and is not biased to contrasts made between populations. During a selective sweep, a beneficial mutation will increase in frequency in the population, resulting in hitchhiking effects of reduced variability in the flanking sequence, high LD on each side of a beneficial mutation and low LD between loci, and a shift in the site frequency spectrum toward low and high-frequency derived variants. We identified a number of putative selective sweep regions, containing various genes for oxidoreductase processes, ion binding/transport, components of the cell membrane, and structural maintenance of chromosomes (Table 4.4). Regions past the threshold have a high probability of

being under positive selection caused by a selective sweep. Of particular interest is the Smc5-Smc6 complex which is involved in DNA repair and maintaining cell cycle arrest following DNA damage in Eukaryotes (Reviewed in Aragón 2018). This positively selected complex may have allowed this invasive pathogen to deal with environmental stresses in North America not typical in its home range in Eurasia.

Aside from evidence of positive selection, we have also found evidence of purifying selection in the North American population of *P. destructans*. The high frequency of common SNPs is consistent with signatures of deleterious mutations and purifying selection against such mutations. Furthermore, analyses of dN/dS ratios have identified a number of genes under purifying selection within almost all North American strains. Of these genes, one is retinoic acid induced 16-like protein which may play an important role in *P. destructans* pathogenesis. Retinoic acid is the biologically active metabolite of vitamin A which controls the normal immune system development as a modulator of both innate and adaptive immune responses in many animals. As the activity of this gene product is likely activated by a component of mammalian immune systems, deleterious mutations in this gene may not be maintained due to selection pressures from host bats (Johnson et al. 2015; Bouma et al. 2010).

4.7 Conclusion

The use of genome sequencing and molecular markers are essential for tracking the spread and evolution of a pathogen population in an ongoing epizootic. Typically, SNPs can be used to determine the rate of mutation accumulation or to resolve population structure in large cohorts. However, base substitution rate is generally low and for a recently expanding clonal pathogen, SNPs provide very limited power in discriminating closely related strains and populations. Here, we have shown the utility of CNVs in distinguishing clonal lineages in the North American *P. destructans* population. Furthermore, CNVs

appear to play a role in generating novel genetic diversity after a bottleneck event, with evidence of adaptive significance. Here, the specific genes with signals of positive selection likely reflect mutations accumulated within the *P. destructans* ancestral range in Europe, and therefore represent possible pre-adaptation prior to the introduction to North America. In addition, we have identified putative regions impacted by a selective sweep within European *P. destructans* populations. However, since introduction, purifying selection is common within the invasive *P. destructans* population. Taken together, the combined analyses using both SNPs and CNVs suggest that a diversity of genetic changes have happened in the North American *P. destructans* population, potentially contributing to its rapid spread and adaptation in this novel ecological niche.

Chapter 5

General Conclusion

5.1 Fungal Epizootics: A Growing Problem

While fungi have shaped the ecosystem in many different ways (Robinson 1990), in recent years fungal pathogens have been responsible for large-scale complications to human health, agriculture, and the biodiversity of wildlife (Savary et al. 2012; Fisher et al. 2020). Fungal outbreaks have been recorded since the early twentieth Century (Pijper, Pullinger, et al. 1927), but only a small proportion of fungal genera are well described in medical literature (Hoog et al. 2016). Outbreaks of systemic fungal disease remained relatively rare in humans until recently. Without precedence, the diagnoses of systemic fungal infections remain difficult (Brown et al. 2012). Furthermore, relatively little attention paid to fungal epidemics and research investment on fungal pathogens remains disproportionate to the incidence of infections: i.e. cryptococcosis, 0.5% of investment with 180 000 cases of mortality, malaria and tuberculosis 35.5% of the total, with 429 000 and 1.6 million cases of mortality, respectively (Moran et al. 2015; Rajasingham et al. 2017).

The increasing prevalence of fungal epidemics emphasizes the importance of understanding how fungal pathogens spread and invade new ecological niches (Seyedmousavi

et al. 2018). Approximately a third of all food crops in North America (N. America) are destroyed by fungal pathogens annually (Fisher et al. 2012). Crop losses due to fungal infections in global production of rice, wheat, maize, potatoes, and soybeans result in the loss of enough food to feed 600 million people (Fisher et al. 2012), which also have a disproportionate impact on human populations in developing countries (Rodrigues 2016; Rodrigues 2018).

Invasive fungal pathogens bring significant concerns for the conservation and health of our ecosystems. The rapid spread and persistence of *Pseudogymnoascus destructans* (*P. destructans*) across N. America has led to the continued loss of bat populations. Many of the bat species impacted by White-Nose Syndrome (WNS) hold important ecological positions in N. American ecosystems, and the loss of these bats may have dramatic ecological and economic consequences. For example, bats are predators of many insect pests, and as their populations decline the ecosystem services that they provide to the agricultural industry could also disappear. At the population level, the loss of diversity in bat populations would result in further destabilization and greater susceptibility to changes in climate or other disruptions to bat health in the future. Given that WNS continues to rapidly expand in N. America, an increased understanding of the causative agent, *P. destructans*, could contribute to wildlife management decisions. As much of the fungal biology of this pathogen remains undescribed, continued investigation into the pathogenicity or growth and survival of *P. destructans* outside of the host could contribute to the development of mitigation of additional infections. Cooperation and integration of mycologist and wildlife biologists would be crucial to control the future spread of WNS

5.2 Summary of Thesis

In Chapter 2 of this thesis, I compared phenotypic diversity and the impact of temperature on conidium viability in *P. destructans* isolates from different areas of the WNS epizootic. This research emphasizes the constraints that could impact conidial germination in the environment, which are likely to be variable across N. America and impact the rates of WNS transmission. The main results of this research suggest that *P. destructans* isolates have lowered tolerance to high temperatures since first introduction to N. America. Among the evolved isolates, novel genetic variations in the form of single nucleotide polymorphisms were also identified. These mutations may be related to the adaptation of *P. destructans* to N. American conditions. Signals of genetic adaptation were identified later in Chapter 4 using a larger cohort of the N. American population that also included copy number variants.

In Chapter 3 of this thesis, I explored population genetic structure and the environmental factors that may have influenced the transmission and gene flow of *P. destructans* between hibernacula. We found evidence that population structure in N. America has been influenced by the level of human activity present across the landscape more so than the null expectation of a stepping-stone model for dispersal. The seasonal prevalence of *P. destructans* can also influence transmission. Therefore, to better understand rates of transmission, measurements of the viable fungal load present on free-flying bats after summer is necessary. Our results suggest that the genetic changes accumulated during the spread of WNS and the impact that they have on the survival and reproduction should be considered in designing further prevention and management strategies. There is increasing evidence that *P. destructans* cells are detectable on bats well into the summer (Ballmann et al. 2017; Carpenter et al. 2016; Huebschman et al. 2019), but the viable fungal load present on hosts during the hibernative season is not yet known.

The analyses explored in Chapter 4, using both Single Nucleotide Polymorphism

(SNP)s and copy number variations (CNVs), identified multiple signatures of selection within the *P. destructans* genome. In particular, copy number variation (CNV)s present a mechanism for the rapid generation of novel genetic diversity in a clonal population. Following a population bottleneck event, mutations under positive selection could have adaptive significance for a pathogen in a novel environment. However, since introduction and during the ensuing rapid population expansion, purifying selection is likely common within the invasive *P. destructans* population in N. America. Interestingly, my analyses revealed that some of the genes under positive selection were likely on the mutations accumulated within the European *P. destructans* ancestral range. However, signatures of adaptive evolution are commonly found in the N. American population.

Tracking the spread of WNS is made possible through the use of genome sequencing and molecular markers. Rapid and effective genotyping methods are essential for monitoring pathogen population causing wildlife diseases, especially WNS, as the high mobility of host species and airborne nature of pathogens themselves present significant challenges in tracking pathogen transmission. In such studies, recent approaches using high-throughput sequencing have improved discriminatory power compared to less robust methods (Santure et al. 2010; Helyar et al. 2011; Fischer et al. 2017). Typically, SNPs can be used to determine the rate of mutation accumulation or to resolve population structure in large cohorts. However, base substitution rate are generally low, and thus SNPs provide very limited power in discriminating closely related strains and populations for a recently expanding clonal pathogen. In comparison, CNVs may accumulate at a rate that outpaces that of SNPs or even microsatellites. In this thesis, the use of different markers in combination have illuminated more than each method shows alone. For instance, genotype data provided supporting evidence for deviations from the null expectations of strict clonality in N. America.

5.3 The Future of WNS in N. America

Despite more than 10 years of investigation of WNS, the specific factors leading to the exploitation of N. American *Myotis* species by *P. destructans* remain unknown (Wibbelt 2018). Similarly, the virulence factors and mechanisms of *P. destructans* pathogenesis are still not well defined. The term "WNS" was coined based on distinct histological and physiological signs leading to mortality (Meteyer et al. 2009; Reeder et al. 2012). As a syndrome is the terminology given for a group of symptoms that commonly occur together, with the direct cause of mortality not necessarily understood, much still remains unknown about the nature of WNS. One key issue is how N. American and Eurasian bats respond differently to *P. destructans* infections. Clear histopathological criteria associated with deadly and non-deadly *P. destructans* infections would help identify the epidemiologic features of WNS within N. America. For example, are complications from skin lesions solely responsible for mortality? Furthermore, if mortality is not associated with the severe lesions in wing tissues, what other factors likely contribute to the fatal outcome of WNS? In order to solve these problems, more research is required in order to protect the remaining *Myotis* populations.

The extirpation of *Myotis* will undoubtedly continue in N. America, and the full eradication of *P. destructans* from environmental reservoirs is not likely possible. The high connectivity of habitat in N. America makes it unlikely that many refuges for host species exist, resulting in the spread of WNS throughout much of the remaining naïve bat populations (O'Regan et al. 2015). Thus, the primary goal in the mitigation of WNS should be in the control/prevention of the spread of infections to other parts of the continent that have experienced little impact so far. Whether human influence has had much of a direct impact on the continued spread of WNS is yet to be determined, yet persistent disinfection protocols limitation of human traffic between hibernacula would help prevent futher spread.

Several different approaches have been proposed to treat WNS infections and decontaminate *P. destructans* from hibernacula. However, the application of antifungal drugs in a fragile cave ecosystem could result in a cascade of unpredictable consequences (Wibbelt 2015). As a result, other treatments have been suggested to apply a more targeted approach in mitigating the impact of WNS infections on the surrounding environment. Localized heating of bat hibernacula could present a non-invasive treatment for WNS (Boyles and Willis 2010), but may have physiological consequences for maintaining torpor for infected bats. As an alternative to antifungal drugs, probiotics can be used to inhibit invasive transient microorganisms (Grice and Segre 2011; Clay 2014) and is one approach considered in the control of WNS infections. Naturally sourced probiotics can provide protection without upsetting natural flora, which is an approach that has been used to combat chytridiomycosis in amphibians (Bletz et al. 2013; Walke et al. 2015). Since *P. destructans* invasion causes a change in the bat's surface microbial community (Lemieux-Labonté et al. 2017), manipulation of this interaction between pathogen and host microbiome could be used to mitigate the impacts of WNS. The activity of various inhibiting bacterial species have already been described (Hamm et al. 2017), and the testing of probiotic applications have so far been limited to demonstrating that the probiotics have no adverse impact on the health of bats (Hoyt et al. 2015a; Cheng et al. 2017).

References Cited

Adams, R. A. and Hayes, M. A. (2008). Water availability and successful lactation by bats as related to climate change in arid regions of western North America. *J. Anim. Ecol.* 77(6), 1115–1121.

Agapow, P.-M. and Burt, A. (2001). Indices of multilocus linkage disequilibrium. *Mol. Ecol. Notes* 1(1-2), 101–102.

Aguileta, G., Lengelle, J., Marthey, S., Chiapello, H., Rodolphe, F., Gendrault, A., Yockteng, R., Vercken, E., Devier, B., Fontaine, M. C., Wincker, P., Dossat, C., Cruaud, C., Couloux, A., and Giraud, T. (2010). Finding candidate genes under positive selection in Non-model species: examples of genes involved in host specialization in pathogens. *Mol. Ecol.* 19(2), 292–306.

Aguileta, G., Lengelle, J., Chiapello, H., Giraud, T., Viaud, M., Fournier, E., Rodolphe, F., Marthey, S., Ducasse, A., Gendrault, A., Poulain, J., Wincker, P., and Gout, L. (2012). Genes under positive selection in a model plant pathogenic fungus, *Botrytis*. *Infect. Genet. Evol.* 12(5), 987–996.

Ahmed, Y. L., Gerke, J., Park, H.-S., Bayram, Ö., Neumann, P., Ni, M., Dickmanns, A., Kim, S. C., Yu, J.-H., Braus, G. H., and Ficner, R. (2013). The velvet family of fungal regulators contains a DNA-binding domain structurally similar to NF-κB. *PLoS Biol.* 11(12), e1001750.

Alachiotis, N. and Pavlidis, P. (2018). RAiSD detects positive selection based on multiple signatures of a selective sweep and SNP vectors. *Commun Biol* 1, 79.

Alexa, A. and Rahnenfuhrer, J. (2010). topGO: enrichment analysis for gene ontology. *R package version* 2(0).

Ali, S., Gladieux, P., Leconte, M., Gautier, A., Justesen, A. F., Hovmøller, M. S., Enjalbert, J., and de Vallavieille-Pope, C. (2014). Origin, migration routes and worldwide population genetic structure of the wheat yellow rust pathogen *Puccinia striiformis* f.sp. *tritici*. *PLoS Pathog.* 10(1), e1003903.

Ali, S., Leconte, M., Walker, A.-S., Enjalbert, J., and de Vallavieille-Pope, C. (2010). Reduction in the sex ability of worldwide clonal populations of *Puccinia striiformis* f.sp. *tritici*. *Fungal Genet. Biol.* 47(10), 828–838.

Aragón, L. (2018). The Smc5/6 Complex: New and old functions of the enigmatic long-distance relative. *Annu. Rev. Genet.* 52, 89–107.

Arnaud-Haond, S., Migliaccio, M., Diaz-Almela, E., Teixeira, S., Van De Vliet, M. S., Alberto, F., Procaccini, G., Duarte, C. M., and Serrao, E. A. (2007). Vicariance patterns in the Mediterranean Sea: east–west cleavage and low dispersal in the endemic seagrass *Posidonia oceanica*. *J. Biogeogr.* 34(6), 963–976.

Attanayake, R. N., Tennekoon, V., Johnson, D. A., Porter, L. D., Rıo-Mendoza, L. del, Jiang, D., and Chen, W. (2014). Inferring outcrossing in the homothallic fungus *Sclerotinia sclerotiorum* using linkage disequilibrium decay. *Heredity* 113(4), 353–363.

Avila-Flores, R. and Fenton, M. B. (2005). Use of spatial features by foraging insectivorous bats in a large urban landscape. *J. Mammal.* 86(6), 1193–1204.

Aylor, D. E. (1990). The role of intermittent wind in the dispersal of fungal pathogens. *Annu. Rev. Phytopathol.* 28(1), 73–92.

Ballmann, A. E., Torkelson, M. R., Bohuski, E. A., Russell, R. E., and Blehert, D. S. (2017). Dispersal hazards of *Pseudogymnoascus destructans* by bats and human activity at hibernacula in summer. *J. Wildl. Dis.* 53(4), 725–735.

Bandouchova, H., Bartonicka, T., Berkova, H., Brichta, J., Cerny, J., Kovacova, V., Kolarik, M., Köllner, B., Kulich, P., Martınková, N., et al. (2015). *Pseudogymnoascus destructans*: evidence of virulent skin invasion for bats under natural conditions, Europe. *Transbound. Emerg. Dis.* 62(1), 1–5.

Baroncelli, R., Amby, D. B., Zapparata, A., Sarrocco, S., Vannacci, G., Le Floch, G., Harrison, R. J., Holub, E., Sukno, S. A., Sreenivasaprasad, S., and Thon, M. R. (2016). Gene family expansions and contractions are associated with host range in plant pathogens of the genus Colletotrichum. *BMC Genomics* 17, 555.

Bates, D., Mächler, M., Bolker, B., and Walker, S. (2015). Fitting linear mixed-effects models using lme4. *J. Stat. Softw* 67(1), 1–48.

Bayram, O. and Braus, G. H. (2012). Coordination of secondary metabolism and development in fungi: the velvet family of regulatory proteins. *FEMS Microbiol. Rev.* 36(1), 1–24.

Bayram, O., Krappmann, S., Ni, M., Bok, J. W., Helmstaedt, K., Valerius, O., Braus-Stromeyer, S., Kwon, N.-J., Keller, N. P., Yu, J.-H., and Braus, G. H. (2008). VelB/VeA/LaeA complex coordinates light signal with fungal development and secondary metabolism. *Science* 320(5882), 1504–1506.

Bazin, É., Mathé-Hubert, H., Facon, B., Carlier, J., and Ravigné, V. (2013). The effect of mating system on invasiveness: some genetic load may be advantageous when invading new environments. *Biol. Invasions* 16(4), 875–886.

Beeson, W. T., Van V., V., Span, E. A., Phillips, C. M., and Marletta, M. A. (2015). Cellulose degradation by polysaccharide monooxygenases. *Annu. Rev. Biochem.* 84(1), 923–946.

Behie, S. W. and Bidochka, M. J. (2014). Nutrient transfer in plant–fungal symbioses. *Trends Plant. Sci.* 19(11), 734–740.

Bell-Pedersen, D., Dunlap, J. C., and Loros, J. J. (1992). The *Neurospora* circadian clock-controlled gene, ccg-2, is allelic to eas and encodes a fungal hydrophobin required for formation of the conidial rodlet layer. *Genes Dev.* 6(12A), 2382–2394.

Bennati-Granier, C., Garajova, S., Champion, C., Grisel, S., Haon, M., Zhou, S., Fanuel, M., Ropartz, D., Rogniaux, H., Gimbert, I., Record, E., and Berrin, J.-G. (2015). Substrate specificity and regioselectivity of fungal AA9 lytic polysaccharide monooxygenases secreted by *Podospora anserina*. *Biotechnol. Biofuels* 8, 90.

Bernard, R. F., Willcox, E. V., Parise, K. L., Foster, J. T., and McCracken, G. F. (2017). White-nose syndrome fungus, *Pseudogymnoascus destructans*, on bats captured emerging from caves during winter in the southeastern United States. *BMC Zool.* 2(1).

Biek, R. and Real, L. A. (2010). The landscape genetics of infectious disease emergence and spread. *Mol. Ecol.* 19(17), 3515–3531.

Blackwell, M. (2011). The fungi: 1, 2, 3 ... 5.1 million species? *Am. J. Bot.* 98(3), 426–438.

Blasi, B., Tafer, H., Tesei, D., and Sterflinger, K. (2015). From glacier to sauna: RNA-Seq of the human pathogen black fungus Exophiala dermatitidis under varying temperature conditions exhibits common and novel fungal response. *PLoS one* 10(6), e0127103.

Blehert, D. S., Hicks, A. C., Behr, M., Meteyer, C. U., Berlowski-Zier, B. M., Buckles, E. L., Coleman, J. T. H., Darling, S. R., Gargas, A., Niver, R., Okoniewski, J. C., Rudd, R. J., and Stone, W. B. (2009). Bat White-Nose syndrome: an emerging fungal pathogen? *Science* 323(5911), 227.

Bletz, M. C., Loudon, A. H., Becker, M. H., Bell, S. C., Woodhams, D. C., Minbiole, K. P. C., and Harris, R. N. (2013). Mitigating amphibian chytridiomycosis with bioaugmentation: characteristics of effective probiotics and strategies for their selection and use. *Ecol. Lett.* 16(6), 807–820.

Boeva, V., Popova, T., Bleakley, K., Chiche, P., Cappo, J., Schleiermacher, G., Janoueix-Lerosey, I., Delattre, O., and Barillot, E. (2012). Control-FREEC: a tool for assessing copy number and allelic content using next-generation sequencing data. *Bioinformatics* 28(3), 423–425.

Bolger, A. M., Lohse, M., and Usadel, B. (2014). Trimmomatic: a flexible trimmer for Illumina sequence data. *Bioinformatics* 30(15), 2114–2120.

Botts, M. R., Giles, S. S., Gates, M. A., Kozel, T. R., and Hull, C. M. (2009). Isolation and characterization of Cryptococcus neoformans spores reveal a critical role for capsule biosynthesis genes in spore biogenesis. *Eukaryot. cell* 8(4), 595–605.

Bouma, H. R., Carey, H. V., and Kroese, F. G. M. (2010). Hibernation: the immune system at rest? *J. Leukoc. Biol.* 88(4), 619–624.

Boyles, J., Storm, J., and Brack Jr, V. (2008). Thermal benefits of clustering during hibernation: a field test of competing hypotheses on Myotis sodalis. *Funct. Ecol.*, 632–636.

Boyles, J. G. and Willis, C. K. (2010). Could localized warm areas inside cold caves reduce mortality of hibernating bats affected by White-Nose syndrome? *Front. Ecol. Environ.* 8(2), 92–98.

Briggler, J. T. and Prather, J. W. (2003). Seasonal use and selection of caves by the eastern pipistrelle bat (Pipistrellus subflavus). *The American midland naturalist* 149(2), 406–412.

Broad Institute (2015). PicardTools.

Brown, G. D., Denning, D. W., Gow, N. A., Levitz, S. M., Netea, M. G., and White, T. C. (2012). Hidden killers: human fungal infections. *Sci. Transl. Med.* 4(165), 165rv13–165rv13.

Brown, J. K. and Hovmøller, M. S. (2002). Aerial dispersal of pathogens on the global and continental scales and its impact on plant disease. *Science* 297(5581), 537–541.

Brundrett, M. C. (2002). Coevolution of roots and mycorrhizas of land plants. *New phytol.* 154(2), 275–304.

Burmester, A., Shelest, E., Glöckner, G., Heddergott, C., Schindler, S., Staib, P., Heidel, A., Felder, M., Petzold, A., Szafranski, K., et al. (2011). Comparative and functional genomics provide insights into the pathogenicity of dermatophytic fungi. *Genome biol.* 12(1), R7.

Burns, L. E., Frasier, T. R., and Broders, H. G. (2014). Genetic connectivity among swarming sites in the wide ranging and recently declining little brown bat (*Myotis lucifugus*). *Ecol. Evol.* 4(21), 4130–4149.

Calvo, A. M., Lohmar, J. M., Ibarra, B., and Satterlee, T. (2016). 18 Velvet Regulation of Fungal Development. In: *Growth, Differentiation and Sexuality*. Springer, 475–497.

Campbell, L. T. and Carter, D. A. (2006). Looking for sex in the fungal pathogens *Cryptococcus neoformans* and *Cryptococcus gattii*. *FEMS Yeast Res.* 6(4), 588–598.

Campbell, L. J., Walsh, D. P., Blehert, D. S., and Lorch, J. M. (2020). Long-Term Survival of *Pseudogymnoascus destructans* at Elevated Temperatures. *J. Wildl. Dis.* 56(2), 278–287.

Carpenter, G. M., Willcox, E. V., Bernard, R. F., and H. Stiver, W. (2016). Detection of *Pseudogymnoascus destructans* on free-flying male bats captured during summer in the southeastern USA. *J. Wildl. Dis.* 52(4), 922–926.

Casadevall, A. (2005). Fungal virulence, vertebrate endothermy, and dinosaur extinction: is there a connection? *Fungal Genet. Biol.* 42(2), 98–106.

Casadevall, A. (2008). Evolution of Intracellular Pathogens. *Annu. Rev. Microbiol.* 62(1), 19–33.

Casadevall, A., Steenbergen, J. N., and Nosanchuk, J. D. (2003). 'Ready made' virulence and 'dual use' virulence factors in pathogenic environmental fungi — the *Cryptococcus neoformans* paradigm. *CURR OPIN MICROBIOL* 6(4), 332–337.

Chafin, T. K. (2019). FGTpartitioner: Parsimonious delimitation of ancestry breakpoints in large genome-wide SNP datasets. *bioRxiv*, 644088.

Chaturvedi, V., Springer, D. J., Behr, M. J., Ramani, R., Li, X., Peck, M. K., Ren, P., Bopp, D. J., Wood, B., Samsonoff, W. A., et al. (2010). Morphological and molecular characterizations of psychrophilic fungus Geomyces destructans from New York bats with white nose syndrome (WNS). *PLoS one* 5(5), e10783.

Cheng, T. L., Mayberry, H., McGuire, L. P., Hoyt, J. R., Langwig, K. E., Nguyen, H., Parise, K. L., Foster, J. T., Willis, C. K. R., Kilpatrick, A. M., and Frick, W. F. (2017). Efficacy of a probiotic bacterium to treat bats affected by the disease White-Nose syndrome. *J. Appl. Ecol.* 54(3), 701–708.

Chibucos, M. C., Crabtree, J., Nagaraj, S., Chaturvedi, S., and Chaturvedi, V. (2013). Draft Genome Sequences of Human Pathogenic Fungus *Geomyces pannorum* Sensu Lato and Bat White Nose Syndrome Pathogen *Geomyces* (*Pseudogymnoascus*) *destructans*. *Genome Announc.* 1(6).

Chow, E. W. L., Morrow, C. A., Djordjevic, J. T., Wood, I. A., and Fraser, J. A. (2012). Microevolution of *Cryptococcus neoformans* driven by massive tandem gene amplification. *Mol. Biol. Evol.* 29(8), 1987–2000.

Cingolani, P., Platts, A., Wang, L. L., Coon, M., Nguyen, T., Wang, L., Land, S. J., Lu, X., and Ruden, D. M. (2012). A program for annotating and predicting the effects of single nucleotide polymorphisms, SnpEff: SNPs in the genome of Drosophila melanogaster strain w1118; iso-2; iso-3. *Fly* 6(2), 80–92.

Clay, K. (2014). EDITORIAL: Defensive symbiosis: a microbial perspective. *Funct. Ecol.* 28(2), 293–298.

Coil, D., Jospin, G., and Darling, A. E. (2015). A5-miseq: an updated pipeline to assemble microbial genomes from Illumina MiSeq data. *Bioinformatics* 31(4), 587–589.

Conesa, A. and Götz, S. (2008). Blast2GO: A comprehensive suite for functional analysis in plant genomics. *Int. J. Plant Genomics* 2008, 619832.

Cryan, P. M. (2011). Wind Turbines as Landscape Impediments to the Migratory Connectivity of Bats. *Environ. Law* 41(2), 355–370.

Cryan, P. M., Meteyer, C. U., Boyles, J. G., and Blehert, D. S. (2010). Wing pathology of White-Nose syndrome in bats suggests life-threatening disruption of physiology. *BMC Biol.* 8, 135.

Davis, M. A., Small, A. J., Kourambas, S., and Hynes, M. J. (1996). The tamA gene of *Aspergillus nidulans* contains a putative zinc cluster motif which is not required for gene function. *J. Bacteriol.* 178(11), 3406–3409.

Davis, W. H. (1970). Hibernation: Ecology and Physiological Ecology. In: *Biology of Bats*, 265–300.

Davy, C. M., Martinez-Nunez, F., Willis, C. K. R., and Good, S. V. (2015). Spatial genetic structure among bat hibernacula along the leading edge of a rapidly spreading pathogen. *Conserv. Genet.* (APRIL), 1013–1024.

de Hoog, G. S., Ahmed, S. A., Danesi, P., Guillot, J., and Gräser, Y. (2018). Distribution of Pathogens and Outbreak Fungi in the Fungal Kingdom. In: *Emerging and Epizootic Fungal Infections in Animals*, 3–16.

De Mendiburu, F. (2014). Agricolae: statistical procedures for agricultural research. *R package version.*

de Vienne, D. M., Refrégier, G., López-Villavicencio, M., Tellier, A., Hood, M. E., and Giraud, T. (2013). Cospeciation vs host-shift speciation: methods for testing, evidence from natural associations and relation to coevolution. *New Phytol.* 198(2), 347–385.

Delcher, A. L., Salzberg, S. L., and Phillippy, A. M. (2003). Using MUMmer to identify similar regions in large sequence sets. *Curr. Protoc. Bioinformatics* Chapter 10, Unit 10.3.

Desprez-Loustau, M.-L., Robin, C., Buée, M., Courtecuisse, R., Garbaye, J., Suffert, F., Sache, I., and Rizzo, D. M. (2007). The fungal dimension of biological invasions. *Trends Ecol. Evol.* 22(9), 472–480.

Dilmaghani, A., Gladieux, P., Gout, L., Giraud, T., Brunner, P. C., Stachowiak, A., Balesdent, M.-H., and Rouxel, T. (2012). Migration patterns and changes in population biology associated with the worldwide spread of the oilseed rape pathogen *Leptosphaeria maculans*. *Mol. Ecol.* 21(10), 2519–2533.

Dixon, M. D. (2012). Relationship between land cover and insectivorous bat activity in an urban landscape. *Urban Ecosyst.* 15(3), 683–695.

Dobrowolski, M. P., Tommerup, I. C., Shearer, B. L., and O'Brien, P. A. (2003). Three Clonal Lineages of *Phytophthora cinnamomi* in Australia Revealed by Microsatellites. *Phytopathology* 93(6), 695–704.

Dorant, Y., Cayuela, H., Wellband, K., Laporte, M., Rougemont, Q., Mérot, C., Normandeau, E., Rochette, R., and Bernatchez, L. (2020). Copy number variants outperform SNPs to reveal genotype-temperature association in a marine species.

Drees, K. P., Lorch, J. M., Puechmaille, S. J., Parise, K. L., Wibbelt, G., Hoyt, J. R., Sun, K., Jargalsaikhan, A., Dalannast, M., Palmer, J. M., Lindner, D. L., Marm Kilpatrick, A., Pearson, T., Keim, P. S., Blehert, D. S., and Foster, J. T. (2017a). Phylogenetics of a Fungal Invasion: Origins and Widespread Dispersal of White-Nose Syndrome. *MBio* 8(6), e01941–17.

Drees, K. P., Palmer, J. M., Sebra, R., Lorch, J. M., Chen, C., Wu, C.-C., Bok, W., Keller, N. P., Blehert, D. S., Cuomo, C. A., Lindner, D. L., and Foster, T. (2016). Use of Multiple Sequencing Technologies To Produce a High-Quality Genome of the Fungus *Pseudogymnoascus destructans* , the Causative Agent of Bat White-Nose Syndrome. *Genome Announc.* 4(3), 4–5.

Drees, K. P., Parise, K. L., Rivas, S. M., Felton, L. L., Bastien, S., Puechmaille, J., Keim, P., and Foster, J. T. (2017b). Characterization of Microsatellites in *Pseudogymnoascus destructans* for White-nose Syndrome Genetic Analysis. *J. Wildl. Dis* 53(4), 0–0.

Duchamp, J. E. and Swihart, R. K. (2008). Shifts in bat community structure related to evolved traits and features of human-altered landscapes. *Landsc. Ecol.* 23(7), 849–860.

Duplessis, S., Cuomo, C. A., Lin, Y.-C., Aerts, A., Tisserant, E., Veneault-Fourrey, C., Joly, D. L., Hacquard, S., Amselem, J., Cantarel, B. L., Chiu, R., Coutinho, P. M., Feau, N., Field, M., Frey, P., Gelhaye, E., Goldberg, J., Grabherr, M. G., Kodira, C. D., Kohler, A., Kües, U., Lindquist, E. A., Lucas, S. M., Mago, R., Mauceli, E., Morin, E., Murat, C., Pangilinan, J. L., Park, R., Pearson, M., Quesneville, H., Rouhier, N., Sakthikumar, S., Salamov, A. A., Schmutz, J., Selles, B., Shapiro, H., Tanguay, P., Tuskan, G. A., Henrissat, B., Van de Peer, Y., Rouzé, P., Ellis, J. G., Dodds, P. N., Schein, J. E., Zhong, S., Hamelin, R. C., Grigoriev, I. V., Szabo, L. J., and Martin, F. (2011). Obligate biotrophy features unraveled by the genomic analysis of rust fungi. *Proc. Natl. Acad. Sci. U. S. A.* 108(22), 9166–9171.

Eide, D. J. (2009). Homeostatic and adaptive responses to zinc deficiency in *Saccharomyces cerevisiae*. *J. Biol. Chem.* 284(28), 18565–18569.

Elliot, S. L., Blanford, S., and Thomas, M. B. (2002). Host–pathogen interactions in a varying environment: temperature, behavioural fever and fitness. *Proc. Royal Soc. B* 269(1500), 1599–1607.

Emerson, J. J., Cardoso-Moreira, M., Borevitz, J. O., and Long, M. (2008). Natural selection shapes genome-wide patterns of copy-number polymorphism in *Drosophila melanogaster*. *Science* 320(5883), 1629–1631.

Ene, I. V., Adya, A. K., Wehmeier, S., Brand, A. C., MacCallum, D. M., Gow, N. A. R., and Brown, A. J. P. (2012a). Host carbon sources modulate cell wall architecture, drug resistance and virulence in a fungal pathogen. *Cell. Microbiol.* 14(9), 1319–1335.

Ene, I. V. and Bennett, R. J. (2014). The cryptic sexual strategies of human fungal pathogens. *Nat. Rev. Microbiol.* 12(4), 239–251.

Ene, I. V., Heilmann, C. J., Sorgo, A. G., Walker, L. A., Koster, C. G. de, Munro, C. A., Klis, F. M., and Brown, A. J. P. (2012b). Carbon source-induced reprogramming of the cell wall proteome and secretome modulates the adherence and drug resistance of the fungal pathogen *Candida albicans*. *PROTEOMICS* 12(21), 3164–3179.

Enjalbert, J., Duan, X., Leconte, M., Hovmøller, M. S., and de Vallavieille-Pope, C. (2005). Genetic evidence of local adaptation of wheat yellow rust (*Puccinia striiformis f. sp. tritici*) within France. *Mol. Ecol.* 14(7), 2065–2073.

Enoch, D., Ludlam, H., and Brown, N. (2006). Invasive fungal infections: a review of epidemiology and management options. *J. Med. Microbiol.* 55(7), 809–818.

Ernst, J. F. (2000). Transcription factors in *Candida albicans* – environmental control of morphogenesis. *Microbiology* 146(8), 1763–1774.

Etten, J. van (2017). R Package gdistance: Distances and Routes on Geographical Grids. *J. Stat. Softw* 76(13).

Facon, B., Genton, B. J., Shykoff, J., Jarne, P., Estoup, A., and David, P. (2006). A general eco-evolutionary framework for understanding bioinvasions. *Trends Ecol. Evol.* 21(3), 130–135.

Feau, N., Lauron-Moreau, A., Piou, D., Marçais, B., Dutech, C., and Desprez-Loustau, M.-L. (2012). Niche partitioning of the genetic lineages of the oak powdery mildew complex. *Fungal Ecol.* 5(2), 154–162.

Felenbok, B., Flipphi, M., and Nikolaev, I. (2001). Ethanol catabolism in *Aspergillus nidulans*: a model system for studying gene regulation. *Prog. Nucleic Acid Res. Mol. Biol.* 69, 149–204.

Fernández-López, J. and Schliep, K. (2019). rWind: download, edit and include wind data in ecological and evolutionary analysis. *Ecography* 42(4), 804–810.

Fidalgo, M., Barrales, R. R., Ibeas, J. I., and Jimenez, J. (2006). Adaptive evolution by mutations in the FLO11 gene. *Proc. Natl. Acad. Sci. U. S. A.* 103(30), 11228–11233.

Fillinger, S., Chaveroche, M. K., Dijck, P. van, Vries, R. de, Ruijter, G., Thevelein, J., and d'Enfert, C. (2001). Trehalose is required for the acquisition of tolerance to a variety of stresses in the filamentous fungus *Aspergillus nidulans*. *Microbiology* 147(Pt 7), 1851–1862.

Fischer, M. C., Rellstab, C., Leuzinger, M., Roumet, M., Gugerli, F., Shimizu, K. K., Holderegger, R., and Widmer, A. (2017). Estimating genomic diversity and population differentiation - an empirical comparison of microsatellite and SNP variation in *Arabidopsis halleri*. *BMC Genomics* 18(1), 69.

Fisher, M. C., Henk, D. a., Briggs, C. J., Brownstein, J. S., Madoff, L. C., McCraw, S. L., and Gurr, S. J. (2012). Emerging fungal threats to animal, plant and ecosystem health. *Nature* 484(7393), 186–194.

Fisher, M. C., Gurr, S. J., Cuomo, C. A., Blehert, D. S., Jin, H., Stukenbrock, E. H., Stajich, J. E., Kahmann, R., Boone, C., Denning, D. W., Gow, N. A. R., Klein, B. S., Kronstad, J. W., Sheppard, D. C., Taylor, J. W., Wright, G. D., Heitman, J., Casadevall, A., and Cowen, L. E. (2020). Threats Posed by the Fungal Kingdom to Humans, Wildlife, and Agriculture. *MBio* 11(3).

Fisher, M., Gow, N., and Gurr, S. (2016). Tackling emerging fungal threats to animal health , food security and ecosystem resilience. *Philos. Trans. R. Soc. Lond. B Biol. Sci.* 371(1709), 1–6.

Fisher, R. A. (2004). The nature of adaptation. In: *Evolution*. Ed. by M. Ridley. 2nd ed. New York: Oxford Univesity Press, 85–91.

Flory, A. R., Kumar, S., Stohlgren, T. J., and Cryan, P. M. (2012). Environmental conditions associated with bat White-Nose syndrome mortality in the north-eastern United States. *J. Appl. Ecol.* 49(3), 680–689.

Foley, J., Clifford, D., Castle, K., Cryan, P., and Ostfeld, R. S. (2011). Investigating and managing the rapid emergence of White-Nose syndrome, a novel, fatal, infectious disease of hibernating bats. *Conserv. Biol.* 25(2), 223–231.

Forsythe, A., Giglio, V., Asa, J., and Xu, J. (2018). Phenotypic divergence along geographic gradients reveals potential for rapid adaptation of the White-nose Syndrome pathogen, *Pseudogymnoascus destructans*, in North America. *Appl. Environ. Microbiol.*, AEM–00863.

Freese, E. B., Chu, M. I., and Freese, E. (1982). Initiation of yeast sporulation by partial carbon, nitrogen, or phosphate deprivation. *J. bacteriol.* 149(3), 840–851.

Frenkel, O., Peever, T. L., Chilvers, M. I., Ozkilinc, H., Can, C., Abbo, S., Shtienberg, D., and Sherman, A. (2010). Ecological genetic divergence of the fungal pathogen *Didymella rabiei* on sympatric wild and domesticated *Cicer spp.* (Chickpea). *Appl. Environ. Microbiol.* 76(1), 30–39.

Frick, W. F., Pollock, J. F., Hicks, A. C., Langwig, K. E., Reynolds, D. S., Turner, G. G., Butchkoski, C. M., and Kunz, T. H. (2010). An emerging disease causes regional population collapse of a common North American bat species. *Science* 329(5992), 679–682.

Froschauer, A. and Coleman, J. (2012). North American bat death toll exceeds 5.5 million from White-Nose syndrome. *Biol. Rep. U.S. Fish Wildl. Serv.*, 1–2.

Gargas, A., Trest, M. T., Christensen, M., Volk, T. J., and Blehert, D. S. (2009). *Geomyces destructans sp. nov.* associated with bat White-Nose syndrome. *Mycotaxon* 108(1), 147–154.

Garrison, E. and Marth, G. (2012). Haplotype-based variant detection from short-read sequencing. *arXiv*, 1207–3907.

Gervais, P. and Marañon, I. M. de (1995). Effect of the kinetics of temperature variation on Saccharomyces cereuisiae viability and permeability. *Biochim. Biophys. Acta Biomembr.* 1235(1), 52–56.

Ghannoum, M. A., Jurevic, R. J., Mukherjee, P. K., Cui, F., Sikaroodi, M., Naqvi, A., and Gillevet, P. M. (2010). Characterization of the oral fungal microbiome (mycobiome) in healthy individuals. *PLoS pathog* 6(1), e1000713.

Gibbons, J. G., Salichos, L., Slot, J. C., Rinker, D. C., McGary, K. L., King, J. G., Klich, M. A., Tabb, D. L., McDonald, W. H., and Rokas, A. (2012). The evolutionary imprint of domestication on genome variation and function of the filamentous fungus *Aspergillus oryzae*. *Curr. Biol.* 22(15), 1403–1409.

Giraud, T., Fortini, D., Levis, C., Leroux, P., and Brygoo, Y. (1997). RFLP markers show genetic recombination in *Botryotinia fuckeliana* (*Botrytis cinerea*) and transposable elements reveal two sympatric species. *Mol. Biol. Evol.* 14(11), 1177–1185.

Giraud, T., Gladieux, P., and Gavrilets, S. (2010). Linking the emergence of fungal plant diseases with ecological speciation. *Trends Ecol. Evol.* 25(7), 387–395.

Gladieux, P., Feurtey, A., Hood, M. E., Snirc, A., Clavel, J., Dutech, C., Roy, M., and Giraud, T. (2015). The population biology of fungal invasions. *Mol. Ecol.* 24(9), 1969–1986.

Gladieux, P., Ropars, J., Badouin, H., Branca, A., Aguileta, G., de Vienne, D. M., Rodrıguez de la Vega, R. C., Branco, S., and Giraud, T. (2014). Fungal evolutionary genomics provides insight into the mechanisms of adaptive divergence in eukaryotes. *Mol. Ecol.* 23(4), 753–773.

Gladieux, P., Zhang, X.-G., Afoufa-Bastien, D., Valdebenito Sanhueza, R.-M., Sbaghi, M., and Le Cam, B. (2008). On the origin and spread of the Scab disease of apple: out of central Asia. *PLoS One* 3(1), e1455.

Gladieux, P., Zhang, X.-G., Róldan-Ruiz, I., Caffier, V., Leroy, T., Devaux, M., Van Glabeke, S., Coart, E., and Le Cam, B. (2010). Evolution of the population structure of *Venturia inaequalis*, the apple scab fungus, associated with the domestication of its host. *Mol. Ecol.* 19(4), 658–674.

Glass, N. L., Jacobson, D. J., and Shiu, P. K. (2000). The genetics of hyphal fusion and vegetative incompatibility in filamentous ascomycete fungi. *Annu. Rev. Genet.* 34(1), 165–186.

Goldman, G. H., McGuire, S. L., and Harris, S. D. (2002). The DNA damage response in filamentous fungi. *Fungal Genet. Biol.* 35(3), 183–195.

Gostinčar, C., Grube, M., de Hoog, S., Zalar, P., and Gunde-Cimerman, N. (2009). Extremotolerance in fungi: evolution on the edge. *FEMS Microbiol. Ecol.* 71(1), 2–11.

Grice, E. A. and Segre, J. A. (2011). The skin microbiome. *Nat. Rev. Microbiol.* 9(4), 244–253.

Gusa, A. and Jinks-Robertson, S. (2019). Mitotic Recombination and Adaptive Genomic Changes in Human Pathogenic Fungi. *Genes* 10(11).

Halkett, F., Simon, J.-C., and Balloux, F. (2005). Tackling the population genetics of clonal and partially clonal organisms. *Trends Ecol. Evol.* 20(4), 194–201.

Hamm, P. S., Caimi, N. A., Northup, D. E., Valdez, E. W., Buecher, D. C., Dunlap, C. A., Labeda, D. P., Lueschow, S., and Porras-Alfaro, A. (2017). Western Bats as a Reservoir of Novel Streptomyces Species with Antifungal Activity. *Appl. Environ. Microbiol.* 83(5).

Hardham, A. R. (2005). *Phytophthora cinnamomi*. *Mol. Plant Pathol.* 6(6), 589–604.

Hartl, L., Zach, S., and Seidl-Seiboth, V. (2012). Fungal chitinases: diversity, mechanistic properties and biotechnological potential. *Appl. Microbiol. Biotechnol.* 93(2), 533–543.

Hayes, M. A. (2012). The *Geomyces* Fungi: Ecology and Distribution. *Bioscience* 62(9), 819–823.

He, Q., Cheng, P., He, Q., and Liu, Y. (2005). The COP9 signalosome regulates the *Neurospora* circadian clock by controlling the stability of the SCFFWD-1 complex. *Genes Dev.* 19(13), 1518–1531.

Hecker, L. I. and Sussman, A. S. (1973). Activity and heat stability of trehalase from the mycelium and ascospores of Neurospora. *J. bacteriol.* 115(2), 582–591.

Heffernan, A. (2017). White-nose syndrome map. Accessed: 2017-4-1.

Heitman, J., Sun, S., and James, T. Y. (2013). Evolution of fungal sexual reproduction. *Mycologia* 105(1), 1–27.

Helyar, S. J., Hemmer-Hansen, J., Bekkevold, D., Taylor, M. I., Ogden, R., Limborg, M. T., Cariani, A., Maes, G. E., Diopere, E., Carvalho, G. R., and Nielsen, E. E. (2011). Application of SNPs for population genetics of nonmodel organisms: new opportunities and challenges. *Mol. Ecol. Resour.* 11 Suppl 1, 123–136.

Hijmans, R. J., Williams, E., and Vennes, C. (2012). Geosphere: spherical trigonometry. *R package version*.

Hiremath, S. and Lehtoma, K. (2006). Ectomycorrhizal fungi association with the American chestnut. In: *Proceedings of the 2006 USDA Interagency Research Forum on Gypsy Moth and other Invasive Species*, 55.

Hollister, J. and Shah, T. (2017). elevatr: Access elevation data from various APIs. *R package version 0. 1* 3.

Hoog, G. S. de, Guarro, J., Gene, J., and Figueras, M. J. (2016). *Atlas of Clinical Fungi version 4.1. 4*. CBS-KNAW Fungal Biodiversity Centre, Utrecht.

Hovmøller, M. S., Yahyaoui, A. H., Milus, E. A., and Justesen, A. F. (2008). Rapid global spread of two aggressive strains of a wheat rust fungus. *Mol. Ecol.* 17(17), 3818–3826.

Hoyt, J. R., Cheng, T. L., Langwig, K. E., Hee, M. M., Frick, W. F., and Kilpatrick, A. M. (2015a). Bacteria isolated from bats inhibit the growth of *Pseudogymnoascus destructans*, the causative agent of White-Nose syndrome. *PLoS One*.

Hoyt, J. R., Langwig, K. E., Okoniewski, J., Frick, W. F., Stone, W. B., and Kilpatrick, A. M. (2015b). Long-Term Persistence of *Pseudogymnoascus destructans*, the Causative Agent of White-Nose Syndrome, in the Absence of Bats. *Ecohealth* 12(2), 330–333.

Hoyt, J. R., Langwig, K. E., White, J. P., Kaarakka, H. M., Redell, J. A., Kurta, A., DePue, J. E., Scullon, W. H., Parise, K. L., Foster, J. T., Frick, W. F., and Kilpatrick, A. M. (2018). Cryptic connections illuminate pathogen transmission within community networks. *Nature* 563(7733), 710–713.

Hubka, V., Peano, A., Cmokova, A., and Guillot, J. (2018). Common and emerging dermatophytoses in animals: well-known and new threats. In: *Emerging and Epizootic Fungal Infections in Animals*. Springer, 31–79.

Hudson, R. R. and Kaplan, N. L. (1985). Statistical properties of the number of recombination events in the history of a sample of DNA sequences. *Genetics* 111(1), 147–164.

Huebschman, J. J., Hoerner, S. A., White, J. P., Kaarakka, H. M., Parise, K. L., and Foster, J. T. (2019). Detection of *Pseudogymnoascus destructans* during Summer on Wisconsin Bats. *J. Wildl. Dis.* 55(3), 673–677.

Huson, D. H. and Bryant, D. (2006). Application of phylogenetic networks in evolutionary studies. *Mol. Biol. Evol.* 23(2), 254–267.

Iliev, I. D., Funari, V. A., Taylor, K. D., Nguyen, Q., Reyes, C. N., Strom, S. P., Brown, J., Becker, C. A., Fleshner, P. R., Dubinsky, M., et al. (2012). Interactions between commensal fungi and the C-type lectin receptor Dectin-1 influence colitis. *Science* 336(6086), 1314–1317.

Inoue, H. and Shimoda, C. (1981). Changes in trehalose content and trehalase activity during spore germination in fission yeast, Schizosaccharomyces pombe. *Arch. Microbiol.* 129(1), 19–22.

Jacobson, E. S. (2000). Pathogenic roles for fungal melanins. *Clin. Microbiol. Rev.* 13(4), 708–717.

Jahn, B., Koch, A., Schmidt, A., Wanner, G., Gehringer, H., Bhakdi, S., and Brakhage, A. a. (1997). Isolation and characterization of a pigmentless-conidium mutant of

Aspergillus fumigatus with altered conidial surface and reduced virulence. *Infect. Immun.* 65(12), 5110–5117.

Johnson, J. S., Reeder, D. A. M., Lilley, T. M., Czirj??k, G., Voigt, C. C., Mcmichael, J. W., Meierhofer, M. B., Seery, C. W., Lumadue, S. S., Altmann, A. J., Toro, M. O., and Field, K. A. (2015). Antibodies to *Pseudogymnoascus destructans* are not sufficient for protection against White-Nose syndrome. *Ecol. Evol.* 5(11), 2203–2214.

Jonasson, K. A. (2017). The effects of sex, energy, and environmental conditions on the movement ecology of migratory bats. PhD thesis.

Joneson, S., Stajich, J. E., Shiu, S.-H., and Rosenblum, E. B. (2011). Genomic transition to pathogenicity in chytrid fungi. *PLoS Pathog.* 7(11), e1002338.

Juge, C., Samson, J., Bastien, C., Vierheilig, H., Coughlan, A., and Piché, Y. (2002). Breaking dormancy in spores of the arbuscular mycorrhizal fungus *Glomus intraradices*: a critical cold-storage period. *Mycorrhiza* 12(1), 37–42.

Jung, K. and Kalko, E. K. (2011). Adaptability and vulnerability of high flying Neotropical aerial insectivorous bats to urbanization. *Divers. Distrib.* 17(2), 262–274.

Jung, K. and Threlfall, C. G. (2016). Urbanisation and Its Effects on Bats—A Global Meta-Analysis. In: *Bats in the Anthropocene: Conservation of Bats in a Changing World*, 13–33.

Kamvar, Z. N., Tabima, J. F., and Grünwald, N. J. (2014). Poppr: an R package for genetic analysis of populations with clonal, partially clonal, and/or sexual reproduction. *PeerJ* 2, e281.

Kardon, T., Noël, G., Vertommen, D., and Schaftingen, E. V. (2006). Identification of the gene encoding hydroxyacid-oxoacid transhydrogenase, an enzyme that metabolizes 4-hydroxybutyrate. *FEBS Lett.* 580(9), 2347–2350.

Katju, V. and Bergthorsson, U. (2013). Copy-number changes in evolution: rates, fitness effects and adaptive significance. *Front. Genet.* 4, 273.

Katju, V. and Lynch, M. (2003). The structure and early evolution of recently arisen gene duplicates in the *Caenorhabditis elegans* genome. *Genetics* 165(4), 1793–1803.

Katz, M. E. and Cheetham, B. F. (2009). Isolation of Nucleic Acids from Filamentous Fungi. In: *Handbook of Nucleic Acid Purification*. Ed. by D. Liu. CRC Press, 191.

Kellis, M., Birren, B. W., and Lander, E. S. (2004). Proof and evolutionary analysis of ancient genome duplication in the yeast *Saccharomyces cerevisiae*. *Nature* 428(3), 617–624.

Kemp, M. U., Van Loon, E. E., Shamoun-Baranes, J., Bouten, W., et al. (2012). RNCEP: global weather and climate data at your fingertips. *Methods Ecol. Evol.* 3(1), 65–70.

Khankhet, J., Vanderwolf, K. J., McAlpine, D. F., McBurney, S., Overy, D. P., Slavic, D., and Xu, J. (2014). Clonal expansion of the *Pseudogymnoascus destructans* genotype in North America is accompanied by significant variation in phenotypic expression. *PLoS One* 9(8), e104684.

Kierepka, E. M. and Latch, E. K. (2015). Performance of partial statistics in individual-based landscape genetics. *Mol. Ecol. Resour.* 15(3), 512–525.

Kohlhaw, G. B. (2003). Leucine biosynthesis in fungi: entering metabolism through the back door. *Microbiol. Mol. Biol. Rev.* 67(1), 1–15.

Kokurewicz, T., Ogórek, R., Pusz, W., and Matkowski, K. (2016). Bats Increase the Number of Cultivable Airborne Fungi in the "Nietoperek" Bat Reserve in Western Poland. *Microb. Ecol.* 72(1), 36–48.

Kolar, C. S. and Lodge, D. M. (2001). Progress in invasion biology: predicting invaders. *Trends Ecol. Evol.* 16(4), 199–204.

Krauel, J. J., McGuire, L. P., and Boyles, J. G. (2018). Testing traditional assumptions about regional migration in bats. *Mammal Res.* 63(2), 115–123.

Kunz, T. H., Torrez, E. B. de, Bauer, D., Lobova, T., and Fleming, T. H. (2011). Ecosystem services provided by bats. *Ann. N. Y. Acad. Sci.* 1223(1), 1–38.

Lakin-Thomas, P. L., Coté, G. G., and Brody, S. (1990). Circadian Rhythms in *Neurospora crassa*: Biochemistry and Genetics. *Crit. Rev. Microbiol.* 17(5), 365–416.

Langwig, K. E., Frick, W. F., Bried, J. T., Hicks, A. C., Kunz, T. H., and Kilpatrick, A. M. (2012). Sociality, density-dependence and microclimates determine the persistence of populations suffering from a novel fungal disease, White-Nose syndrome. *Ecol. Lett.* 15(9), 1050–1057.

Langwig, K. E., Frick, W. F., Reynolds, R., Parise, K. L., Drees, K. P., Hoyt, J. R., Cheng, T. L., Kunz, T. H., Foster, J. T., and Kilpatrick, A. M. (2015). Host and pathogen ecology drive the seasonal dynamics of a fungal disease, White-Nose syndrome. *Proc. Biol. Sci.* 282(1799), 20142335.

Lauer, S., Avecilla, G., Spealman, P., Sethia, G., Brandt, N., Levy, S. F., and Gresham, D. (2018). Single-cell copy number variant detection reveals the dynamics and diversity of adaptation. *PLoS Biol.* 16(12), e3000069.

Le Gac, M., Hood, M. E., Fournier, E., and Giraud, T. (2007). Phylogenetic evidence of host-specific cryptic species in the anther smut fungus. *Evolution* 61(1), 15–26.

Le Van, A., Gladieux, P., Lemaire, C., Cornille, A., Giraud, T., Durel, C.-E., Caffier, V., and Le Cam, B. (2012). Evolution of pathogenicity traits in the apple scab fungal pathogen in response to the domestication of its host. *Evol. Appl.* 5(7), 694–704.

Lemieux-Labonté, V., Simard, A., Willis, C. K. R., and Lapointe, F.-J. (2017). Enrichment of beneficial bacteria in the skin microbiota of bats persisting with White-Nose syndrome. *Microbiome* 5(1), 115.

Leopardi, S., Blake, D., and Puechmaille, S. J. (2015). White-Nose Syndrome fungus introduced from Europe to North America. *Curr. Biol.* 25(6), R217–9.

Lespinet, O., Wolf, Y. I., Koonin, E. V., and Aravind, L. (2002). The role of lineage-specific gene family expansion in the evolution of eukaryotes. *Genome Res.* 12(7), 1048–1059.

Leushkin, E. V., Logacheva, M. D., Penin, A. A., Sutormin, R. A., Gerasimov, E. S., Kochkina, G. A., Ivanushkina, N. E., Vasilenko, O. V., Kondrashov, A. S., and Ozerskaya, S. M. (2015). Comparative genome analysis of Pseudogymnoascus spp. reveals primarily clonal evolution with small genome fragments exchanged between lineages. *BMC Genomics* 16(1), 400.

Leutner, B. and Horning, N. (2017). RStoolbox: tools for remote sensing data analysis. *R package version 0. 1* 7.

Levasseur, A., Drula, E., Lombard, V., Coutinho, P. M., and Henrissat, B. (2013). Expansion of the enzymatic repertoire of the CAZy database to integrate auxiliary redox enzymes. *Biotechnol. Biofuels* 6(1), 41.

Li, H. and Durbin, R. (2010). Fast and accurate long-read alignment with Burrows-Wheeler transform. *Bioinformatics* 26(5), 589–595.

Li, Y.-D., Liang, H., Gu, Z., Lin, Z., Guan, W., Zhou, L., Li, Y.-Q., and Li, W.-H. (2009). Detecting positive selection in the budding yeast genome. *J. Evol. Biol.* 22(12), 2430–2437.

Lilley, T. M., Anttila, J., and Ruokolainen, L. (2018). Landscape structure and ecology influence the spread of a bat fungal disease. *Funct. Ecol.* 32(11), 2483–2496.

Lin, X., Litvintseva, A. P., Nielsen, K., Patel, S., Floyd, A., Mitchell, T. G., and Heitman, J. (2007). αADα hybrids of *Cryptococcus neoformans*: Evidence of same-sex mating in nature and hybrid fitness. *PLoS Genet.* 3(10), 1975–1990.

Lind, A. L., Wisecaver, J. H., Lameiras, C., Wiemann, P., Palmer, J. M., Keller, N. P., Rodrigues, F., Goldman, G. H., and Rokas, A. (2017). Drivers of genetic diversity in secondary metabolic gene clusters within a fungal species. *PLoS Biology* 15(11), e2003583.

Lindenbaum, P. (2015). JVarkit: java-based utilities for Bioinformatics. *FigShare, doi* 10, m9.

Lindner, D. L., Gargas, A., Lorch, J. M., Banik, M. T., Glaeser, J., Kunz, T. H., and Blehert, D. S. (2011). DNA-based detection of the fungal pathogen *Geomyces destructans* in soils from bat hibernacula. *Mycologia* 103(2), 241–246.

Liu, Z., Pagani, M., Zinniker, D., DeConto, R., Huber, M., Brinkhuis, H., Shah, S. R., Leckie, R. M., and Pearson, A. (2009). Global cooling during the Eocene-Oligocene climate transition. *Science* 323(5918), 1187–1190.

Longmead, B. and Salzberg, S. L. (2012). Fast gapped-read alignment with Bowtie2. *Nat. Methods.*

Lorch, J. M., Meteyer, C. U., Behr, M. J., Boyles, J. G., Cryan, P. M., Hicks, A. C., Ballmann, A. E., Coleman, J. T. H., Redell, D. N., Reeder, D. M., and Blehert, D. S. (2011). Experimental infection of bats with *Geomyces destructans* causes White-Nose syndrome. *Nature* 480(7377), 376–378.

Lorch, J. M., Muller, L. K., Russell, R. E., O'Connor, M., Lindner, D. L., and Blehert, D. S. (2013). Distribution and environmental persistence of the causative agent of White-Nose syndrome, *Geomyces destructans*, in bat hibernacula of the eastern United States. *Appl. Environ. Microbiol.* 79(4), 1293–1301.

Lorch, J. M., Palmer, J. M., Lindner, D. L., Ballmann, A. E., George, K. G., Griffin, K., Knowles, S., Huckabee, J. R., Haman, K. H., Anderson, C. D., Becker, P. A., Buchanan, J. B., Foster, J. T., and Blehert, D. S. (2016). First Detection of Bat White-Nose Syndrome in Western North America. *mSphere* 1(4).

Lučan, R. K., Bandouchova, H., Bartonička, T., Pikula, J., Zahradnıková Jr, A., Zukal, J., and Martınková, N. (2016). Ectoparasites may serve as vectors for the White-Nose syndrome fungus. *Parasit. Vectors* 9(1), 16.

Lulloff, S. J., Hahn, B. L., and Sohnle, P. G. (2004). Fungal susceptibility to zinc deprivation. *J. Lab. Clin. Med.* 144(4), 208–214.

Lutzoni, F., Pagel, M., and Reeb, V. (2001). Major fungal lineages are derived from lichen symbiotic ancestors. *Nature* 411(6840), 937–940.

MacPherson, S., Larochelle, M., and Turcotte, B. (2006). A fungal family of transcriptional regulators: the zinc cluster proteins. *Microbiol. Mol. Biol. Rev.* 70(3), 583–604.

Manning, V. A., Pandelova, I., Dhillon, B., Wilhelm, L. J., Goodwin, S. B., Berlin, A. M., Figueroa, M., Freitag, M., Hane, J. K., Henrissat, B., Holman, W. H., Kodira, C. D., Martin, J., Oliver, R. P., Robbertse, B., Schackwitz, W., Schwartz, D. C., Spatafora, J. W., Turgeon, B. G., Yandava, C., Young, S., Zhou, S., Zeng, Q., Grigoriev, I. V., Ma, L.-J., and Ciuffetti, L. M. (2013). Comparative genomics of a plant-pathogenic fungus, *Pyrenophora tritici-repentis*, reveals transduplication and the impact of repeat elements on pathogenicity and population divergence. *G3-Genes. Genom. Genet.* 3(1), 41–63.

Marroquin, C. M., Lavine, J. O., and Windstam, S. T. (2017). Effect of Humidity on Development of *Pseudogymnoascus destructans* , the Causal Agent of Bat White-Nose Syndrome. *Northeast. Nat.* 24(1), 54–64.

Martel, A., Pasmans, F., Fisher, M. C., Grogan, L. F., Skerratt, L. F., and Berger, L. (2018). Chytridiomycosis. In: *Emerging and epizootic fungal infections in animals.* Springer, 309–335.

Martinez, D., Larrondo, L. F., Putnam, N., Gelpke, M. D. S., Huang, K., Chapman, J., Helfenbein, K. G., Ramaiya, P., Detter, J. C., Larimer, F., Coutinho, P. M., Henrissat, B., Berka, R., Cullen, D., and Rokhsar, D. (2004). Genome sequence of the lignocellulose degrading fungus *Phanerochaete chrysosporium* strain RP78. *Nat. Biotechnol.* 22(6), 695–700.

Mathews, F., Roche, N., Aughney, T., Jones, N., Day, J., Baker, J., and Langton, S. (2015). Barriers and benefits: implications of artificial night-lighting for the distribution of common bats in Britain and Ireland. *Philos. Trans. R. Soc. Lond. B Biol. Sci.* 370(1667).

Mboup, M., Leconte, M., Gautier, A., Wan, A. M., Chen, W., de Vallavieille-Pope, C., and Enjalbert, J. (2009). Evidence of genetic recombination in wheat yellow rust populations of a Chinese oversummering area. *Fungal Genet. Biol.* 46(4), 299–307.

Mboup, M., Bahri, B., Leconte, M., de Vallavieille-Pope, C., Kaltz, O., and Enjalbert, J. (2012). Genetic structure and local adaptation of European wheat yellow rust populations: the role of temperature-specific adaptation. *Evol. Appl.* 5(4), 341–352.

McDowell, J. M. (2011). Genomes of obligate plant pathogens reveal adaptations for obligate parasitism. *Proc. Natl. Acad. Sci. U. S. A.* 108(22), 8921–8922.

McNab, B. K. (1974). The behavior of temperate cave bats in a subtropical environment. *Ecology* 55(5), 943–958.

Meteyer, C. U., Buckles, E. L., Blehert, D. S., Hicks, A. C., Green, D. E., Shearn-bochsler, V., Thomas, N. J., Gargas, A., and Behr, M. J. (2009). Histopathologic criteria to confirm White-Nose syndrome in bats. *J. Vet. Diagn. Invest.* 21(4), 411–414.

Meyer, A. D., Stevens, D. F., and Blackwood, J. C. (2016). Predicting bat colony survival under controls targeting multiple transmission routes of White-Nose syndrome. *J. Theor. Biol.* 409, 60–69.

Miller-Butterworth, C. M., Vonhof, M. J., Rosenstern, J., Turner, G. G., and Russell, A. L. (2014). Genetic structure of little brown bats (*Myotis lucifugus*) corresponds with spread of White-Nose syndrome among hibernacula. *J. Hered.* 105(3), 1–11.

Monis, P. T., Caccio, S. M., and Thompson, R. C. A. (2009). Variation in *Giardia*: towards a taxonomic revision of the genus. *Trends Parasitol.* 25(2), 93–100.

Moore, G. W. and Sullivan, G. N. (1978). *Speleology: the study of caves*. Zephyrus Press.

Moran, M., Chapman, N., Abela-Oversteegen, L., Doubell, A., Whittall, C., Howard, R., Farrell, P., Halliday, D., and Hirst, C. (2015). Neglected disease research and development: The Ebola effect. *Policy Cures*, 69.

Morisak, K. M. (2018). Variation of *Pseudogymnoascus destructans* Spore Loads and Risk of Human Vectored Transport. PhD thesis. University of Akron.

Munkacsi, A. B., Stoxen, S., and May, G. (2008). *Ustilago maydis* populations tracked maize through domestication and cultivation in the Americas. *Proc. Biol. Sci.* 275(1638), 1037–1046.

Mysyakina, I. S., Kochkina, G. A., Ivanushkina, N. E., Bokareva, D. A., and Feofilova, E. P. (2016). Germination of spores of mycelial fungi in relation to exogenous dormancy. *Microbiology* 85(3), 290–294.

Narra, H. P. and Ochman, H. (2006). Of What Use Is Sex to Bacteria? *Curr. Biol.* 16(17), R705–R710.

Nelson, C. W., Moncla, L. H., and Hughes, A. L. (2015). SNPGenie: estimating evolutionary parameters to detect natural selection using pooled next-generation sequencing data. *Bioinformatics* 31(22), 3709–3711.

Nguyen, N. H., Suh, S.-O., and Blackwell, M. (2007). Five novel *Candida* species in insect-associated yeast clades isolated from Neuroptera and other insects. *Mycologia* 99(6), 842–858.

Ni, M. and Yu, J.-H. (2007). A novel regulator couples sporogenesis and trehalose biogenesis in *Aspergillus nidulans*. *PLoS One* 2(10), e970.

Norquay, K. J. O., Martinez-Nuñez, F., Dubois, J. E., Monson, K. M., and Willis, C. K. R. (2013). Long-distance movements of little brown bats (*Myotis lucifugus*). *J. Mammal.* 94(2), 506–515.

Novacek, M. J. (1985). Evidence for echolocation in the oldest known bats. *Nature* 315(6015), 140–141.

O'Regan, S. M., Magori, K., Pulliam, J. T., Zokan, M. A., Kaul, R. B., Barton, H. D., and Drake, J. M. (2015). Multi-scale model of epidemic fade-out: Will local extirpation events inhibit the spread of white-nose syndrome? *Ecol. Appl.* 25(3), 621–633.

O'Donoghue, A. J., Knudsen, G. M., Beekman, C., Perry, J. A., Johnson, A. D., DeRisi, J. L., Craik, C. S., and Bennett, R. J. (2015). Destructin-1 is a collagen-degrading

endopeptidase secreted by Pseudogymnoascus destructans, the causative agent of white-nose syndrome. *PNAS* 112(24), 7478–7483.

Ohm, R. A., Feau, N., Henrissat, B., Schoch, C. L., Horwitz, B. A., Barry, K. W., Condon, B. J., Copeland, A. C., Dhillon, B., Glaser, F., Hesse, C. N., Kosti, I., LaButti, K., Lindquist, E. A., Lucas, S., Salamov, A. A., Bradshaw, R. E., Ciuffetti, L., Hamelin, R. C., Kema, G. H. J., Lawrence, C., Scott, J. A., Spatafora, J. W., Turgeon, B. G., Wit, P. J. G. M. de, Zhong, S., Goodwin, S. B., and Grigoriev, I. V. (2012). Diverse lifestyles and strategies of plant pathogenesis encoded in the genomes of eighteen Dothideomycetes fungi. *PLoS Pathog.* 8(12), e1003037.

Olsen, L., Choffnes, E. R., Relman, D. A., Pray, L., et al. (2011). Fungal diseases: an emerging threat to human, animal and plant health. Workshop summary. In: *Fungal diseases: an emerging threat to human, animal and plant health. Workshop summary.*

Palmer, J. M., Drees, K. P., Foster, J. T., and Lindner, D. L. (2018). Extreme sensitivity to ultraviolet light in the fungal pathogen causing White-Nose syndrome of bats. *Nat. Commun.* 9(1), 35.

Palmer, J. M., Kubatova, A., Novakova, A., Minnis, A. M., Kolarik, M., and Lindner, D. L. (2014). Molecular Characterization of a Heterothallic Mating System in *Pseudogymnoascus destructans*, the Fungus Causing White-Nose Syndrome of Bats. *G3-Genes. Genom. Genet.* 4(September), 1–11.

Papadatou, E., Ibáñez, C., Pradel, R., Juste, J., and Gimenez, O. (2011). Assessing survival in a multi-population system: a case study on bat populations. *Oecologia* 165(4), 925–933.

Park, H.-S., Ni, M., Jeong, K. C., Kim, Y. H., and Yu, J.-H. (2012). The role, interaction and regulation of the velvet regulator VelB in *Aspergillus nidulans*. *PLoS One* 7(9), e45935.

Park, J., Park, J., Jang, S., Kim, S., Kong, S., Choi, J., Ahn, K., Kim, J., Lee, S., Kim, S., Park, B., Jung, K., Kim, S., Kang, S., and Lee, Y.-H. (2008). FTFD: an

informatics pipeline supporting phylogenomic analysis of fungal transcription factors. *Bioinformatics* 24(7), 1024–1025.

Park, K. J., Jones, G., and Ransome, R. D. (2000). Torpor, arousal and activity of hibernating Greater Horseshoe Bats (*Rhinolophus ferrumequinum*). *Funct. Ecol.* 14(5), 580–588.

Park, S.-Y., Choi, J., Lim, S.-E., Lee, G.-W., Park, J., Kim, Y., Kong, S., Kim, S. R., Rho, H.-S., Jeon, J., Chi, M.-H., Kim, S., Khang, C. H., Kang, S., and Lee, Y.-H. (2013). Global Expression Profiling of Transcription Factor Genes Provides New Insights into Pathogenicity and Stress Responses in the Rice Blast Fungus. *PLoS Pathog.* 9(6), e1003350.

Peng, Y., Leung, H. C. M., Yiu, S. M., and Chin, F. Y. L. (2012). IDBA-UD: a de novo assembler for single-cell and metagenomic sequencing data with highly uneven depth. *Bioinformatics* 28(11), 1420–1428.

Peterman, W. E. (2018). ResistanceGA: An R package for the optimization of resistance surfaces using genetic algorithms. *Methods Ecol. Evol.* 9(6), 1638–1647.

Petkova, D., Novembre, J., and Stephens, M. (2016). Visualizing spatial population structure with estimated effective migration surfaces. *Nat. Genet.* 48(1), 94–100.

Pettit, J. L. and O'Keefe, J. M. (2017). Impacts of White-Nose Syndrome Observed During Long-Term Monitoring of a Midwestern Bat Community. *J. Fish and Wildl. Manag.* 8(1), 69–78.

Philibert, A., Desprez-Loustau, M.-L., Fabre, B., Frey, P., Halkett, F., Husson, C., Lung-Escarmant, B., Marçais, B., Robin, C., Vacher, C., and Makowski, D. (2011). Predicting invasion success of forest pathogenic fungi from species traits. *J. Appl. Ecol.* 48(6), 1381–1390.

Pigliucci, M. (2001). *Phenotypic Plasticity: Beyond Nature and Nurture*. JHU Press.

Pijper, A., Pullinger, B. D., et al. (1927). An Outbreak of Sporotrichosis among South African Native Miners. *Lancet*, 914–15.

Pikula, J., Amelon, S. K., Bandouchova, H., Bartonička, T., Berkova, H., Brichta, J., Hooper, S., Kokurewicz, T., Kolarik, M., Köllner, B., et al. (2017). White-nose syndrome pathology grading in Nearctic and Palearctic bats. *PLoS One* 12(8), e0180435.

Popa-Lisseanu, A. G. and Voigt, C. C. (2009). Bats on the Move. *J. Mammal.* 90(6), 1283–1289.

Poplin, R., Ruano-Rubio, V., DePristo, M. A., Fennell, T. J., Carneiro, M. O., Van der Auwera, G. A., Kling, D. E., Gauthier, L. D., Levy-Moonshine, A., Roazen, D., et al. (2017). Scaling accurate genetic variant discovery to tens of thousands of samples. *BioRxiv*, 201178.

Powell, A. J., Conant, G. C., Brown, D. E., Carbone, I., and Dean, R. A. (2008). Altered patterns of gene duplication and differential gene gain and loss in fungal pathogens. *BMC Genomics* 9, 147.

Puechmaille, S. J., Fuller, H., and Teeling, E. C. (2011a). Effect of Sample Preservation Methods on the Viability of *Geomyces destructans* , the Fungus Associated with White-Nose Syndrome in Bats. *Acta Chiropt.* 13(1), 217–221.

Puechmaille, S. J., Wibbelt, G., Korn, V., Fuller, H., Forget, F., Mühldorfer, K., Kurth, A., Bogdanowicz, W., Borel, C., Bosch, T., Cherezy, T., Drebet, M., Görföl, T., Haarsma, A.-J., Herhaus, F., Hallart, G., Hammer, M., Jungmann, C., Le Bris, Y., Lutsar, L., Masing, M., Mulkens, B., Passior, K., Starrach, M., Wojtaszewski, A., Zöphel, U., and Teeling, E. C. (2011b). Pan-European distribution of White-Nose syndrome fungus (*Geomyces destructans*) not associated with mass mortality. *PLoS One* 6(4), e19167.

Qian, W. and Zhang, J. (2014). Genomic evidence for adaptation by gene duplication. *Genome Res.* 24(8), 1356–1362.

R Core Team (2015). R: A Language and Environment for Statistical Computing.

Raboin, L.-M., Selvi, A., Oliveira, K. M., Paulet, F., Calatayud, C., Zapater, M.-F., Brottier, P., Luzaran, R., Garsmeur, O., Carlier, J., and D'Hont, A. (2007). Evidence

for the dispersal of a unique lineage from Asia to America and Africa in the sugarcane fungal pathogen *Ustilago scitaminea*. *Fungal Genet. Biol.* 44(1), 64–76.

Rachowicz, L. J., Hero, J.-M., Alford, R. a., Taylor, J. W., Morgan, J. a. T., Vredenburg, V. T., Collins, J. P., and Briggs, C. J. (2005). The Novel and Endemic Pathogen Hypotheses: Competing Explanations for the Origin of Emerging Infectious Diseases of Wildlife. *Conserv. Biol.* 19(5), 1441–1448.

Raj, A., Stephens, M., and Pritchard, J. K. (2014). fastSTRUCTURE: variational inference of population structure in large SNP data sets. *Genetics* 197(2), 573–589.

Rajasingham, R., Smith, R. M., Park, B. J., Jarvis, J. N., Govender, N. P., Chiller, T. M., Denning, D. W., Loyse, A., and Boulware, D. R. (2017). Global burden of disease of HIV-associated cryptococcal meningitis: an updated analysis. *Lancet Infect. Dis.* 17(8), 873–881.

Rajkumar, S. S., Li, X., Rudd, R. J., Okoniewski, J. C., Xu, J., Chaturvedi, S., and Chaturvedi, V. (2011). Clonal genotype of *Geomyces destructans* among bats with White Nose Syndrome, New York, USA. *Emerg. Infect. Dis.* 17(7), 1273–1276.

Range-Wide Indiana Bat Summer Survey Guidelines (2018). Tech. rep. U.S. Fish and Wildlife Service.

Raudabaugh, D. B. and Miller, A. N. (2013). Nutritional capability of and substrate suitability for *Pseudogymnoascus destructans*, the causal agent of bat White-Nose syndrome. *PLoS One* 8(10), e78300.

Read, N. D. and Roca, M. G. (2006). Vegetative hyphal fusion in filamentous fungi. In: *Cell-Cell Channels*. Springer, 87–98.

Redon, R., Ishikawa, S., Fitch, K. R., Feuk, L., Perry, G. H., Andrews, T. D., Fiegler, H., Shapero, M. H., Carson, A. R., Chen, W., Cho, E. K., Dallaire, S., Freeman, J. L., González, J. R., Gratacòs, M., Huang, J., Kalaitzopoulos, D., Komura, D., MacDonald, J. R., Marshall, C. R., Mei, R., Montgomery, L., Nishimura, K., Okamura, K., Shen, F., Somerville, M. J., Tchinda, J., Valsesia, A., Woodwark, C., Yang,

F., Zhang, J., Zerjal, T., Zhang, J., Armengol, L., Conrad, D. F., Estivill, X., Tyler-Smith, C., Carter, N. P., Aburatani, H., Lee, C., Jones, K. W., Scherer, S. W., and Hurles, M. E. (2006). Global variation in copy number in the human genome. *Nature* 444(7118), 444–454.

Reeder, D. M., Frank, C. L., Turner, G. G., Meteyer, C. U., Kurta, A., Britzke, E. R., Vodzak, M. E., Darling, S. R., Stihler, C. W., Hicks, A. C., Jacob, R., Grieneisen, L. E., Brownlee, S. A., Muller, L. K., and Blehert, D. S. (2012). Frequent arousal from hibernation linked to severity of infection and mortality in bats with White-Nose syndrome. *PLoS One* 7(6), e38920.

Reeder, S. M., Palmer, J. M., Prokkola, J. M., Lilley, T. M., Reeder, D. M., and Field, K. A. (2017). *Pseudogymnoascus destructans* transcriptome changes during White-Nose syndrome infections. *Virulence* 8(8), 1695–1707.

Refrégier, G., Le Gac, M., Jabbour, F., Widmer, A., Shykoff, J. A., Yockteng, R., Hood, M. E., and Giraud, T. (2008). Cophylogeny of the anther smut fungi and their caryophyllaceous hosts: prevalence of host shifts and importance of delimiting parasite species for inferring cospeciation. *BMC Evol. Biol.* 8, 100.

Ren, P., Haman, K. H., Last, L. a., Rajkumar, S. S., Kevin Keel, M., and Chaturvedi, V. (2012). Clonal spread of *Geomyces destructans* among bats, Midwestern and Southern United States. *Emerg. Infect. Dis.* 18(5), 883–885.

Reynolds, H. T. and Barton, H. A. (2013). White-Nose Syndrome: Human Activity in the Emergence of an Extirpating Mycosis. *Microbiol. Spectr.* 1(2).

Reynolds, H. T. and Barton, H. a. (2014). Comparison of the White-Nose syndrome agent Pseudogymnoascus destructans to cave-dwelling relatives suggests reduced saprotrophic enzyme activity. *PLoS One* 9(1), e86437.

Reynolds, H. T., Ingersoll, T., and Barton, H. A. (2015). Modeling the environmental growth of *Pseudogymnoascus destructans* and its impact on the White-Nose syndrome epidemic. *J. Wildl. Dis.* 51(2), 318–331.

Rieux, A., Soubeyrand, S., Bonnot, F., Klein, E. K., Ngando, J. E., Mehl, A., Ravigne, V., Carlier, J., and Lapeyre de Bellaire, L. de (2014). Long-distance wind-dispersal of spores in a fungal plant pathogen: estimation of anisotropic dispersal kernels from an extensive field experiment. *PLoS One* 9(8), e103225.

Rinker, D. C., Specian, N. K., Zhao, S., and Gibbons, J. G. (2019). Polar bear evolution is marked by rapid changes in gene copy number in response to dietary shift. *Proc. Natl. Acad. Sci. U. S. A.* 116(27), 13446–13451.

Robert, V. A. and Casadevall, A. (2009). Vertebrate endothermy restricts most fungi as potential pathogens. *J. Infect. Dis.* 200(10), 1623–1626.

Robinson, J. M. (1990). Lignin, land plants, and fungi: Biological evolution affecting Phanerozoic oxygen balance. *Geology* 18(7), 607–610.

Rodrigues, M. L. (2016). Funding and Innovation in Diseases of Neglected Populations: The Paradox of Cryptococcal Meningitis. *PLoS Negl. Trop. Dis.* 10(3), e0004429.

Rodrigues, M. L. (2018). Neglected disease, neglected populations: the fight against *Cryptococcus* and cryptococcosis. *Mem. Inst. Oswaldo Cruz* 113(7), e180111.

Romani, L. (2004). Immunity to fungal infections. *Nat. Rev. Immunol.* 4(1), 11–24.

Rosas, A. L. and Casadevall, A. (2001). Melanization decreases the susceptibility of Cryptococcus neoformans to enzymatic degradation. *Mycopathologia* 151(2), 53–56.

Rosenblum, E. B., Poorten, T. J., Joneson, S., and Settles, M. (2012). Substrate-specific gene expression in *Batrachochytrium dendrobatidis*, the chytrid pathogen of amphibians. *PLoS One* 7(11), e49924.

Ruedi, M. and Mayer, F. (2001). Molecular systematics of bats of the genus Myotis (Vespertilionidae) suggests deterministic ecomorphological convergences. *Mol. Phylogenet. Evol.* 21(3), 436–448.

Samson, R. A. (1972). Notes on *Pseudogymnoascus*, *Gymnoascus*, and related genera. *Acta Bot. Neerl.* 21(5), 517–527.

Santure, A. W., Stapley, J., Ball, A. D., Birkhead, T. R., Burke, T., and Slate, J. (2010). On the use of large marker panels to estimate inbreeding and relatedness: empirical and simulation studies of a pedigreed zebra finch population typed at 771 SNPs. *Mol. Ecol.* 19(7), 1439–1451.

Sarikaya Bayram, O., Bayram, O., Valerius, O., Park, H. S., Irniger, S., Gerke, J., Ni, M., Han, K.-H., Yu, J.-H., and Braus, G. H. (2010). LaeA control of velvet family regulatory proteins for light-dependent development and fungal cell-type specificity. *PLoS Genet.* 6(12), e1001226.

Sattar, A., Xie, S., Hafeez, M. A., Wang, X., Hussain, H. I., Iqbal, Z., Pan, Y., Iqbal, M., Shabbir, M. A., and Yuan, Z. (2016). Metabolism and toxicity of arsenicals in mammals. *Environ. Toxicol. Pharmacol.* 48, 214–224.

Savary, S., Ficke, A., Aubertot, J.-N., and Hollier, C. (2012). Crop losses due to diseases and their implications for global food production losses and food security. *Food Secur.* 4(4), 519–537.

Schneider, C. A., Rasband, W. S., and Eliceiri, K. W. (2012). NIH Image to ImageJ: 25 years of image analysis. *Nat. Methods* 9(7), 671–675.

Scrucca, L., Fop, M., Murphy, T. B., and Raftery, A. E. (2016). mclust 5: clustering, classification and density estimation using Gaussian finite mixture models. *R J.* 8(1), 289.

Sendor, T. and Simon, M. (2003). Population dynamics of the pipistrelle bat: effects of sex, age and winter weather on seasonal survival. *J. Anim. Ecol.* 72(2), 308–320.

Seyedmousavi, S., de Hoog, G. S., Guillot, J., and Verweij, P. E. (2018). *Emerging and Epidemic Fungal Infections in Animals*. Springer.

Seyedmousavi, S., Guillot, J., Arné, P., de Hoog, G. S., Mouton, J. W., Melchers, W. J. G., and Verweij, P. E. (2015). *Aspergillus* and aspergilloses in wild and domestic animals: a global health concern with parallels to human disease. *Med. Mycol.* 53(8), 765–797.

Shafer, A. B. A., Cullingham, C. I., Côté, S. D., and Coltman, D. W. (2010). Of glaciers and refugia: a decade of study sheds new light on the phylogeography of northwestern North America. *Mol. Ecol.* 19(21), 4589–4621.

Sharma, L., Sousa, M., Faria, A. S., Nunes-Pereira, M., Cabral, J. A., Phillips, A. J. L., Marques, G., and Paiva-Cardoso, M. d. N. (2019). Worldwide recombination in emergent White-Nose syndrome pathogen *Pseudogymnoascus destructans*. *bioaRxiv*.

Sibley, L. D. and Ajioka, J. W. (2008). Population structure of *Toxoplasma gondii*: clonal expansion driven by infrequent recombination and selective sweeps. *Annu. Rev. Microbiol.* 62, 329–351.

Simpson, J. T. and Durbin, R. (2012). Efficient de novo assembly of large genomes using compressed data structures. *Genome Res.* 22(3), 549–556.

Sjödin, P. and Jakobsson, M. (2012). Population Genetic Nature of Copy Number Variation. *Methods Mol. Biol.*, 209–223.

Smit, A., Hubley, R., and Green, P. (n.d.). RepeatMasker ().

Smith, A. D. and McWilliams, S. R. (2016). Bat activity during autumn relates to atmospheric conditions: implications for coastal wind energy development. *J. Mammal.* 97(6), 1565–1577.

Soanes, D. M., Alam, I., Cornell, M., Wong, H. M., Hedeler, C., Paton, N. W., Rattray, M., Hubbard, S. J., Oliver, S. G., and Talbot, N. J. (2008). Comparative genome analysis of filamentous fungi reveals gene family expansions associated with fungal pathogenesis. *PLoS One* 3(6), e2300.

Spanu, P. D. (2012). The genomics of obligate (and nonobligate) biotrophs. *Annu. Rev. Phytopathol.* 50, 91–109.

Spanu, P. D., Abbott, J. C., Amselem, J., Burgis, T. A., Soanes, D. M., Stüber, K., Ver Loren van Themaat, E., Brown, J. K. M., Butcher, S. A., Gurr, S. J., Lebrun, M.-H., Ridout, C. J., Schulze-Lefert, P., Talbot, N. J., Ahmadinejad, N., Ametz, C., Barton, G. R., Benjdia, M., Bidzinski, P., Bindschedler, L. V., Both, M., Brewer, M. T.,

Cadle-Davidson, L., Cadle-Davidson, M. M., Collemare, J., Cramer, R., Frenkel, O., Godfrey, D., Harriman, J., Hoede, C., King, B. C., Klages, S., Kleemann, J., Knoll, D., Koti, P. S., Kreplak, J., López-Ruiz, F. J., Lu, X., Maekawa, T., Mahanil, S., Micali, C., Milgroom, M. G., Montana, G., Noir, S., O'Connell, R. J., Oberhaensli, S., Parlange, F., Pedersen, C., Quesneville, H., Reinhardt, R., Rott, M., Sacristán, S., Schmidt, S. M., Schön, M., Skamnioti, P., Sommer, H., Stephens, A., Takahara, H., Thordal-Christensen, H., Vigouroux, M., Wessling, R., Wicker, T., and Panstruga, R. (2010). Genome expansion and gene loss in powdery mildew fungi reveal tradeoffs in extreme parasitism. *Science* 330(6010), 1543–1546.

Spanu, P. and Kämper, J. (2010). Genomics of biotrophy in fungi and oomycetes—emerging patterns. *Curr. Opin. Plant Biol.* 13(4), 409–414.

Springer, M. S., Teeling, E. C., Madsen, O., and Stanhope M J andde Jong, W. W. (2001). Integrated fossil and molecular data reconstruct bat echolocation. *Proc. Natl. Acad. Sci. U. S. A.* 98(11), 6241–6246.

Staats, C. C., Kmetzsch, L., Schrank, A., and Vainstein, M. H. (2013). Fungal zinc metabolism and its connections to virulence. *Front. Cell. Infect. Microbiol.* 3, 65.

Steele, C. and Wormley, F. L. (2012). Immunology of fungal infections: lessons learned from animal models. *Curr. Opin. Microbiol* 15(4), 413–419.

Steele, S. (1972). Sugars and sugar alcohols in relation to life cycle phases of Geotrichum candidum. *Trans. Brit.* 59(3), 502–506.

Steenwyk, J. L. and Rokas, A. (2018). Copy Number Variation in Fungi and Its Implications for Wine Yeast Genetic Diversity and Adaptation. *Front. Microbiol.* 9, 288.

Steenwyk, J. L., Soghigian, J. S., Perfect, J. R., and Gibbons, J. G. (2016). Copy number variation contributes to cryptic genetic variation in outbreak lineages of *Cryptococcus gattii* from the North American Pacific Northwest. *BMC Genomics* 17(1), 700.

Steenwyk, J. and Rokas, A. (2017). Extensive Copy Number Variation in Fermentation-Related Genes Among *Saccharomyces cerevisiae* Wine Strains. *G3-Genes. Genom. Genet.* 7(5), 1475–1485.

Swezey, C. and Garrity, C. (2011). Geographical and Geological Data From Caves and Mines Infected With White-Nose Syndrome (Wns) Before September 2009 in the Eastern United States. *J. Cave Karst Stud.* 73(3), 125–157.

Taylor, P. D., Mackenzie, S. A., Thurber, B. G., Calvert, A. M., Mills, A. M., McGuire, L. P., and Guglielmo, C. G. (2011). Landscape Movements of Migratory Birds and Bats Reveal an Expanded Scale of Stopover. *PLoS One* 6(11), e27054.

Thapa, V., Turner, G. G., Hafenstein, S., Overton, B. E., Vanderwolf, K. J., and Roossinck, M. J. (2009). Using a Novel Partitivirus in *Pseudogymnoascus destructans* to Understand the Epidemiology of White-Nose Syndrome. *PLoS Pathog.* 12(12), e1006076.

Thogmartin, W. E., Andrew King, R., Szymanski, J. A., and Pruitt, L. (2012). Space-time models for a panzootic in bats, with a focus on the endangered Indiana bat. *J. Wildl. Dis.* 48(4), 876–887.

Thomas, D. W., Dorais, M., and Bergeron, J.-M. (1990). Winter Energy Budgets and Cost of Arousals for Hibernating Little Brown Bats, *Myotis lucifugus*. *J. Mammal.* 71(3), 475–479.

Thomas, D. W. (1995). The physiological ecology of hibernation in vespertilionid bats. In: *Symposia of the Zoological Society of London*. Vol. 67, 233–244.

Thompson, D. A. and Regev, A. (2009). Fungal regulatory evolution: cis and trans in the balance. *FEBS Lett.* 583(24), 3959–3965.

Tirosh, I., Weinberger, A., Carmi, M., and Barkai, N. (2006). A genetic signature of interspecies variations in gene expression. *Nat. Genet.* 38(7), 830–834.

Trivedi, J., Lachapelle, J., Vanderwolf, K. J., Misra, V., Willis, C. K. R., Ratcliffe, J. M., Ness, R. W., Anderson, J. B., and Kohn, L. M. (2017). Fungus Causing White-Nose

Syndrome in Bats Accumulates Genetic Variability in North America with No Sign of Recombination. *mSphere* 2(4), e00271–17.

Turner, G. G., Reeder, D., and Coleman, J. T. H. (2011). A Five-year Assessment of Mortality and Geographic Spread of White-Nose Syndrome in North American Bats, with a Look at the Future. Update of White-Nose Syndrome in Bats. *Bat research news* 52, 13.

University of New Hampshire. (2017). Pseudogymnoascus destructans Raw sequence reads. Title of the publication associated with this dataset: National Library of Medicine (US), National Center for Biotechnology Information.

US Fish and Wildlife Service (2016). White-nose syndrome decontamination protocol Version 4.12. 2016. Web.

US Forest Service (2016). Whole genome sequencing of *Pseudogymnoascus destructans* and six closely related Pseudogymnoascus species. Title of the publication associated with this dataset: National Library of Medicine (US), National Center for Biotechnology Information.

Vacher, C., Vile, D., Helion, E., Piou, D., and Desprez-Loustau, M.-L. (2008). Distribution of parasitic fungal species richness: influence of climate versus host species diversity. *Divers. Distrib.* 14(5), 786–798.

Verant, M. L., Boyles, J. G., Waldrep Jr, W., Wibbelt, G., and Blehert, D. S. (2012). Temperature-dependent growth of *Geomyces destructans*, the fungus that causes bat White-Nose syndrome. *PLoS One* 7(9), e46280.

Vogan, A. A., Khankhet, J., Samarasinghe, H., and Xu, J. (2016). Identification of QTLs Associated with Virulence Related Traits and Drug Resistance in *Cryptococcus neoformans*. *G3-Genes. Genom. Genet.* 6(9), 2745–2759.

Vonhof, M. J., Russell, A. L., and Miller-Butterworth, C. M. (2015). Range-Wide Genetic Analysis of Little Brown Bat (*Myotis lucifugus*) Populations: Estimating the Risk of Spread of White-Nose Syndrome. *PLoS One* 10(7), e0128713.

Walke, J. B., Becker, M. H., Loftus, S. C., House, L. L., Teotonio, T. L., Minbiole, K. P. C., and Belden, L. K. (2015). Community Structure and Function of Amphibian Skin Microbes: An Experiment with Bullfrogs Exposed to a Chytrid Fungus. *PLoS One* 10(10), e0139848.

Warnecke, L., Turner, J. M., Bollinger, T. K., Lorch, J. M., Misra, V., Cryan, P. M., Wibbelt, G., Blehert, D. S., and Willis, C. K. R. (2012). Inoculation of bats with European *Geomyces destructans* supports the novel pathogen hypothesis for the origin of White-Nose syndrome. *Proc. Natl. Acad. Sci. U. S. A.* 109(18), 6999–7003.

Wei, T. and Simko, V. (2017). *R package "corrplot": Visualization of a Correlation Matrix.*

Wibbelt, G. (2015). Out of the dark abyss: White-Nose syndrome in bats. *Vet. Rec.* 177(3), 70–72.

Wibbelt, G. (2018). White-Nose Syndrome in Hibernating Bats. In: *Emerging and Epizootic Fungal Infections in Animals.* Ed. by S. Seyedmousavi, G. S. de Hoog, J. Guillot, and P. E. Verweij. Cham: Springer International Publishing, 289–307.

Wibbelt, G., Kurth, A., Hellmann, D., Weishaar, M., Barlow, A., Veith, M., Prüger, J., Görföl, T., Grosche, L., Bontadina, F., Zöphel, U., Seidl, H. P., Seidl, H. P., and Blehert, D. S. (2010). White-nose syndrome fungus (*Geomyces destructans*) in bats, Europe. *Emerg. Infect. Dis.* 16(8), 1237–1243.

Wilder, A. P., Frick, W. F., Langwig, K. E., and Kunz, T. H. (2011). Risk factors associated with mortality from White-Nose syndrome among hibernating bat colonies. *Biol. Lett.* 7(6), 950–953.

Willis, C. K. R., Menzies, A. K., Boyles, J. G., and Wojciechowski, M. S. (2011). Evaporative water loss is a plausible explanation for mortality of bats from White-Nose syndrome. *Integr. Comp. Biol.* 51(3), 364–373.

Wohlbach, D. J., Thompson, D. A., Gasch, A. P., and Regev, A. (2009). From elements to modules: regulatory evolution in Ascomycota fungi. *Curr. Opin. Genet. Dev.* 19(6), 571–578.

Wyatt, T. T., Wösten, H. A. B., and Dijksterhuis, J. (2013). Fungal spores for dispersion in space and time. *Adv. Appl. Microbiol.* 85, 43–91.

Xu, J., Saunders, C. W., Hu, P., Grant, R. A., Boekhout, T., Kuramae, E. E., Kronstad, J. W., Deangelis, Y. M., Reeder, N. L., Johnstone, K. R., Leland, M., Fieno, A. M., Begley, W. M., Sun, Y., Lacey, M. P., Chaudhary, T., Keough, T., Chu, L., Sears, R., Yuan, B., and Dawson Jr, T. L. (2007). Dandruff-associated *Malassezia* genomes reveal convergent and divergent virulence traits shared with plant and human fungal pathogens. *Proc. Natl. Acad. Sci. U. S. A.* 104(47), 18730–18735.

Zaffarano, P. L., McDonald, B. A., and Linde, C. C. (2009). Phylogeographical analyses reveal global migration patterns of the barley scald pathogen *Rhynchosporium secalis*. *Mol. Ecol.* 18(2), 279–293.

Zhang, F., Gu, W., Hurles, M. E., and Lupski, J. R. (2009). Copy Number Variation in Human Health, Disease, and Evolution. *ANNU REV GENOM HUM G* 10(1), 451–481.

Zhu, Y.-G., Yoshinaga, M., Zhao, F.-J., and Rosen, B. P. (2014). Earth abides arsenic biotransformations. *Annu. Rev. Earth Planet Sci.* 42, 443–467.